UNIVERSIDADE FEDERAL DO PARANÁ

JULIA TRANCOSO FERNANDES DOS SANTOS

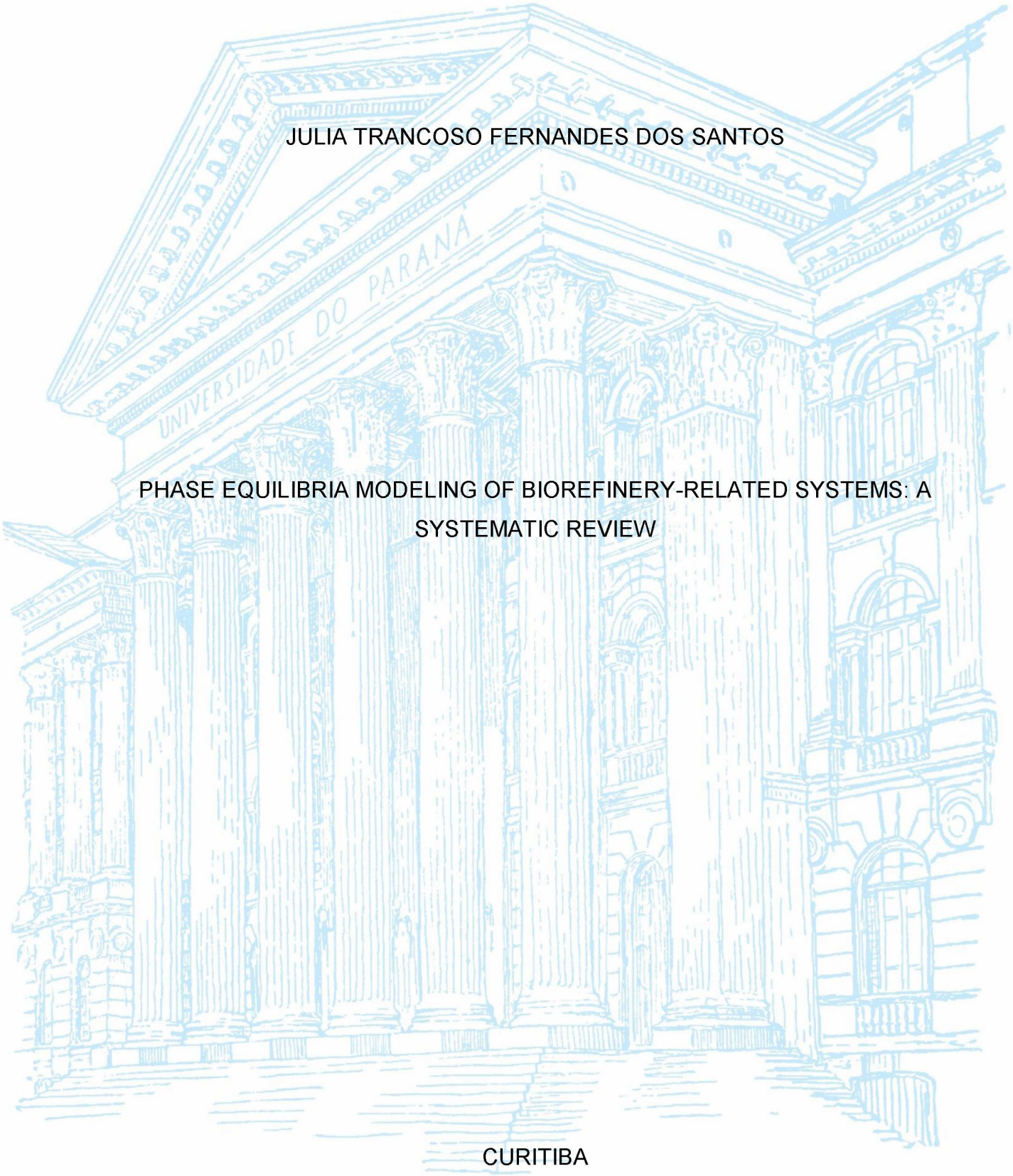

PHASE EQUILIBRIA MODELING OF BIOREFINERY-RELATED SYSTEMS: A SYSTEMATIC REVIEW

CURITIBA

2020

JULIA TRANCOSO FERNANDES DOS SANTOS

PHASE EQUILIBRIA MODELING OF BIOREFINERY-RELATED SYSTEMS: A SYSTEMATIC REVIEW

Dissertação apresentada ao curso de Pós-Graduação em Engenharia Química, Setor de Tecnologia, Universidade Federal do Paraná, como requisito parcial à obtenção do título de Mestre em Engenharia Química.

Orientador: Prof. Dr. Marcos Lúcio Corazza.

CURITIBA

2020

Catalogação na Fonte: Sistema de Bibliotecas, UFPR
Biblioteca de Ciência e Tecnologia

T772p Trancoso, Julia
Phase equilibria modeling of biorefinery-related systems: a systematic review [recurso eletrônico] / Julia Trancoso. – Curitiba, 2020.

Dissertação - Universidade Federal do Paraná, Setor de Tecnologia, Programa de Pós-Graduação em Engenharia Química, 2020.

Orientador: Marcos Lúcio Corazza

1. Termodinâmica. 2. Energia elétrica e calor – Cogeração. 3. Reaproveitamento (Sobras, refugos, etc.). 4. Combustíveis fósseis. 5. Biorrefinarias. I. Universidade Federal do Paraná. II. Corazza, Marcos Lúcio. III. Título.

CDD: 536.7

Bibliotecário: Elias Barbosa da Silva CRB-9/1894

ATA Nº145

ATA DE SESSÃO PÚBLICA DE DEFESA DE MESTRADO PARA A OBTENÇÃO DO GRAU DE MESTRE EM ENGENHARIA QUÍMICA

No dia dezoito de janeiro de dois mil e vinte e um às 14:00 horas, na sala Microsoft Teams, Plataforma online em função da portaria 754/2020 da Reitoria - UFPR, foram instaladas as atividades pertinentes ao rito de defesa de dissertação da mestranda **JULIA TRANCOSO FERNANDES DOS SANTOS**, intitulada**: Phase equilibria modeling of biorefinery-related system: a systematic review**, sob orientação do Prof. Dr. MARCOS LÚCIO CORAZZA. A Banca Examinadora, designada pelo Colegiado do Programa de Pós-Graduação em ENGENHARIA QUÍMICA da Universidade Federal do Paraná, foi constituída pelos seguintes Membros: MARCOS LÚCIO CORAZZA (UNIVERSIDADE FEDERAL DO PARANÁ), SELVA PEREDA (UNIVERSIDAD NACIONAL DEL SUR), ALEXANDRE FERREIRA SANTOS (UNIVERSIDADE FEDERAL DO PARANÁ).

A presidência iniciou os ritos definidos pelo Colegiado do Programa e, após exarados os pareceres dos membros do comitê examinador e da respectiva contra argumentação, ocorreu a leitura do parecer final da banca examinadora, que decidiu pela APROVAÇÃO. Este resultado deverá ser homologado pelo Colegiado do programa, mediante o atendimento de todas as indicações e correções solicitadas pela banca dentro dos prazos regimentais definidos pelo programa. A outorga de título de mestre está condicionada ao atendimento de todos os requisitos e prazos determinados no regimento do Programa de Pós-Graduação. Nada mais havendo a tratar a presidência deu por encerrada a sessão, da qual eu, MARCOS LÚCIO CORAZZA, lavrei a presente ata, que vai assinada por mim e pelos demais membros da Comissão Examinadora.

CURITIBA, 18 de Janeiro de 2021.

Assinatura Eletrônica
18/01/2021 16:08:11.0
MARCOS LÚCIO CORAZZA
Presidente da Banca Examinadora (UNIVERSIDADE FEDERAL DO PARANÁ)

Assinatura Eletrônica
18/01/2021 15:54:53.0
SELVA PEREDA
Avaliador Externo (UNIVERSIDAD NACIONAL DEL SUR)

Assinatura Eletrônica
18/01/2021 15:53:12.0
ALEXANDRE FERREIRA SANTOS
Avaliador Interno (UNIVERSIDADE FEDERAL DO PARANÁ)

TERMO DE APROVAÇÃO

Os membros da Banca Examinadora designada pelo Colegiado do Programa de Pós-Graduação em ENGENHARIA QUÍMICA da Universidade Federal do Paraná foram convocados para realizar a arguição da dissertação de Mestrado de **JULIA TRANCOSO FERNANDES DOS SANTOS** intitulada: **Phase equilibria modeling of biorefinery-related system: a systematic review**, sob orientação do Prof. Dr. MARCOS LÚCIO CORAZZA, que após terem inquirido a aluna e realizada a avaliação do trabalho, são de parecer pela sua APROVAÇÃO no rito de defesa.

A outorga do título de mestre está sujeita à homologação pelo colegiado, ao atendimento de todas as indicações e correções solicitadas pela banca e ao pleno atendimento das demandas regimentais do Programa de Pós-Graduação.

CURITIBA, 18 de Janeiro de 2021.

Assinatura Eletrônica
18/01/2021 16:08:11.0
MARCOS LÚCIO CORAZZA
Presidente da Banca Examinadora (UNIVERSIDADE FEDERAL DO PARANÁ)

Assinatura Eletrônica
18/01/2021 15:54:53.0
SELVA PEREDA
Avaliador Externo (UNIVERSIDAD NACIONAL DEL SUR)

Assinatura Eletrônica
18/01/2021 15:53:12.0
ALEXANDRE FERREIRA SANTOS
Avaliador Interno (UNIVERSIDADE FEDERAL DO PARANÁ)

To my grandmother, Vera, who taught me that: “knowledge is never too much since it does not take space”.

AKNOWLEDGEMENT

To my mother, Lilian, for being the best number 1 fan that anyone could have, your love and support always remind me of who I am in the difficult moments.

To my love, Carlos Eduardo, for being the best life partner I could imagine, your cuddles and coffees made this work much easier.

To all my friends, for always listening to my speeches on thermodynamics, even without any knowledge on the subject.

To my research colleagues and best friends, Luis Ricardo S. Kanda, Estela K. Gelinski, and Estephanie N. Escobar, for all the technical and non-technical conversations that made the laboratory my second home.

To Professors Marcos L. Corazza and Alexandre F. Santos, for always welcoming and guiding me on my professional journey, that I can be a professional as efficient and at the same time kind as you.

To Federal University of Paraná, for being an icon in the production and defense of quality public education in our country.

To CAPES for the financial support granted.

“Nothing in life is to be feared, it is only to be understood.”

Marie Skłodowska Curie

RESUMO

A busca por ideias sustentáveis ganhou destaque nas últimas décadas em todos os níveis da sociedade, uma vez que se tornou imperativo o desenvolvimento econômico, social e ambiental de forma integrada. Nesse contexto, as biorrefinarias apresentam-se atualmente como a tecnologia que melhor cobre todos esses parâmetros, pois agregam os benefícios do reaproveitamento de resíduos, da cogeração de energia e da substituição de combustíveis fósseis. Assim, o estudo das várias matrizes biológicas aplicáveis e a exploração das capacidades técnicas destes processos tornam-se altamente atrativos. A modelagem termodinâmica atua neste cenário como uma poderosa ferramenta para prever o comportamento desses sistemas ainda não totalmente compreendidos, bem como para otimizar os parâmetros de projeto de usinas de biorrefino, sendo, portanto, essencial para o desenvolvimento desta tecnologia. Desse modo, este trabalho teve como objetivo sistematizar, a partir da metodologia PRISMA para revisões sistemáticas, as informações publicadas entre 2010 e 2020 sobre modelagem de equilíbrios de fases em sistemas relacionados a biorrefinaria, a fim de organizar o que já se sabe sobre o assunto. Como resultado, 236 artigos foram categorizados em termos de ano, país, tipo de equilíbrio de fase e modelo termodinâmico empregado. Além disso, as previsões do comportamento de fase de diferentes modelos nas mesmas condições de processo foram comparadas qualitativamente, estabelecendo a equação PC-SAFT como o modelo termodinâmico que melhor representa a grande diversidade de sistemas de interesse para biorrefinarias em uma ampla gama de condições.

Palavras-chave: Revisão sistemática. Equilíbrio de fases. Termodinâmica. Biorrefinarias.

ABSTRACT

The search for sustainable ideas has gained prominence in recent decades at all levels of society since it has become imperative an economic, social, and environmental development in an integrated manner. In this context, biorefineries currently present themselves as the technology that best covers all of these parameters, as they add the benefits of waste reuse, energy cogeneration, and fossil fuel substitution. Thus, the study of the various applicable biological matrices and the exploration of the technical capabilities of these processes become highly attractive. Thermodynamic modeling acts in this scenario as a powerful tool for predicting the behavior of these systems not yet fully understood, as well as to optimize the design parameters of biorefining plants, being, therefore, essential for the development of this technology. Thereby, this work aimed to systematize, using the PRISMA statement for systematic reviews, the information published between 2010 and 2020 on phase equilibria modeling in systems related to biorefineries in order to organize what is already known about the subject. As a result, 236 papers were categorized in terms of the year, country, type of phase equilibria, and thermodynamic model used. In addition, the phase behavior predictions of different models under the same process conditions were qualitatively compared, establishing PC-SAFT as the thermodynamic model that best represents the great diversity of systems of interest for biorefineries in a wide range of conditions.

Keywords: Systematic review. Phase equilibria. Thermodynamics. Biorefineries.

FIGURES

TABLES

NOMENCLATURES

Roman Alphabet

A^R	Residual Helmholtz free energy
A_w	Van der Waals group surface area
G^E	Excess Gibbs free energy
G_{ij}	NRTL interaction coefficient
M^E	General excess property
M^R	General residual property
N_{AV}	Avogadro constant
P_c	Critical pressure
T_R	Reduced temperature
T_c	Critical temperature
V_w	Van der Waals group volume
X^A	Molar fraction of unbound molecules at site A
a^{assoc}	Association energy contribution
a^{att}	Attraction energy contribution
a^{chain}	Chain formation energy contribution
a_{eff}	Effective contact area
a^{fv}	Volume free energy contribution
a_i	Activity
a_{ij}	UNIQUAC binary interaction parameter
a^{seg}	Segment energy contribution
f_{pol}	COSMO defined factor
g_{ij}	NRTL binary interaction parameter
$k^{A_iB_j}$	Bonding volume
k_{ij}	Binary interaction parameter
p_s	Polarity profile
$\mathcal{H}$	Henry's constant
A	Helmholtz free energy
F	General function
G	Gibbs free energy

H	Enthalpy
M	Number of association sites in the molecule
P	Pressure
R	Universal gas constant
S	Entropy
T	Temperature
U	Intern energy
V	Volume
W	Segment exchange energy
Z	Compressibility factor
a	Van der Waals interaction parameter
b	Van der Waals volume parameter
d	Diameter
e	Interaction operator
f	Fugacity
g	Radial distribution function
k	Boltzmann constant
n	Total number of mols
p	Partial pressure
q	Area parameter
r	Volume parameter
x	Molar fraction
z	Coordinator number

Greek Alphabet

α_{ij}	NRTL non-randomness parameter
$\epsilon^{A_iB_j}$	SAFT association energy
ϵ_0	Permittivity of a vacuum
Γ	Individual group contribution
Δ	Association strength
Λ	Wilson interaction coefficient
Ω	Grand Potential
α	Temperature dependence function for EoS

γ	Activity coefficient
ϵ	Permittivity
η	Reduced density
θ	Area fraction
λ	Wilson binary interaction parameter
μ	Chemical potential
ν	Molar volume
ρ	Molar density
σ	Polarity
τ	NRTL and UNIQUAC energy parameter
υ	Number of functional groups
φ	Fugacity coefficient
ϕ	Volume fraction
χ	Flory-Huggins interaction parameter
ω	Acentric factor

Abbreviations

ASOG	Analytical Solution of Groups
CAGR	Compound Annual Growth Rate
CICECO	Centre for research in Ceramics and Composite materials
COSMO	Conductor-like Screening Model
COSMO-RS	Conductor-like Screening Model – Real Solvents
COSMO-SAC	Conductor-like Screening Model - Segment Activity Coefficient
CPA	Cubic Plus Association
CSM	Continuum Solvation Model
DOE	Department of Energy
EMBRAPA	Empresa Brasileira de Pesquisa Agropecuária
EoS	Equation of State
GC	Group Contribution
GCA	Group Contribution with Association
IEA	International Energy Agency
IFP	Institut Français du Pétrole

LLE	Liquid-Liquid Equilibria
NREL	National Renewable Energy Laboratory
NRTL	Non-Random Two-Liquid
PC-SAFT	Perturbed-Chain Statistical Associating Fluid Theory
PLAPIQUI	Planta Piloto de Ingeniería Química
PR	Peng Robinson
PRISMA	Preferred Reporting Items for Systematic reviews and Meta-Analyses
PSRK	Predictive Soave Redlich Kwong
R&D	Research & Development
RK	Redlich Kwong
RMSD	Root Mean Square Deviation
SAFT	Statistical Associating Fluid Theory
SLE	Solid-Liquid Equilibria
SRK	Soave Redlich Kwong
UFPR	Universidade Federal do Paraná
UNICAMP	Universidade de Campinas
UNIFAC	UNIQUAC Functional Activity Coefficients
UNIQUAC	Universal Quasi-Chemical
VdW	Van der Waals
VdW2	Van der Waals quadratic mixing rule
VLE	Vapor-Liquid Equilibria
VLLE	Vapor-Liquid-Liquid Equilibria

CONTENTS

1 INTRODUCTION

1.1 RESEARCH MOTIVATION

The concept of "sustainable development" defined, according to the United Nations Assembly, as the development of the current generation without the commitment of future generations, has been gaining notable importance in recent decades. This theme has become imperative on all fronts of society, given the urgency of environmental problems, the food crisis, and the challenge of the coming "cosmic era" that is approaching. Under these conditions, governmental policies to align incentives to seek renewable energy sources and sustainable technologies have intensified, with a constant demand for processes increasingly integrated with economic, social, and environmental issues (SADHUKHAN et al., 2016).

Biomass appears in this context as a promising alternative to the fossil economy, since the possibility of being produced from different sources provides greater flexibility and security to the market, in addition to its environmental benefits. Thus, studies on the possibilities of using different biological matrices, together with the optimization of the energy integration and efficiency in the conversion of reactions in biomass processing plants support the advancement of the concept of biorefineries (GONZÁLEZ PRIETO et al., 2015).

Despite enormous sustainable economic potentials, biomass has become a pole of research focus only recently, and its processing imposes numerous scientific challenges to be overcome for its large-scale application to become a reality. In this sense, thermodynamic modeling acts as a powerful tool for the better understood of these systems, because it can be used to predict thermodynamics properties, phase behavior, and efficiency of processes. All of these data are crucial for the industrial equipment design, as well as for the definition of process conditions and production strategies in its various stages (ABUTAQIYA, 2018).

In the biorefining sector, the combination of sophistication to handle compounds with large interaction and size differences, and simplicity to allow implementation in a programming environment is the major challenge. Given the complexity of the problem, there is still a lot of ambiguity in thermodynamic modeling in systems-related to biorefineries, which requires continuous investment in the search for a better understanding of this theme (GUO et al., 2012).

1.2 OBJECTIVES

In the context of the growing interest in possible products and processes by biorefining and the importance of thermodynamics in the development of these systems, the objectives of this work were:

1. Understand the development of thermodynamic modeling of phase equilibria over time and the considerations made for modifying models and/or creating new ones;
2. Review the state of the art published in the last decade on thermodynamic modeling of phase equilibria in biorefineries systems using the PRISMA systematic method of searching information;
3. Catalog these works in an overview of publications by year, country, thermodynamic models used and type of equilibrium studied;
4. Highlight relevant points as research groups with greater impact and compounds most studied;
5. Investigate the pros and cons of the thermodynamic models cited in these papers in the context of biorefineries;
6. Perform a critical analysis of which thermodynamic model is the best alternative to represent the phase equilibria of systems related to biorefineries.

1.3 THESIS OUTLINE

To achieve the objectives presented above, this work was assembled in six more sections. **Chapter 2** and **Chapter 3** consist of the presentation of theoretical concepts related to biorefineries, phase equilibria, and thermodynamic modeling. In **Chapter 4**, these topics are connected to formulate the fundamental question that was expected to be answered in this work. **Chapter 5** presents the methodology for the systematic review carried out, the criteria adopted and the final screening results. **Chapter 6** shows the categorization of evaluated studies and finalize with the qualitative comparison of the different thermodynamic models under the same process conditions. For a more didactic development, both the theoretical concepts and the results were categorized into three main classes of thermodynamic models with

specific colors: classical in blue, statistical in yellow, and quantum chemistry in red The last section, **Chapter 7**, lodges an overview of the thesis, highlighting the more important results obtained. This reasoning can best be viewed in Figure 1.

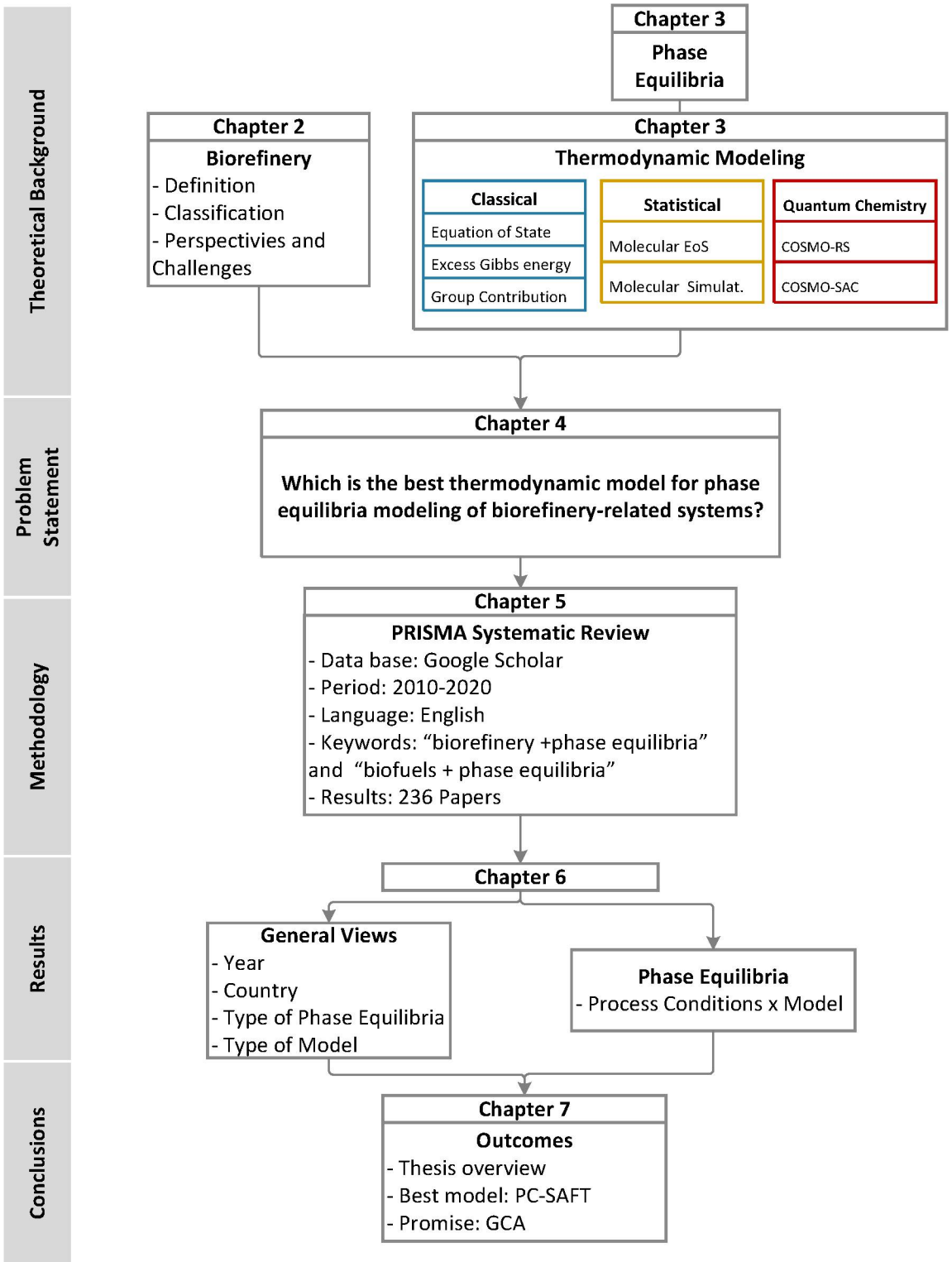

Figure 1 – Conceptual flowchart with the presentation of the reasoning developed in the formulation of this work.

Source: Author's figure (2020).

2 BIOREFINERIES

2.1 CONCEPTS AND DEFINITIONS

The concept of biorefinery was originated in the late 1990s as a result of the increasing trends of biomass use as a renewable feedstock for the production of non-food products, such as plastics, biosurfactants, and, mainly, biofuels. This term, however, is still under development and, despite the wide discussion about its use, there are no established models and standards, which results in several definitions created by different authors and agencies to elucidate its meaning (EMBRAPA, 2011).

The International Energy Agency (IEA) Bioenergy, for example, prepared, in 2010, the most recent known definition, in which the biorefining is exposed as the sustainable processing of biomass in marketable products and energy (IEA, 2010). According to the United States Department of Energy (DOE), on the other hand, the biorefinery is a processing plant where sources of biomass are extracted and converted into a spectrum of products with market value (DOE, 2008). Still, for the American National Renewable Energy Laboratory (NREL), biorefineries are all industries that integrate biomass conversion processes and equipment for the production of fuels, energy, or chemical products (NREL, 2008). It is possible to notice that, in reality, these definitions only differentiate the focus of the description, while the first one emphasizes the process sustainability, the second focuses on products of interest to the market, and the last one points the process integration.

Another definition to be discussed is the proposal by Fatih Demirbas (2009), which makes the important analogy between biorefineries and classical oil refineries. Many authors use this approach as the basis for their work. Fernando et al. (2006), for example, states that subjecting the biomass to complex processes generating different products is equivalent to the processing undergone by oil and natural gas to obtain a variety of compounds. Maity (2015) also highlights that, like the oil refinery, biorefineries can obtain intermediate products for the generation of other substances. Jong and Jungmeier (2015) point out yet the number of intermediate products that both generate as the greatest similarity between these processes, while the biggest difference is about the nature of the raw material, homogeneous for refineries and heterogeneous for biorefineries. The consequence of this heterogeneity is the need for a combination of varied processes, increasing the difficulty and costs of biorefining.

Despite the small differences in the focus of the application, all of these definitions maintain the same basis encompassing, among other aspects, the integration of balances of mass and energy, life cycle, regional socio-economic development, generation and consumption of distributed products and services, and mitigation of greenhouse gas emissions (Figure 2) (EMBRAPA, 2011). Thus, even without a final decision on the concept of biorefineries, large amounts of public and private efforts have focused on the development of this technology, given its compliance with the requirements of the so-called green chemistry, which has become an important socio-economic worldwide goal in recent decades.

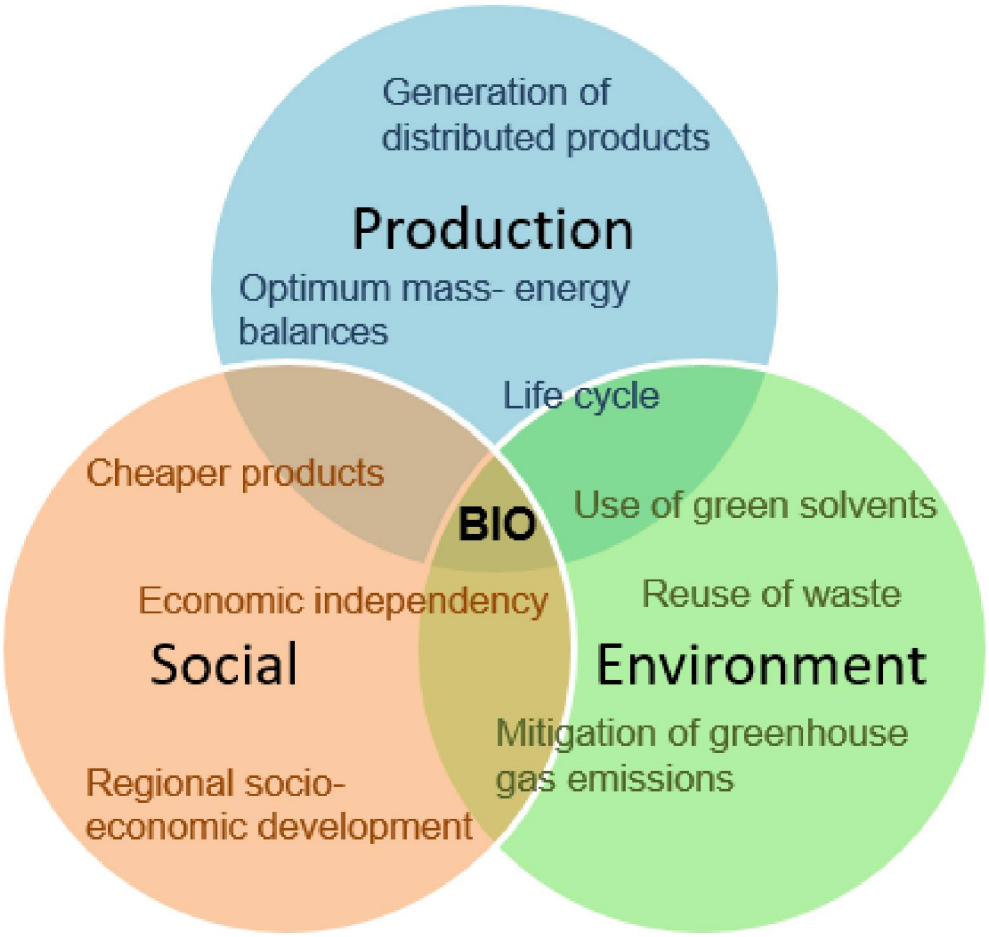

Figure 2 – Schematic representation of different aspects integrated in the most recent biorefinery concept.

Source: Author's figure (2020).

2.2 BIOREFINERIES CLASSIFICATION

As the biorefinery concept is still under development, a standard classification for these systems is not yet available. Most classifications are based on raw material, process technology, state of the platform technology, main product or intermediate produced, but the main problem is that a broad spectrum of different types of biorefineries is growing, and some general categories need to been identified (CHERUBINI et al., 2009).

In this context, Cherubini et al. (2009) developed the most recent idea of classification that includes the biorefinery systems in only a limited number of generic types. For that, each plant, individually, can be defined by the following main characteristics, in order of importance:

i. Platforms: intermediate elements obtained from the raw material and that generate a range of products in the biorefinery;

ii. Products: refer to the main market of the biorefinery and can be divided into two major groups: alternative energies production, like biofuels, electric energy and/or heat; or non-energy products, that are sold or modified to generate bioproducts with higher added value;

iii. Raw materials: classified in primary, harvested from forest or agricultural fields; secondary, residues from the main process, such as black liquor; and tertiary, waste human or industrial post-consumption;

iv. Processes: divided into mechanical/physical, biochemical, chemical, or thermochemical - described as a path or conversion route from the raw material to the product, through platforms and processes.

It is important to remember, however, that the purpose of biorefineries is integration for maximum use of biomass, energy, and processes. Therefore, some processes are suitable for more than one platform, and some platforms can be interconnected as well. Figure 3 presents an example of the application of the Cherubini's method to the most promising individual biorefinery systems in toward the 2020s. It can be seen that even with a well-established method, the classification of a biorefinery can be complicated.

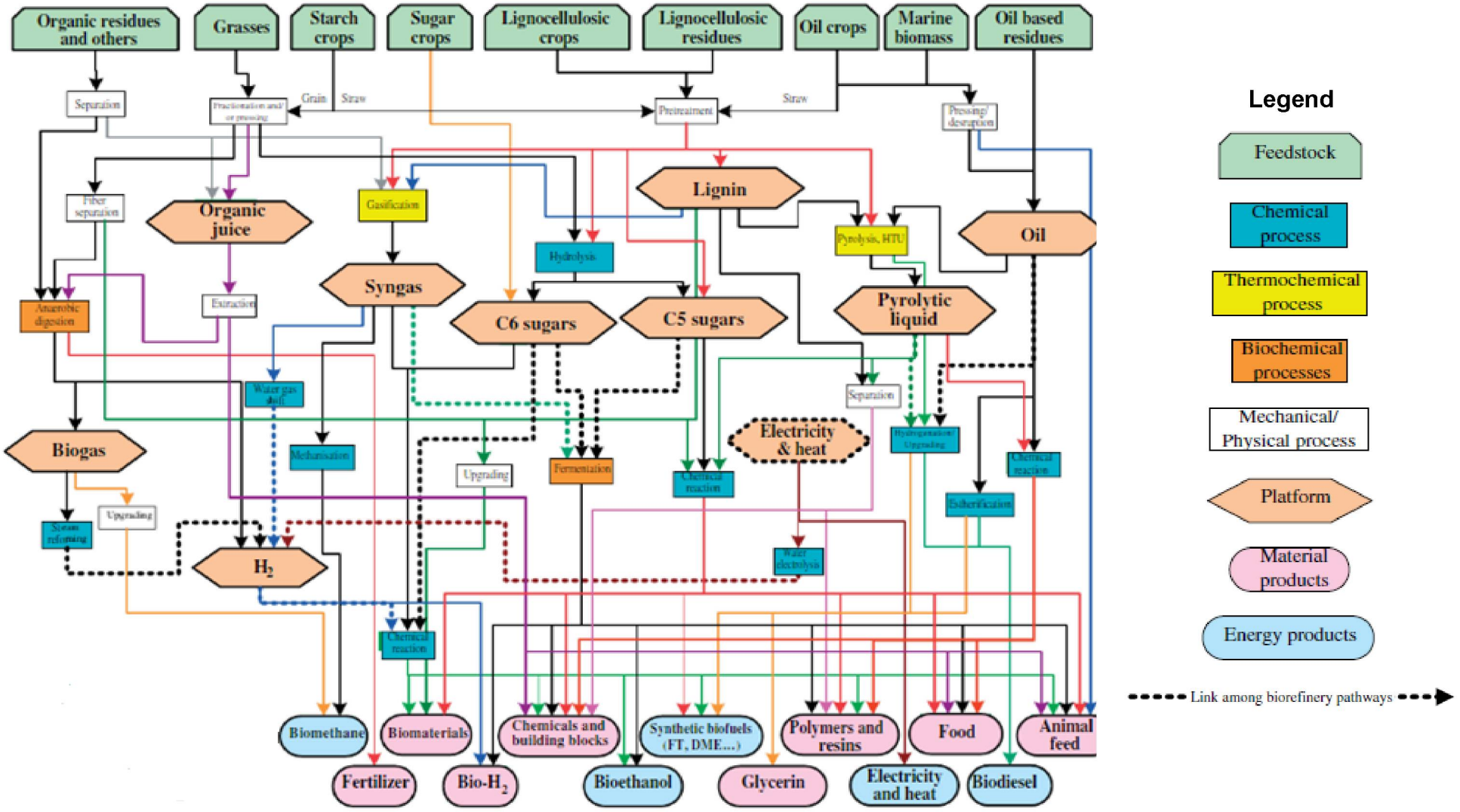

Figure 3 - Network where the most promising individual biorefinery systems toward the 2020s are combined using the methodology proposed by Cherubini et al (2015).

Source: Adapted from Cherubini et al. (2009).

In this work, it was only considered the classification in terms of generation of the plant, which is determined by the raw materials used as explained above and as can be seen in more details in Table 1.

Table 1 – Classification of biorefineries in generations by raw material and solvents used in the plant.

Generation	Raw Materials
1st	Harvest from forest or agricultural fields, containing sugars, starches or oils
2nd	Residual raw materials from agriculture or agroforestry activities, containing cellulose and hemicellulose woody or fibrous
3rd	Microalgae and photosynthetic microbes that produce lipids or hydrocarbons, optimized by the emerging field of synthetic biology
4th	Waste human or industrial post-consumption; new green solvents

Source: Cherubini et al. (2009); Branco (2014).

2.3 PERSPECTIVES AND FUTURE CHALLENGES

This century has faced crises in various sectors of society due to the incessant rise (approximately 7% per year) of energy and chemistry compounds demands, motivated by the rapid increase of the world's population, and the search for better living standards. As a result, in addition to the gradual depletion of resources, the planet is dealing with multiple environmental problems as the deterioration of its natural biomes, severe rates of harmful gas emissions, and the greenhouse effect. Therefore, there is a growing need to change the world economic model, dependent at the moment on unsustainable fossil fuels, to a cyclical economy model, based on the use of renewable resources and technologies (MAITY, 2015).

The oil crisis in the 1970s coupled with the importance of the transport sector, which in 2019 accounted for approximately 28% of world energy consumption ($2.95\ 10^{16}$ kJ), meant that the first efforts for this sustainable movement focused on biofuels research and development (IEA, 2020). Thus, in 2009, according to the International Energy Agency (IEA), biomass (biofuels and waste together) already contributed alone more than 50% of the world's renewable energy, achieving 10.2% of total contribution (Figure 4) (IEA, 2011).

In this regard, many countries have established government guidelines to achieve global goals for sustainable production. The US Department of Energy (DOE), for example, set as target replace 30% of the oil transport fuel with biofuels by 2025,

which would mean that more than 50% of the necessary liquid fuel would be covered by bio-based products.

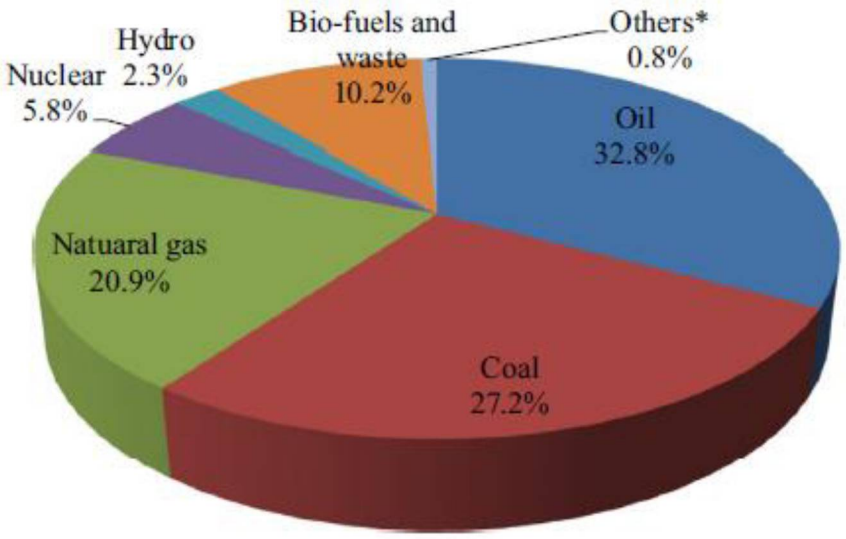

Figure 4 - Global energy scenario in the year 2009. *Other includes geothermal, solar, wind, heat, etc. Source: International Energy Agency (2011).

In Europe, the current regulations regarding the substitution of non-renewable resources with biomass in the area of transport, are given by the directive 2003/30/EC, adopted in 2003. This document aims to replace 2% of all petrol and diesel used as fuels for transportation by biomass until December 2005 and 5.75% until December 2010, receiving an investment of 9 billion euros (LOVINS et al., 2008). Parikka (2004) has reported that these goals are certainly achievable, given that the current sustainable global biomass energy potential is 10^{20} joules per year, of which only 40% is currently used. Although the economy of energy can be based on several alternative raw materials, the economy of substances is not as diverse, depending fundamentally on the biomass of plants. Thus, the development of this sector and, more recently, of the concept of bio-economics have made other products and processes gain space (MAITY, 2015).

For all these reasons, the global biorefinery market, including energy and non-energy products and processes, has received increasing credit. In 2014, for example, this sector received $432.4 billion in investment, according to the Prescient & Strategic Intelligence Company. The BCC Research Group, in turn, pointed out that this growth will go from $466.6 billion in 2016 to $714.6 billion by 2021, with a compound annual growth rate (CAGR) of 8.9% for the period (BCC, 2016). More

recently, the Technavio Group presented an even more impressive CAGR expectation of almost 12% during the 2018-2022 period. In this last analysis, it was also shown that the biotechnology segment, with a value of $224.8 billion in 2014, should reach $447.3 billion by 2020 since in 2017 it already held 52% of the sector (BUSINESS WIRE, 2018).

Despite these achievements and the great potential of biorefining systems, there are still challenges to be overcome. Some applications, for example, are ready now, but their impact is limited by current technologies and raw materials. The future challenges are therefore directly related to commercial and policy support for the growth of this industry and, equally important, research and development, aiming to solve the following problems pointed by Maity (2015):

i. Feedstock diversity: physical properties, chemical compositions, and costs of raw materials used in these systems vary considerably, making it difficult to develop replicable biomass;

ii. Seasonal variation: biomass is in general perennials plants, which makes operations with certain raw material intermittent, hindering the continuous processes desired in the industry;

iii. Land usage: huge quantities of biomass are required to fulfill the long-term goal of complete replacement of petroleum-derived products. Obtaining this amount, however, should not invade agricultural lands, as it may have an adverse impact on food supply;

iv. Consistent R&D investments: many significant contributions in developing feedstock and technologies remain in the early stages of development.

This work focused on contributing to problem **i.**, when trying to select a standard thermodynamic model that best represents the phase behavior of this very diverse range of feedstock in an effective way.

3 THERMODYNAMICS BACKGROUND

The basic concepts of thermodynamics can be found in a multitude of textbooks. This chapter, however, aims to build the evolution of thermodynamic modeling to the present day, including more recent in the analysis. In addition, an effort was made to explain the origins of each expression, its limitations and differences in more detail than usual. Finally, the schemes for presenting this timeline, the main areas of application, and the current problems of each equation can still be used as a short didactic guide on thermodynamic modeling.

3.1 PHASE EQUILIBRIA

The general characteristics of thermodynamic equilibrium can be stated, as defined by Sandler et al. (2006) by the following four criteria:

i. The state properties do not vary with time;
ii. The system is uniform or is formed by uniform subsystems, that is, there are no internal temperature, pressure, velocity, or concentration gradients;
iii. All net fluxes of mass, heat, and work between the system and its surroundings are zero;
iv. The net rate of all chemical reactions is zero.

This state can be expressed mathematically starting with the equation known as the fundamental law of thermodynamics, which combines the first and second laws of thermodynamics, referring to the conservation of energy and the direction of processes, respectively. For reversible open systems, in which interactions between the system and its surroundings occur only in the form of heat and flow work, this relation can be written as Eq.1 (KORETSKY, 2012):

$$dU = TdS - PdV + \sum_i \mu_i dn_i \tag{1}$$

Where T and P are the temperature and pressure, respectively, and μ_i is the chemical potential of component "i", while dU, dS, dV, and dn_i refer, in this order, to

the small changes in energy, entropy, volume, and mass of the system resulting from its interactions with the surroundings. It is important to note that this simplified expression excluded surface and tensile effects, acceleration, change of position in the gravitational or electromagnetic field, chemical, and nuclear reactions.

Now, according to the definition of entropy given by the second law of thermodynamics, it is also known that any isolated system that is not in equilibrium will tend to increase its entropy to reach it, being S maximum at this point (SANDLER et al., 2006). Thus, it makes sense to reorganize Eq.1 in terms of explicit entropy:

$$dS = \frac{1}{T}dU + \frac{P}{T}dV - \frac{1}{T}\sum_i \mu_i dn_i \tag{2}$$

To be a maximum point, the derivative presented in Eq.2 must be null. Therefore, the following set of equations for i components and π phases characterize the basic criteria for thermodynamic phase equilibrium in an isolated system:

$$T(1) = T(2) = \cdots = T(\pi) \qquad \text{Thermal Equilibrium}$$
$$P(1) = P(2) = \cdots = P(\pi) \qquad \text{Mechanical Equilibrium}$$
$$\mu_i(1) = \mu_i(2) = \cdots = \mu_i(\pi) \qquad \text{Chemical Equilibrium}$$

Eq.1 is considered the fundamental law of thermodynamics due to its symmetry, in which each differential is related to an extensive quantity and each coefficient to an intensive quantity. However, other extensive thermodynamic potentials can be obtained using the namely Legendre transformations. This mathematical tool allows changing the independent variables to those that are more practical, maintaining the properties of a fundamental equation. The other three fundamental equations as thermodynamic potentials named enthalpy (H), Helmholtz free energy (A), and Gibbs free energy (G) are presented below (PRAUSNITZ, 1999):

$$dH = TdS + VdP + \sum_i \mu_i dn_i \tag{3}$$

$$dA = -SdT - PdV + \sum_i \mu_i dn_i \tag{4}$$

$$dG = -SdT + VdP + \sum_i \mu_i dn_i \tag{5}$$

Observing these equations, it is possible to define then the chemical potential (μ_i) as the derivative of an extensive property in relation to the component under consideration (i), keep all other variables constant (SISCO, 2018).

$$\mu_i = \left(\frac{\partial U}{\partial n_i}\right)_{S,V,n_{j\neq i}} = \left(\frac{\partial H}{\partial n_i}\right)_{S,P,n_{j\neq i}} = \left(\frac{\partial A}{\partial n_i}\right)_{T,V,n_{j\neq i}} = \left(\frac{\partial G}{\partial n_i}\right)_{T,P,n_{j\neq i}} \quad (6)$$

By this definition, however, it is not possible to calculate an absolute value for the chemical potential, since its relation with the other variables is given by differential equations. Besides that, the concept of μ_i is still quite abstract, so it is desirable to express it in terms of measurable quantities. G. N. Lewis, in 1901, was the first to propose a solution to these problems. In order to establish the relation between chemical potential and factors that can be determined experimentally, he started from the definition of μ_i for a pure, ideal gas, which has T and P as independent variables.

$$d\mu_i = -SdT + VdP \quad (7)$$

Considering an isothermal process, the first term in the right hand side of Eq.7 is canceled. Then, applying the ideal gas equation for the volume (V), he calculated the variation of the chemical potential starting from a standard state of reference to the state of interest (PRAUSNITZ, 1999).

$$\int_{\mu_i^o}^{\mu_i} d\mu_i = RT \int_{P^0}^{P} \frac{1}{P}\, dP \quad (8)$$

$$\mu_i - \mu_i^o = RTln\frac{P}{P^0} \quad (9)$$

In these equations, R is the universal gas constant, and μ_i^o and P^0 are, respectively, the chemical potential and the pressure of the component in a standard reference state chosen arbitrarily but at the same temperature of the interest system.

Subsequently, Lewis generalized this principle to any solid, liquid, or gaseous system, pure or mixed, ideal or not by defining an auxiliary function, called fugacity

(PRAUSNITZ, 1999). For a multicomponent system, the contribution of component i to the chemical potential of the solution is given by Eq.10:

$$\mu_i - \mu_i^o = RTln\frac{\widehat{f}_i}{\widehat{f}_i^0} \tag{10}$$

Comparing Eq.9 and 10 it is possible to note that for a pure, ideal gas, the fugacity is equal to the pressure. For a component in a mixture of ideal gases, it is then reasonable to assume that fugacity is equal to the partial pressure (p_i) of the component. Because all systems approach ideal-gas behavior at very low pressures, the definition of fugacity is completed by the following limit (KORETSKY, 2012):

$$\lim_{P\to 0}\left(\frac{\widehat{f}_i}{p_i}\right) = 1 \tag{11}$$

Lewis also defined the fugacities ratio in Eq.10 as the activity (a_i), an indicator of how "active" a substance is, measured by the difference between the component's fugacity at the state of interest and that in the considered standard state (Eq.12). If this reference state is an ideal gas, this relation becomes the ratio express in the limit definition in Eq.11, which is defined, in turn, as the fugacity coefficient ($\widehat{\varphi}_i$) (Eq.13). On the other hand, if the standard state used is an ideal solution, the new ratio expression is defined as the activity coefficient (γ_i) (Eq.14) (PRAUSNITZ, 1999).

$$a_i = \frac{\widehat{f}_i}{\widehat{f}_i^0} \tag{12}$$

$$\widehat{\varphi}_i = \frac{\widehat{f}_i}{p_i} \tag{13}$$

$$\gamma_i = \frac{\widehat{f}_i}{\widehat{f}_i^{ideal}} \tag{14}$$

More important yet, is the fact that Eq.10 allows a new formulation of the chemical equilibrium in terms of the fugacity (KORETSKY, 2012):

$$\hat{f}_i(1) = \hat{f}_i(2) = \cdots = \hat{f}_i(\pi) \qquad \text{Chemical Equilibrium}$$

This relationship is of great value, as it replaces the equilibrium condition in terms of chemical potential for a more useful function, dependent on controllable variables, without loss of generality. Great efforts have been made in recent decades to correlates fugacity with measurable variables in a broad and efficient way. In the next section, the development of these correlations was more detailed.

3.2 THERMODYNAMICS MODELING

3.2.1 Classical Thermodynamics

3.2.1.1 Equations of State (EoS)

For cases in which the reference state in Eq.10 is chosen as the ideal gas, the so called residual function (M^R) is obtained. This important thermodynamic concept is defined as the difference between the property in the real state, that is, in the state of interest, and the property that an ideal gas would have under these same temperature and pressure conditions (KORETSKY, 2012).

$$M^R = M(T,P) - M^{ideal\ gas}(T,P) \tag{15}$$

The residual Helmholtz free energy, for example, can be obtained by integrating the Eq.4:

$$dA = -SdT - PdV + \sum_i \mu_i dn_i \tag{4}$$

Since the states, by definition, are at the same temperature and composition, the first and the third terms on the right hand side of Eq.4 are canceled and the integration is performed only in terms of volume. For this, it is necessary, first, to determine the limits of integration. For the state of interest, this value is given as the interest volume itself, while for ideal gas representation, in which there are no molecular interactions, the volume is defined as infinite (PRAUSNITZ, 1999):

$$\int_{A^{ideal\ gas}}^{A} dA = \int_{\infty}^{V} -PdV \tag{16}$$

The left hand side of Eq.16 results exactly in the definition presented above for residual functions. Derive then this expression in relation to the number of moles of the component of interest (i):

$$\left(\frac{\partial A^R}{\partial n_i}\right)_{T,V,n_{j\neq i}} = \frac{\partial\left(\int_{\infty}^{V} -PdV\right)}{\partial n_i} \tag{17}$$

It is possible to observe the definition of chemical potential (Eq.6) on the left hand side of Eq.17, which can then be related to fugacity by Eq.10. The right hand side, on the other hand, can be developed using the ideal gas equation. The final expression obtained is presented below:

$$\mu_i - \mu_i^{ideal\ gas} = RTln\frac{\widehat{f}_i}{p_i} = RTln\widehat{\varphi}_i = \int_{V}^{\infty}\left[\left(\frac{\partial P}{\partial n_i}\right)_{T,V,n_{j\neq i}} - \frac{RT}{V}\right]dV - RTlnZ \tag{18}$$

Where Z is the compressibility factor.

For the Gibbs free energy, a similar method can be made. In this case, however, the integration limits are defined in terms of pressure, which for an ideal gas behavior must be low or, in a limit, zero. Eq.19 presented the final expression obtained for this case (PRAUSNITZ, 1999):

$$\mu_i - \mu_i^{ideal\ gas} = RTln\frac{\widehat{f}_i}{p_i} = RTln\widehat{\varphi}_i = \int_{0}^{P}\left(\left(\frac{\partial V}{\partial n_i}\right)_{T,P,n_{j\neq i}} - \frac{RT}{P}\right)dP \tag{19}$$

Equations 18 and 19 enable to compute thermodynamic properties for any substance relative to the ideal gas state, under the same conditions. To evaluate the integrals, however, the volumetric information of the component requires a function valid in all integration region (PRAUSNITZ, 1999).

$$P = F(V, T, n_i) \tag{20}$$

$$V = F(P, T, n_i) \tag{21}$$

These F functions are called Equation of States (EoS), once it allows calculating a property from another two that define a state. In this scenario, for phase equilibrium problems, the pressure explicit equation is more useful, since it provides the volume of each phase under study, while the volume explicit expression has only one result. For this reason, most EoSs are founded in the first form (VAN NESS, 2007).

The first equation of this class was proposed by Johannes van der Waals (vdW), in 1873. In order to describe in a single model both the dispersed and the condensed phase, vdW revised the ideal gas proposal in order to include the contributions of size and molecular interaction of the system (VAN NESS, 2007).

In considering the size of molecules, van der Waals invalidated the ideal hypothesis that they do not occupy space, making the total volume of the ideal equation is no longer accessible. It was, therefore, necessary to replace this term with the new concept of available volume, given by the difference between the total system molar volume (v) and the volume occupied by the molecules, or excluded volume (b).

The second ideal hypothesis of non-interaction, in turn, was nullified when vdW included in its formulation the forces of attraction given by dipole-dipole, induction, and dispersion (London) interactions, which are now generically known as van der Waals' forces. Experimentally, it is known that these forces have a dependence on distance in the order of r^{-6}, which redefined for the volume parameter, results in a term proportional to v^{-2}. It is important to note that these interaction forces have an inversely proportional relation with the pressure of the system, as they hinder the collision of molecules on the walls of the recipient (KORETSKY, 2012).

The final expression obtained by van der Waals is presented in Eq.22 and, an equivalent form, in Eq.23:

$$P = \frac{RT}{v - b} - \frac{a}{v^2} \tag{22}$$

$$Pv^3 - (RT + Pb)v^2 + av - ab = 0 \tag{23}$$

Eq.23 is also known as the cubic Equation of State since for a given pair of P and T, there are three roots for the volume (KORETSKY, 2012):

i. For temperatures beyond critical, there is only one real root, while the other two are imaginary complex conjugates;
ii. At the critical point, the three roots are real and equal;
iii. In the case of sub-critical temperatures, the smallest and the largest roots are taken as the specific volume of the liquid and the vapor phase in equilibrium, respectively. The intermediate root is physically meaningless.

The behavior of a generalized cubic function can be seen in Figure 5, where the red lines represent the isotherms and the yellow area gave the vapor-liquid equilibrium region.

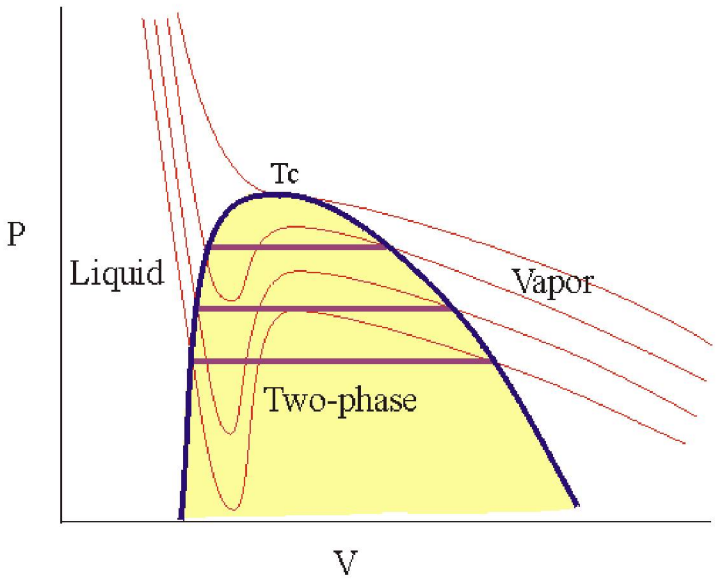

Figure 5 – Representation of the behavior of a generalized Cubic Equation of State function. Source: Rowley (2020).

In turn, the coefficients a and b are positive constants obtained through calculations of statistical mechanics, theoretically related to attraction and repulsion forces, respectively. This determination, however, is performed in practice by adjusting experimental data, or still by the relation of these parameters with the critical properties of the component. This last option is possible due to the inflection point present in the critical isotherm as shown in Figure 5, which is defined mathematically as expressed in the following equation (Eq.24) (KORETSKY, 2012):

$$\left(\frac{\partial P}{\partial v}\right)_{T_c} = \left(\frac{\partial^2 P}{\partial v^2}\right)_{T_c} = 0 \tag{24}$$

After manipulation, the result is:

$$a = \frac{27(RT_c)^2}{64P_c} \tag{25}$$

$$b = \frac{RT_c}{8P_c} \tag{26}$$

Where, the index "c" means critical property.

For mixtures, these parameters need a mixing rule to total the contributions of the pure components. Nowadays, there are robust rules, as proposed by Huron and Vidal (1979), in which the parameter a above is rewritten to be a function of a modified NRTL expression at infinite pressure, obtaining good results even in systems with strong polar compounds such as water (GMEHLING et al., 2015). Despite this, the van der Waals quadratic mixing rule with two independent parameters (vdW2) below is the most used mainly due to its simplicity (SISCO, 2018):

$$A = \sum_i \sum_j n_i n_j \sqrt{a_i a_j}(1 - k_{ij}) \tag{27}$$

$$B = \sum_i n_i \, b_i \tag{28}$$

In these expressions, k_{ij} is a binary interaction parameter between the components i and j obtained by adjusting experimental data of the mixture under study.

Subsequent EoSs added some experimental modifications to van der Waals' initial idea. The first of these equations to be successful was the Redlich-Kwong (RK) Equation of State, proposed by Otto Redlich and Joseph Neng Shun Kwong, in 1949. Its main contribution was the reformulation of the attraction contribution term, including an empirical correction for the temperature influence (REDLICH; KWONG, 1949).

$$P = \frac{RT}{v - b} - \frac{a}{\sqrt{T}.v.(v + b)} \tag{29}$$

Soave (1972) optimized this temperature dependence reformulating the a parameter as:

$$a_i(T) = a_{ic}.\alpha_i(T) \tag{30}$$

Where a_{ic} is the vdW parameter given by the critical properties of the component "i" and $\alpha_i(T)$ is a dimensionless factor that becomes unitary when the reduced temperature ($T_{R_i} = T/T_{c_i}$) is also one. A set of values for α_i can be fitted from the experimental vapor pressure data of the component and then the linearization of the $\alpha_i^{0.5}$ found and ${T_{R_i}}^{0.5}$ relation is performed. Forcing these lines of different components to pass through the point $T_{R_i} = 0.7$, when α_i depends only on the assumed acentric factor (ω), the following function is obtained (SOAVE, 1972):

$$\alpha_i = \left[1 + (0.48 + 1.574\omega_i - 0.176\omega_i^2)(1 - \sqrt{T_R})\right]^2 \tag{31}$$

Soave-Redlich-Kwong (SRK) Equation of State is presented in Eq.32:

$$P = \frac{RT}{v - b} - \frac{a(T)}{v(v + b)} \tag{32}$$

In 1976, Ding-Yu Peng and Donald Robinson, in turn, proposed an improvement in SRK expression. For that, they indicated a new relation for the molar volume and the size of the molecules (b), aiming to consider the magnitude of this last factor at very high pressures (PENG; ROBINSON, 1976).

$$P = \frac{RT}{v - b} - \frac{a(T, \omega)}{v(v + b) + b(v - b)} \tag{33}$$

Furthermore, a new α function was developed (Eq.34) considering the vapor pressure data in the range from the normal boiling point to the critical point of each

substance, instead of just the vapor pressure calculated at $T_{R_i} = 0.7$ based on the value of acentric factor proposed by Soave (PENG; ROBINSON, 1976).

$$\alpha = \left[1 + (0.37464 + 1.54226\omega - 0.26992\omega^2)(1 - \sqrt{T_R})\right]^2 \quad (34)$$

There are also Equations of States with a strong theoretical base in mechanical statistical, such as the Virial, Beattie-Bridgeman and Benedict-Webb-Rubin Equations of States. The coefficients of these expressions depend only on the temperature and composition of the mixture, and are directly related to intermolecular interactions. However, due to their relative simplicity, cubic Equations of State are the most used in engineering applications.

3.2.1.2 G^E Models

Although Equations of State are defined generically and can be applied to any phase, in general, their results to condensed phase are doubtful. This is mainly due to the following restrictions:

i. With ideal gas as the reference state, condensed phase require volumetric data and an efficient function over the entire density range from the ideal-gas (zero density) to the density of interest, including the two-phase region, which generally are not easily available (PRAUSNITZ, 1999);
ii. Most of these equations consider only physical forces (vdW forces), while in condensed state chemical forces (covalent bonds, hydrogen bonds, solvation, and association) have a considerable role in molecular interactions.

To solve the first problem, therefore, a more practical way for calculation of fugacities in condensed phase is needed. In this context, an alternative method, named excess Gibbs free energy (G^E) models, were developed using the ideal solution as reference state, which is related to the activity coefficient by Eq.14:

$$\gamma_i = \frac{\hat{f}_i}{\hat{f}_i^{ideal}} \quad (14)$$

An ideal solution is defined as one in which, at constant temperature and pressure, the molecular potentials are the same for all components in the mixture. In other words, where all components interact with themselves and others with the same intensity. Besides that, the fugacity of each component of the mixture presents a linear dependency on its molar fraction (x_i) (KORETSKY, 2012; PRAUSNITZ, 1999).

This linearization is achieved in two limit situations, which generates two possibilities of standard state. The first one occurs when the molar fraction of the component tends to unity. In this case, as a molecule interacts almost exclusively with molecules of the same type, interactions can be considered equal and the solution, ideal. In this scenario, the Lewis/Randall rule (Eq.35) is defined, and the ideal fugacity is replaced by the fugacity of the pure component itself (f_i) (KORETSKY, 2012).

$$\widehat{f}_i^{ideal} = x_i f_i \tag{35}$$

On the other hand, when the molar fraction of the component tends to zero, the molecule interacts mainly with molecules of a different type. Despite the different components, the molecular interactions obtained are equal, making the solution, once again, ideal. In this case, Henry's law (Eq.36) is valid and the ideal fugacity of the component can be replaced by the Henry's constant ($\mathcal{H}_i$), determined experimentally (KORETSKY, 2012; PRAUSNITZ, 1999).

$$\widehat{f}_i^{ideal} = x_i \mathcal{H}_i \tag{36}$$

Once the standard state for the condensed phase has been defined, it is possible to realize a procedure similar to that performed for the Equations of State, where Eq.10 and Eq.6 are related.

It is noted, however, that the change of reference state means that another thermodynamic concept needs to be defined in place of residual functions. This new concept is called excess function (M^E), defined as the difference between a thermodynamic property real value and that which the same property has as an ideal solution state, at the same temperature, pressure, and composition (KORETSKY, 2012; PRAUSNITZ, 1999).

$$M^E = M(T, P, n_i) - M^{ideal\ solution}(T, P, n_i) \tag{37}$$

Applying these concepts, Eq.6 and Eq.10 are related by Eq. 38:

$$\mu_i - \mu_i^{ideal\ solution} = RTln\frac{\widehat{f}_i}{\widehat{f}_i^{ideal}} = RTln\gamma_i = \left(\frac{\partial G^E}{\partial n_i}\right)_{T,P,n_{j\neq i}} \tag{38}$$

In general, the Lewis-Randall state is adopted as reference. In this sense, all development carried out from here will have this starting point.

It is important to highlight that when the reference state is an ideal gas, a constant temperature is fixed for the integration of Eq.10, which allows the use of free energy in terms of Gibbs and Helmholtz. However, when the standard state is an ideal solution, the temperature, but also the pressure is fixed. As a result, the excess Gibbs free energy is the only possible function for the developments to follow.

At this point, it is noted the need for some G^E function valid for the entire composition range of interest, so that Eq.38 can be evaluated. This function can be represented in the form shown in Eq.39, which has the same meaning for G^E models as Eq.20 and Eq.21 have for EoS.

$$G^E = F(n_i) \tag{39}$$

Margules, in 1890, was the first to propose an equation to express analytically the function F above. His work has no theoretical base, and aimed to represent the compounds merely by adjusting a polynomial expansion that satisfies the following criteria for binary systems (CHEN; MATHIAS, 2002; PRAUSNITZ, 1999):

i. When the solution has only the pure component ($x_1\ or\ x_2 = 1$), it becomes an ideal solution and, consequently, the excess Gibbs free energy must be null; (PRAUSNITZ, 1999);

ii. The activity coefficients of the two components are correlated by Gibbs-Duhem equation.

The most simple equation that fulfills these principles is the called one-parameters Margules or two-suffix Margules equation (Eq.40):

$$G^E = Ax_1x_2 \tag{40}$$

Where A is an empirical constant given as a function of pressure and, more significantly, the temperature of the system. There are other Margules equations with more parameters of polynomial expansion. It is expected that the more terms are added to the expression, the better the performance of the model, however, even for larger order, this equation only obtain approximate values for systems where the components are similar in size, shape, and chemical nature. In addition, the expansion to multicomponent systems requires further assumptions or interaction parameters of higher order than the binaries normally used, which are often difficult to obtain experimentally (PRAUSNITZ, 1999).

The first attempt at a model for ideal solutions developed on a theoretical base was made in 1910, by Van Laar, one of the students and, later, coworker of van der Waals. For this purpose, he assumed that, for mixtures of liquids at constant temperature and pressure, there are no excess volume or excess entropy (regular solution) and, therefore, the vdW Equation of State can be used to represent the volumetric properties of the mixture (SANDLER et al., 2006; PRAUSNITZ, 1999). The Van Laar equation for binary systems is presented in Eq.41:

$$G^E = x_1x_2\left(\frac{AB}{Ax_1 + Bx_2}\right) \tag{41}$$

Where A and B are coefficients that depend on temperature and pure components properties. When these terms are the same Eq.41 returns to the Margules equation (Eq.40).

The use of the premises and, mainly, of the van der Waals mixing rules, however, makes the activity coefficients obtained by this method always lower than one, which restricts its predict capacity only positive deviations from ideality. For this reason, despite the theoretical development, the Van Laar model, when applied, has its constants determined experimentally (KORETSKY, 2012; PRAUSNITZ, 1999).

In this sense, the first thermodynamic model for condensed phases with a theoretical basis actually applied was proposed, independently, by Flory (1941) and Huggins (1942). Aiming to describe mixtures of very different size molecules, including solutions of polymers, Flory and Huggins dismissed Van Laar's earlier consideration of regular solutions. Thus, to focus on this entropy of the mixture, they first assume athermal solutions ($\Delta H = 0$), which is a good approximation for mixtures of components that are similar in their chemical characteristics, even if their sizes are different (PRAUSNITZ, 1999; SANDLER et al., 2006).

To do so, they applied the quasi-crystalline lattice model, which assumes that molecules of condensed phases tend to remain in a small region, in a more or less fixed position in space, forming a regular array, called lattice (Figure 6).

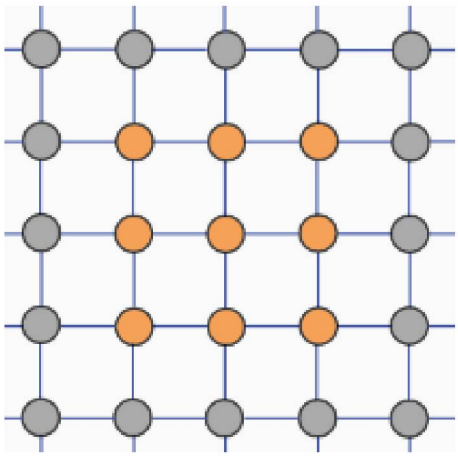

Figure 6 – Representation of the hypothetical arrangement proposed by the lattice model in which each molecule has a fixed position in space resulting in a well-defined array.
Source: HQS Quantum Simulations (2020).

Based on statistical arguments and well-defined assumptions an equation for entropy, named combinatorial contribution, was obtained (Eq.42) as a function only of the composition and structural parameters of pure components (PRAUSNITZ, 1999; SANDLER et al., 2006).

$$S^E = -R\left(x_1 ln\frac{\phi_1}{x_1} + x_2 ln\frac{\phi_2}{x_2}\right) \tag{42}$$

Where ϕ_i is the volume fraction of component "i".

Then, to extend this result to real, non-athermal solutions, a semi-empirical term, called residual contribution, was added to Eq.42. This term includes deviations

due to intermolecular forces and free volumes of the components (Eq.43) (PRAUSNITZ, 1999; SANDLER et al., 2006).

$$H^E = RT\chi\left(x_1 + \frac{v_2}{v_1}x_2\right)\phi_1\phi_2 \tag{43}$$

The symbol χ represents a dimensionless parameter named Flory-Huggins interaction parameter, which is determined by the energies that characterize the interactions between pairs of components (PRAUSNITZ, 1999).

As Gibbs free energy is defined as the difference between enthalpy and entropy multiplied by the temperature, the Flory-Huggins equation in terms of G^E is given by Eq.44:

$$G^E = RT\left[\left(x_1 ln\frac{\phi_1}{x_1} + x_2 ln\frac{\phi_2}{x_2}\right) + \chi\left(x_1 + \frac{v_2}{v_1}x_2\right)\phi_1\phi_2\right] \tag{44}$$

Wilson (1964), in turn, tried to improve the Flory-Huggins model using concepts of the local composition theory. This reasoning has the main assumption that, given a central molecule in the lattice of Figure 6, its neighborhood depends on the differences in size and interaction energies of this central molecule with other species. Thus, around each molecule, there is a local composition different from that in bulk. The local composition expression proposed by Wilson is presented in Eq.45:

$$\frac{x_{ji}}{x_{ii}} = \frac{x_j e\left(\frac{-g_{ji}}{RT}\right)}{x_i e\left(\frac{-g_{ii}}{RT}\right)} \tag{45}$$

Continuously, Wilson used the expression for athermal mixtures (Eq.42) replacing the overall volume fraction with his proposal of local fraction (WILSON, 1964). Wilson's final G^E equation is presented in Eq.46:

$$G^E = -RT\sum_{i=1}^{m} x_i ln\left(\sum_{j=1}^{m} x_j \Lambda_{ij}\right) \tag{46}$$

Where Λ_{ij} satisfies the following definitions: $\Lambda_{ii} = 0$ and $\Lambda_{ij} \neq \Lambda_{ji}$.

This parameter is related to pure component molar volumes and to characteristic energy, given by the difference between interactions of same type and non-similar molecules. Wilson's equation has the advantage that any number of components can be fitted with only binaries parameters. However, despite being applicable to a wide variety of systems, this model is unable to describe partial miscibility, not predicting liquid-liquid equilibrium when Λ_{ij} is close to unity (WILSON, 1964).

Renon and Prausnitz (1968) solved this problem in their proposal named Non-Random Two-Liquid (NRTL) model. For this, they rewrote Wilson's suggestion for local composition (Eq.45), multiplying it by a constant in accordance with statistical-mechanical Guggenheim's quasi-chemical lattice theory (1952).

$$\frac{x_{ji}}{x_{ii}} = \frac{x_j e\left(\frac{-\alpha_{ij} g_{ji}}{RT}\right)}{x_i e\left(\frac{-\alpha_{ij} g_{ii}}{RT}\right)} \tag{47}$$

Besides that, they obtained an expression for G^E using Scott's two-liquid theory of binary mixtures (1956), in place of Flory Huggins previously used (RENON; PRAUSNITZ 1968). The final NRTL equation is shown below:

$$G^E = -RT \sum_{i=1}^{m} x_i \frac{\sum_{j=1}^{m} \tau_{ji} G_{ji} x_j}{\sum_{l=1}^{m} G_{li} x_l} \tag{48}$$

NRTL is a three parameters model. Two of them are included in the term τ_{ji} and measure energy interactions, in a similar way to Λ_{ij} of Wilson's model. The other parameter is the multiplication constant added to Eq.47 (α_{ij}), included in the term G_{ji}, which provides a measure of the non-randomness of the mixture. Although α_{ij} can be adjusted experimentally, a large number of binary systems indicate that its value is in the range of variation [0.2; 0.47], being a typical choice 0.3. It is also noted that, when α_{ij} is zero, the mixture is assumed completely random and the Eq.48 reduces to the two-suffix Margules equation (PRAUSNITZ, 1968).

Nevertheless, aiming to overcome the restriction for completely miscible mixtures, maintaining the advantage of only two adjustment parameters of Wilson's model, Abrams and Prausnitz (1975) derived the universal quasi-chemical theory (UNIQUAC) model. This equation extends the already mentioned Guggenheim theory for nonrandom mixtures to solutions containing molecules of different sizes and shapes. This was achieved by replacing the Guggenheim's boundary of equi-sized spherical molecules with the combinatorial factor proposed by Staverman (1950) for mixtures of molecules with arbitrary size and shape. As a result, the G^E equation obtained has a combinatorial and a residual contribution, in a similar way to the Flory-Huggins expression (Eq.44):

$$(G^E)^{combinatorial} = RT \sum_{i=1}^{m} x_i ln \frac{\phi_i}{x_i} + \frac{z}{2} \sum_{i=1}^{m} q_i x_i ln \frac{\theta_i}{\phi_i} \tag{49}$$

Where ϕ_i is the volume and θ_i is the area fraction, related to the molecules' external surface area. The parameter z is the coordinator number defined by Abrams as 10.

$$(G^E)^{residual} = -RT \sum_{i=1}^{m} x_i q_i ln \left(\sum_{j=1}^{m} \theta_j \tau_{ji} \right) \tag{50}$$

The parameter τ_{ji}, in turn, gives the intermolecular forces and depends on two adjustable binary parameters.

The UNIQUAC equation is not just a generalization of Guggenheim's model, but also of all commonly used expressions for the excess Gibbs free energy, can be reduced to any of them by some simplifications. The main advantage of UNIQUAC equation is that, with only two adjustable parameters per binary, it gives a good representation of both vapor-liquid and liquid-liquid equilibria for a variety of nonelectrolyte liquid mixtures (PRAUSNITZ 1968).

All excess Gibbs free energy functions presented in this section and its related expressions, including parameters and activity coefficient final equations were listed in Appendix 1.

3.2.1.3 Group Contribution

The last method comprised within classical thermodynamics refers to the group contribution models. This proposal emerged as a relatively simple predictive tool for mixtures where only fragmentary data or no data at all are available. Therefore, it is assumed that the mixture consists not of molecules but of functional groups, which behave completely independent of the molecule in which they appear (Figure 7). As a result, it is then possible to calculate the solution properties by properly weighted sums of individual contributions from each structural group interactions. The fundamental advantage of this procedure is that the number of possible distinct functional groups is much smaller than the number of distinct molecules.

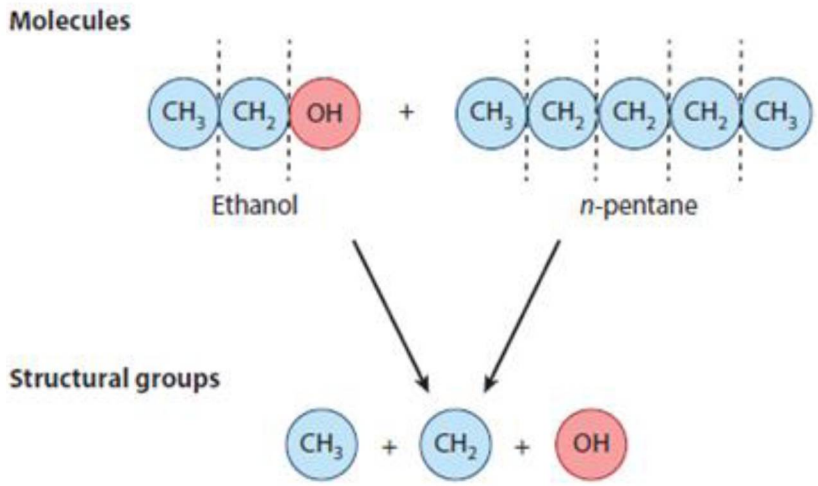

Figure 7 – Representation of the division of a molecule into its base structural groups, which are then counted individually by the Group Contribution methods.
Source: Gmehling et al. (2015).

It was during the 50s and 60s in an experimental program carried out by G. M. Sletmoe (Shell Development Co.), with the objective of using mixtures of solvents and resins efficiently, that Deal and Derr (1969) published the final version of the first group contribution model, named Analytical Solution of Groups (ASOG). This theory is in many ways similar to that of the UNIQUAC model, where it has a configurational part, which provides the contribution due to differences in molecular size, and a residual part that provides the contribution due to molecular interactions (Eq.51). This distinction is necessary since the sized effects cannot be associated with group interactions (GMEHLING et al., 2015 ; WILSON; DEAL 1962).

$$ln\gamma_i = (ln\gamma_i)^{combinatorial} + (ln\gamma_i)^{residual} \quad (51)$$

The first part is then estimated by using the athermal Flory-Huggins equation. The residual part, in turn, is obtained by the Wilson proposal, given by the difference between the sum of individual contributions of each group (Γ_k) and the sum of the individual contributions in the conventional standard state ($\Gamma_k^{(i)}$), normally defined as the "pure group" (Eq.52).

$$(ln\gamma_i)^{residual} = \sum_i v_k^{(i)}(ln\Gamma_k - \Gamma_k^{(i)}) \quad (52)$$

Where $v_k^{(i)}$ is the number of functional groups k in component i, and Γ_k is a composition function given, in practice, by a graphical relation derived from an appropriate set of experimental data (WILSON; DEAL, 1962).

ASOG model had been largely superseded by Fredenslund and Prausnitiz, (1975) proposal, that combining the groups' concept with the UNIQUAC equation, arriving at the UNIQUAC Functional Group Activity Coefficients (UNIFAC) model. This method has the advantage that the UNIQUAC model contains per se a combinatorial part (Eq.49), which can be used directly being the pure component properties r_i and q_i are now calculated as the sum of the group volume (r_i) and area (q_i) parameters:

$$r_i = \sum_k v_k^{(i)} \frac{V_{w_k}}{15.17} \quad (53)$$

$$q_i = \sum_k v_k^{(i)} \frac{A_{w_k}}{2.5 \cdot 10^9} \quad (54)$$

Where V_{w_k} and A_{w_k} are van der Waals group volume and surface areas, given by Bondi (1968). The normalization factors are those given by Abrams and Prausnitz (1975). Besides that, the individual contributions of each group (Γ_k) in the residual part of the activity coefficient, is calculated by the solution-of-groups concept:

$$ln\Gamma_k = \frac{A_{w_k}}{2.5 \cdot 10^9}\left[1 - \ln(\sum_m \theta_m \tau_{mk}) - \sum_m \frac{\theta_m \tau_{mk}}{\sum_n \theta_n \tau_{nm}}\right] \quad (55)$$

Eq.55 also holds for $\Gamma_k^{(i)}$. The parameters θ_m and τ_{mk} are the already defined parameters for the UNIQUAC model related to the area fraction of group m, and an empirical measure of the energy of interaction between groups m and n, respectively (FREDENSLUND; PRAUSNITIZ, 1975).

In spite of the reliable results for VLE, UNIFAC shows a few weaknesses. For example, unsatisfactory results are obtained for activity coefficients at infinite dilution, and only poor agreement is obtained for excess enthalpies, which lead to a wrong description of the activity coefficients as a function of temperature. Furthermore, poor results for asymmetric systems were obtained, mainly caused by the inadequate combinatorial part used (GMEHLING et al., 2015).

To improve its results, modified UNIFAC models were developed, mainly using a different combinatorial part and adding temperature dependent group interaction parameters. The most important of these modifications were made by Weidlich and Gmehling (1999), at the University of Dortmund (UNIFAC-Dortmund), in which the group interaction parameters are fitted not only to VLE, but also to other reliable phase equilibrium and excess properties data in a wide temperature range.

Because of the importance of a reliable predictive method with a large range of applicability for process development, the continuous extension and revision of the group interaction parameter matrix is carried out within a company consortium supported by approximately 50 companies (GMEHLING et al., 2015).

3.2.2 Statistical Thermodynamics

3.2.2.1 Molecular EoS

The Statistical Associating Fluid Theory (SAFT) is based on the first-order perturbation theory developed by Wertheim, in 1984. This principle is presented as one of the tools of statistical mechanics to quantify interactions present in association fluids, thus allowing accounting how behaviors at the microscopic level alter the average properties of the fluid at the macro level (CHAPMAN et al., 1989; WERTHEIM, 1983,

1984). For this, Wertheim proposed the incorporation of steric and interaction effects for simple and multipolar fluids with highly directional forces, by expanding Helmholtz free energy in a series of molecular distribution functions and association potentials. As a result, a reasonably simple relation was obtained between the residual Helmholtz free energy and a function that characterizes the association force (WERTHEIM, 1983, 1984).

In this context, the SAFT equation of state was developed by Chapman et al. (1989) as the sum of three terms of this residual Helmholtz free energy expansion, which represent contributions of different intermolecular forces. To this end, they considered a reference term given by the interactions between hard spheres fluid segments and added to it two perturbations related to the formation of chains by covalent bonds, and to associative forces such as hydrogen bonds (Figure 8).

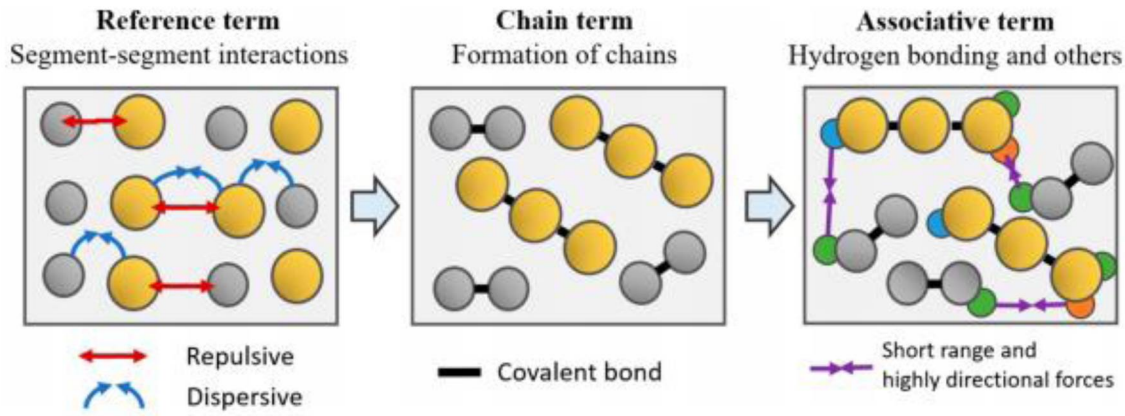

Figure 8 – The three terms included by Chapman et al. (1989) in the development of the original SAFT equation.

Source: Crespo; Coutinho (2019).

Mathematically, these terms can be represented as in Eq.56:

$$\frac{A^R(T,V,n)}{RT} = a^{seg} + a^{chain} + a^{assoc} \tag{56}$$

The first term (a^{seg}) in this expression is calculated using the interactive potential equation of hard spheres proposed by Carnahan and Starling (1969):

$$\frac{a^{seg}}{RT} = \frac{4\eta - 3\eta^2}{(1-\eta)^2} \tag{57}$$

Where η is the reduced density defined for mixtures as:

$$\eta = \frac{\pi N_{AV}}{6} \rho d^3 \sum_i x_i m_i \tag{58}$$

In Eq.58, m_i is the number of spherical segments in component "i" and the sum $\sum_i x_i m_i$ is the ratio of the segment number to the molecule number in the fluid. Besides that, N_{AV} is the Avogadro constant, ρ is the molar density, and d is the segment diameter.

The second term (a^{chain}) in Eq.56 is given by the following equation:

$$\frac{a^{chain}}{RT} = \sum_i x_i (1 - m_i) \ln(g_{ii}(d_{ii})^{hs}) \tag{59}$$

Where g_{ii} is the pair correlation function for the interaction between two of these spheres, evaluated in the contact radius of hard spheres $(d_{ii})^{hs}$.

The third term (a^{assoc}) in Eq.56, in turn, is responsible for the presence of specific site-site interactions between segments and can be calculated by Eq.60.

$$\frac{a^{assoc}}{RT} = \sum_i x_i \left[\sum_{A_i} \left[ln X^{A_i} - \frac{X^{A_i}}{2} \right] + \frac{M_i}{2} \right] \tag{60}$$

Where M_i is the number of association sites in the molecule "i" and X^{A_i} is the molar fraction of unbound molecules "i" at site A (Eq.61).

$$X^{A_i} = \frac{1}{1 + \rho \sum_j x_j \sum_{B_j} X^{B_j} \Delta^{A_i B_j}} \tag{61}$$

In Eq.61, $\Delta^{A_i B_j}$ is the association strength, which describes the association between site A on a molecule of species i and site B on a molecule of species j. This term is defined as:

$$\Delta^{A_iB_j} = {d_{ij}}^3 g_{ij}(d_{ij})^{seg} k^{A_iB_j} \left[\exp\left(\frac{\epsilon^{A_iB_j}}{kT}\right) - 1\right] \quad (62)$$

Where $\epsilon^{A_iB_j}$ is the association energy, k is the Boltzmann's constant, $k^{A_iB_j}$ is the bounding volume, d_{ij} is the segment diameter, and g_{ij} is the radial distribution function, which, for hard spheres, is approximately given by the following expression:

$$g_{ij}(d_{ij})^{seg} = g_{ij}(d_{ij})^{hs} = \frac{1 - \frac{1}{2}\eta}{(1-\eta)^3} \quad (63)$$

Most variants of SAFT retain the fundamental form presented in Eq.56, although some may add terms or modify the reference or the distribution function used. Table 2 presents all the statistical models that appeared in this review divided into two major groups, those derived from the original SAFT equation (SAFT Type) and those derived from the PC-SAFT model (PC-SAFT Type).

Table 2 - Statistical models present in this review and their particular considerations.

Model	Consideration
SAFT	Hard spheres potential for spherical segments as reference
SAFT-VR	Hard spheres potential show Variable Range (VR) interaction
GC-SAFT-VR	Group Contribution (GC) rules to applying SAFT-VR
SAFT-γ	γ intermolecular potential as reference
soft-SAFT	Lennard–Jones potential as reference
PC-SAFT	Perturbation Chain (PC) theory by Barker-Henderson as reference
ePC-SAFT	PC-SAFT with a Debye-Hückel contribution for Electrolyte
GC-PC-SAFT	Group Contribution (GC) rules to parametrizing the associating parameters
PPC-SAFT	Adding a Polar term to PC-SAFT
ePPC-SAFT	PPC-SAFT with a Debye-Hückel contribution for Electrolyte
PCIP-SAFT	Adding a Induced Polar (IP) term to PC-SAFT
GC-PPC-SAFT	Adding a Polar term to GC-PC-SAFT

Source: Adapted from Chapman et al. (1989); Perdomo; Villegas (2010); Haley; Cabe (2015); Perdomo et al. (2014); Llovelll; Veja (2015); Gross; Sadowski (2001); Mohammad et al. (2016); Auger et al. (2016); Ahmed et al. (2017); Klajmon et al.(2015); Hemptinne et al. (2011,2014).

It is also highlighted other proposals that tried to reconcile the statistical theory with other methods previously discussed. Two of them stood out in this review: the CPA and GCA equations.

The Cubic Plus Association (CPA) model was proposed by Kontogeorgis et al. (1996) and is based on the combination of a cubic EoS, the original proposal used Soave Redlich Kwong equation, as a physical term with the association term of the SAFT theory, presented in Eq.60. The final equation obtained is presented in Eq.64:

$$P = \frac{RT}{v-b} - \frac{a}{v.(v+b)} + \frac{RT}{v}\rho\sum_{A}\left[\frac{1}{X^A} - \frac{1}{2}\right]\frac{\partial X^A}{\partial \rho} \tag{64}$$

The Group Contribution with Association (GCA) model, in turn, is the first EoS of the SAFT family that uses a GC approach of the Wertheim model. This method was proposed by Gros et al. (1996) and presents three contributions to the residual Helmholtz energy: free volume (a^{fv}), attraction (a^{att}), and association (a^{assoc}).

$$\frac{A^R(T,V,n)}{RT} = a^{fv} + a^{att} + a^{assoc} \tag{65}$$

Where the free volume and attractive contributions are based on Carnahan-Starling and Non Random Two Liquids (NRTL) models, respectively, maintaining the same formulation as in the original GC-EoS proposed by Skjold-Jørgensen (1988).

$$\frac{a^{fv}}{RT} = 3\frac{\lambda_1\lambda_2}{\lambda_3}(Y-1) + \frac{\lambda_2^3}{\lambda_3^2}(Y^2 - Y - \ln(Y)) + n.ln(Y) \tag{66}$$

With $Y = \left(1 - \frac{\pi\lambda_3}{6V}\right)^{-1}$ and $\lambda_k = \sum_j^{NC} n_j d_j^k$.

$$\frac{a^{att}}{RT} = -\frac{\left(\frac{Z}{2}\right)\left(\sum_i^{NC}\sum_j^{NG} n_i v_{ij} q_j\right)^2 . \sum_j^{NG}\theta_j \sum_k^{NG}\frac{\theta_k \tau_{kj} g_{kj}}{\sum_l^{NC}\theta_l \tau_{lj}}}{RTV} \tag{67}$$

Last, the associating term is given by a group contribution version of the SAFT associating parameter, differing from Eq.60 only in the calculation of the total number of moles, since here this term is weighted by the number of association groups present in the molecule (GONZÁLEZ PRIETO et al.,2015).

3.2.2.2 Molecular Simulations

Molecular simulations have become an important area, especially for the condensed phase, since the thermophysical properties can be derived in a single theoretical framework. These methods consider small size systems, on a typical scale of a few nanometers, and determine their behavior by carefully calculating the interactions between their components (UNGERER et al., 2007). Due to the fact that each molecule interacts with several surrounding ones, this description is a very difficult task, requiring a large set, typically at least several hundred molecules, to be considered a good representation of the system (ECKERT; KLAMT, 2002).

Different statistical ensembles can be used in these simulations, each of them characterized by the constrained variables and by its probability density (Table 3). For a given problem, the selection of the ensemble is made in such a way that the constraints correspond to variables that are controlled in the experimental set-up. The variables that are not constrained are fluctuating, and their statistical averages provide predictions that may be compared with experimental results. The ensemble which is the most widely used for phase equilibrium calculations is the Gibbs ensemble, in which two phases are introduced without an explicit interface, imposing the global volume of the two phases, or the pressure, the temperature, and the total number of molecules as constrained (PANAGIOTOPOULOS, 1992; UNGERER et al., 2007).

Table 3 – Statistical ensembles and their main applications.

Statistical ensemble	Imposed variables	Variable optimized	Applications
Canonical ensemble	N,V,T	A	Phase properties
Microcanonical ensemble	N,V,E	S	Phase properties
Grand canonical ensemble	μ,V,T	Ω	Adsorption isotherms
Isothermal-isobaric ensemble	N,P,T	G	Phase properties
Gibbs ensemble	N,V,T N,P,T	G	Phase equilibrium

Source: Adapted from Urgerer et al. (2007); Chapman (2020).

There are two methods most widely used to simulate these statistical ensembles, both of which use force fields to describe the intra and intermolecular interactions. The first is molecular dynamics (MD), which consists of integrating Newton's equations of motion over time for all particles, and the second is Monte Carlo

(MC) simulation, in which a statistical method is used to generate representative system configurations based on the probability distribution of potential energy (Figure 9) (PANAGIOTOPOULOS, 1992).

These simulations are highly parameterized, having the ability to model the different types of interactions that atoms of interest can have with geometric and molecular details. However, as these calculations scale with the number of atoms considered, now and in the near future, these simulations are very time-consuming, ranging from a few hours to several weeks, even on the fastest computers. Nevertheless, these results are still restricted by the fundamental approximation, and the appropriate treatment of some interactions (ECKERT; KLAMT, 2002; UNGERER et al., 2007).

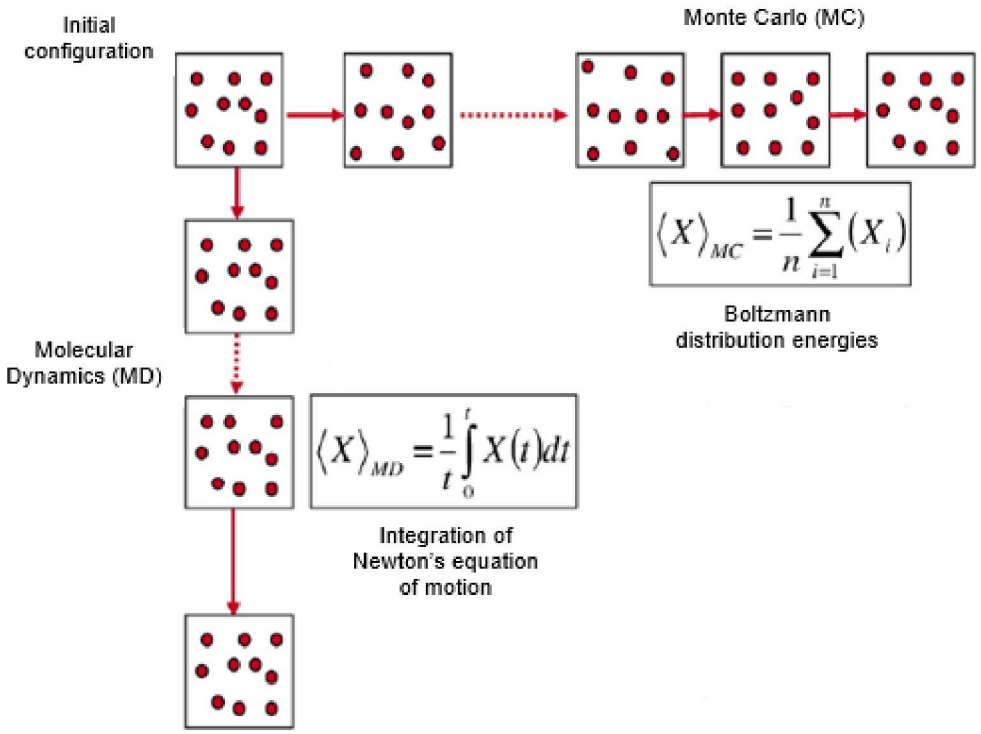

Figure 9 - The two ways of simulating a statistical ensemble: Molecular dynamics (MD) and Monte Carlo (MC). Both averages are equivalent due to the Ergodic hypothesis.
Source: Adapted from Ungerer et al. (2007).

3.2.3 Quantum Chemistry

3.2.3.1 COSMO-RS

Andreas Klamt proposed a completely different point of view, with a new model based on molecular quantum chemistry calculations, which, combined with exact

statistical thermodynamics, provides the necessary information for the evaluation of molecular interactions in the condensed phase, being independent of experimental data and generally applicable. The energy expression used in this case, in contrast to the force field expressions of molecular simulations, does not depend on the 3D geometry of the molecules but is reduced to the relatively much simpler statistical thermodynamics of independent pair-wise interacting surface (ECKERT; KLAMT, 2002; KLAMT, 1995; KLAMT et al., 2010).

For that, Klamt started from the modification that he proposed together with Schürmann (1993) for the dielectric continuum solvation model (CSM). CSM is an extension of the basic quantum methods for isolated molecules at a temperature of 0 K, which focuses mainly on the representation of a molecule or a small cluster of the solute with some solvent molecules, representing the influence of the rest of the solvent by a continuum surrounding them, defined as the dielectric continuum. The contribution proposed then by the aforementioned authors consists of replacing the dielectric with a much simpler conductor parameterized on the solvation energies of organic compounds, mostly water. This new method is known as the Conductor-like Screening Model (COSMO) (ECKERT; KLAMT, 2002; KLAMT, 1995; KLAMT et al., 2010).

In COSMO quantum calculations, the solute is treated as if it is embedded in a virtual conductor, generating a discrete molecular surface or "cavity" around the molecule. From this surface, each discrete segment is characterized by its area and the screening charge density. Klamt et al. (2010) described these calculations in eight steps, which can be summarized by the vanishing of the total electrostatic potential and the polarization charges on the entire surface, the analytical calculation of the gradient of the total QC/COSMO energy, and the geometry of the molecule towards the lowest energy in an iterated way until self-consistency. As result, this algorithm yields the energy, the electron and polarization charge densities, and the geometry of the molecule in a virtual conductor, called "the COSMO state". All this relevant information is stored in a COSMO file, available in several quantum chemical software.

In 1995, Klamt combined the COSMO model with statistical thermodynamics, which is called the Conductor-like Screening Model for Realistic Solvation (COSMO-RS). In this way, starting from a conductor in which each molecule has its COSMO information, it is possible to approximate the condensed phase as an ensemble of closely packed ideally screened molecules, as shown in Figure 10 (ECKERT; KLAMT, 2002; KLAMT, 1995; KLAMT et al., 2010).

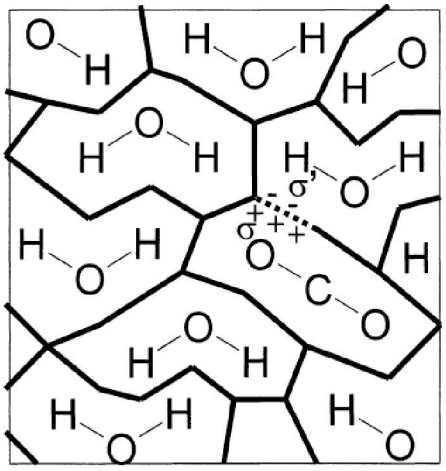

Figure 10 - COSMO-RS view of surface-contact interactions of molecular cavities.
Source: Eckert; Klamt (2002).

Thus, the link between microscopic surface-interaction energies and macroscopic thermodynamic properties is provided by the average of all possible configurations of the ensemble, obtained by statistical thermodynamic calculations.

The chemical potential of a surface segment, for example, is exactly determined by the integration over all potential partners in the mixture (Eq.69) (ECKERT; KLAMT, 2002; KLAMT, 1995; KLAMT et al., 2010). Larsen and Rasmussen (1986) published later an algorithm show that this expression is equivalent to the exact solution of a quasi-chemical lattice approach.

$$\mu_s(\sigma) = -\frac{kT}{a_{eff}} ln \int p_s(\sigma) exp\left\{-\frac{a_{eff}}{kT}(e_{int}(\sigma,\sigma') - \mu_s(\sigma'))\right\} d\sigma \qquad (68)$$

Where $\mu_s(\sigma)$ is the chemical potential per surface area, $p_s(\sigma)$ is the solvent σ-profile, that in simple words, is a characteristic function that specifies how much the solvent or mixture is attracted to a surface area of polarity σ, a_{eff} is the effective contact area, and e_{int} is the interaction operator, which gives the energetic costs of making a contact between $\sigma - \sigma'$. Equation 69 is an implicit equation and must be solved iteratively.

Individual σ-profiles of molecules, in turn, are given as probability distributions. In this way, it is possible to derive a probability function as a histogram of the molecular COSMO surface with respect to the polarization charge density σ, using a Gaussian weight of width contact radius (ECKERT; KLAMT, 2002; KLAMT, 1995; KLAMT et al., 2010). An example of the molecule σ-profile is shown in Figure 11.

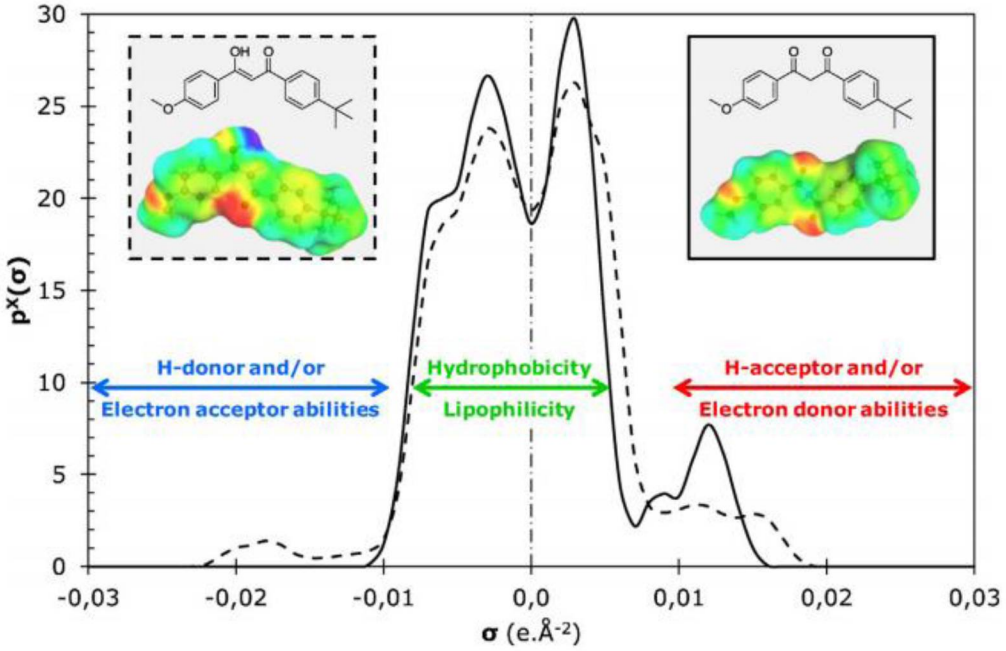

Figure 11 – Representation of σ-profile of avobenzone in ketone form (solid line) and enol form (dashed line).

Source: Benazzouz et al. (2014).

The color-coding of COSMO is established as blue stands for a strongly negative, green for neutral, and red for strongly positive polarization charge density (σ) of the surface area. The signals are inversely related to the polarization charge density and the molecular polarity of the molecule since the conductor compensates this with opposite charge density (ECKERT; KLAMT, 2002; KLAMT, 1995; KLAMT et al., 2010).

3.2.3.2 COSMO-SAC

Lin and Sandler (2002) suggested a variation of COSMO-RS by the called COSMO-SAC, where SAC denotes Segment Activity Coefficient. Both models share similarities in the calculations, being the main difference the expression used for accounting the σ profiles in properties determination. In COSMO-SAC the restoring free energy for a specie "i" in the solvent is obtained from:

$$\frac{\Delta G_i^{res}}{RT} = n \sum_{\sigma_m} p(\sigma_m) ln\Gamma_{solvent}(\sigma_m) \tag{69}$$

Where n is the total number of segments in the mixture, and $\Gamma_{solvent}(\sigma_m)$ is the activity coefficient for segment σ_m given by:

$$ln\Gamma_{solvent}(\sigma_m) = -ln\left\{\sum_{\sigma_n} p(\sigma_n)\Gamma_{solvent}(\sigma_n)exp\left[\frac{-\Delta W(\sigma_m,\sigma_n)}{RT}\right]\right\} \quad (70)$$

Here, the segment exchange energy (ΔW) is obtained as a function of the permittivity of a vacuum (ϵ_0):

$$\Delta W(\sigma_m,\sigma_n) = f_{pol}\left(\frac{0.3a_{eff}^{3/2}}{2\epsilon_0}\right)(\sigma_m+\sigma_n)^2 \quad (71)$$

Finally, the factor f_{pol} is defined as a function of permittivity (ϵ):

$$f_{pol} = 1 - f(\epsilon) \quad (72)$$

The most advantage of COSMO-SAC to the previous model is the satisfaction of the thermodynamic consistency relations (Gibbs−Duhem). Besides that, in the COSMO-RS model not all calculation details are published, which makes it impossible for others to independently test and develop this method (FINGERHUT et al., 2017).

COSMO-based models are promising candidates to address the scarcity of phase equilibrium data, due to their strictly predictive character. However, these methods are still under development and the lack of parameters makes them not yet as accurate as group contribution methods. Nonetheless, efforts have been made to improve their accuracy for different types of fluid and mixtures, such as COSMO-RS (Ol), COSMO-vac, or COSMO-3D (FINGERHUT et al., 2017).

3.2.4 Summary of Content

In the previous sections, the development of thermodynamic modeling overtime was presented. It was tried to concisely show the premises of each method, as well as to highlight the origins of their limitations. Still, an effort was made to point out how the next model tried to overcome previous problems and what differs it from the others. With the intention of recapitulating this construction, Figure 12 indicates the evolution of thermodynamic models in a timeline.

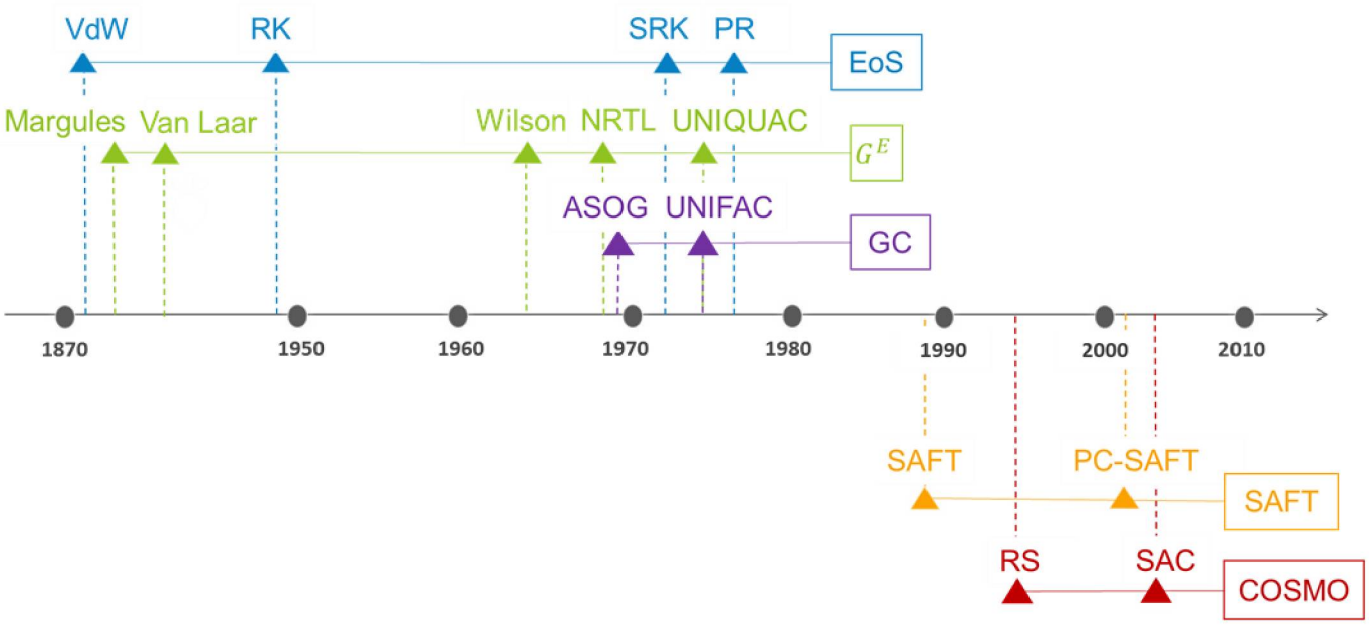

Figure 12 - Evolution of thermodynamic models over the years. Classical models are above, while statistical models (yellow), and quantum chemistry models (red) are below the timeline.
Source: Author's figure (2020).

Table 4 also summarizes the main application areas and problems currently faced by each class of thermodynamic models.

Table 4 – Class of thermodynamic models discussed in this work with their main applications and problems founded in theirs areas.

	Model	Applications	Problem
Classical	Equation of State	Gas processing, Petrochemicals VLE, Process close or above critical conditions	Data, Parameters, Liquids density
	G^E	Petrochemical LLE, Non ideal solutions	Data, Parameters, VLLE, multicomponent systems
	Group Contribution	When there is no data available	Data, Isomers, Chiral compounds
Statistical	SAFT	Associate compounds, Hydrogen bonds	Data, Parameters, Critical conditions
	PC-SAFT	Associate compounds, Polar systems, Polymers; Pharmaceutics	
Quantum	COSMO	Complex molecules	Computational effort for molecules out of database, Still in development

Source: Adapted from Chen; Mathias (2002); Von Solms et al. (2006); Klamt et al. (2010).

4 PROBLEM STATEMENT

Heretofore, this work has presented the reasons why biorefineries have become a topic of great importance nowadays and how their development is fundamental to the sustainable development of society. Among the challenges encountered in advancing these systems, this work then focused on those related to the thermodynamic modeling of these diverse systems, more specifically phase equilibria modeling. This stems from the fact that equilibrium properties and an understanding of why and how interactions between different phases occur are essential requirements for the design of separation operations, which are, in a typical large-scale chemical plant, about 50% of total investment (SANDLER et al., 2006). Thereby, the main challenge of this work is to answer the question:

"Which is the best thermodynamic model for phase equilibria modeling of biorefinery-related systems?"

In this way, it was essential to understand the conceptual differences between the thermodynamic models, and how the diversity of the systems of interest can interfere in the performance of each one of them. To this end, a large number of works on phase equilibria modeling in systems found in biorefineries were categorized and analyzed. This was accomplished through the scientific method of systematizing information, PRISMA, with the purpose of establishing if there is a thermodynamic model that best represents mostly, if not all, of these systems.

5 METHODOLOGY

5.1 PRISMA STATEMENT

The Preferred Reporting Items for Systematic reviews and Meta-Analyses (PRISMA) was established in Ottawa, Canada, in June 2005. The guidelines of this statement were defined after an executive committee, contend 29 participants, including review authors, methodologists, and clinicians, examine the quality of systematic reviews in an extensive literature search to identify methodological papers (LIBERATI et al., 2009).

The PRISMA directive aims to assist authors in improving their technical reports, reducing the excessive number of reviews that address the same question, and providing greater transparency on systematic reviews formulation. In addition, the committee reviewed and expanded the checklist and the flow diagram used as a basis for systematic studies (LIBERATI et al., 2009). As a result, a flowchart with the following four steps makes up this methodology:

i. Identification: definition of the main problem and keywords to be used in literature search, as well as the database and information sources to be explored in this search;
ii. Screening: first selection among the results obtained in the identification stage, evaluating possibly useful studies, duplicate papers, inaccessible links;
iii. Eligibility: criteria used to refine the research, as years considered, language, publication status;
iii. Included: categorization of the studies selected, organizing them in analysis "blocks". It is an important highlight that the number of included articles might be smaller or larger than the number of studies, because articles may report on multiple studies, and results from a particular study may be published in several articles.

The final version of the checklist, in turn, has 27 items. Both tools, as well as other supporting information can be found for download on the PRIMAS website (http://www.prisma-statement.org/).

5.2 PRISMA APPLICATION

The PRISMA methodology described in the previous section was applied in the elaboration of the systematic review carried out in this work, in order to synthesize the phase equilibria modeling of greatest interest systems to biorefineries.

The researched literature was obtained by the search engine Google Scholar, which includes major scientific publishers (Elsevier/ScienceDirect, Emerald, SpringerLink, and Wiley), and also studies that were not published in journals. For that, initially, the search keywords were defined as the two groups: ‘‘biorefinery + phase equilibria” and “biofuels + phase equilibria”. This definition was the most difficult step in the review procedure, as it should be comprehensive enough to generate reliable results, while it should apply rigorous screening criteria so that the analysis sticks to the main problem. The second group was added, due to the fact that the initial efforts and most of the studies related to biorefineries still have as main objective the substitution of fossil fuels for biodiesel. Thus, many works in this research area place greater emphasis on biofuels than on biorefineries themselves.

Then, a practical screening was carried out on the set of selected studies, based on information derived from titles and abstracts. This procedure was realized several times between May and December 2020, to ensure certainty of the numbers and to include possible works published during the construction of this thesis. The search words yielded 3082 studies, excluding patents, citations, doctoral and master’s theses, and defining publications from 2010 or later as a period of interest, aiming to work with recent information. Besides that, only papers in English were considered for this analysis, to make this review replicable for readers.

In the second step, the screening criteria were applied to the full texts. Thus, were identified studies that did not meet the inclusion criteria, as systems were not related to biorefineries, studies did not have a modeling procedure, or because the model was used to obtained other thermodynamic information such as solubility, chemical kinetics, or volumetric properties. Also, in order to facilitate the comparison carried out in section 6.2, and also for that the selection of papers could be performed more quickly, it was only included studies where the phase equilibria were presented in a graphic format, such as *Txy, Pxy*, tie-lines or binodal curves.

The data obtained in the last search was considered for the analysis in the next section since it presented the largest number of papers included among all

searches performed. These numbers are presented in detail in Figure 13. PRISMA 27 items-checklist, in turn, can be found in Appendix 2.

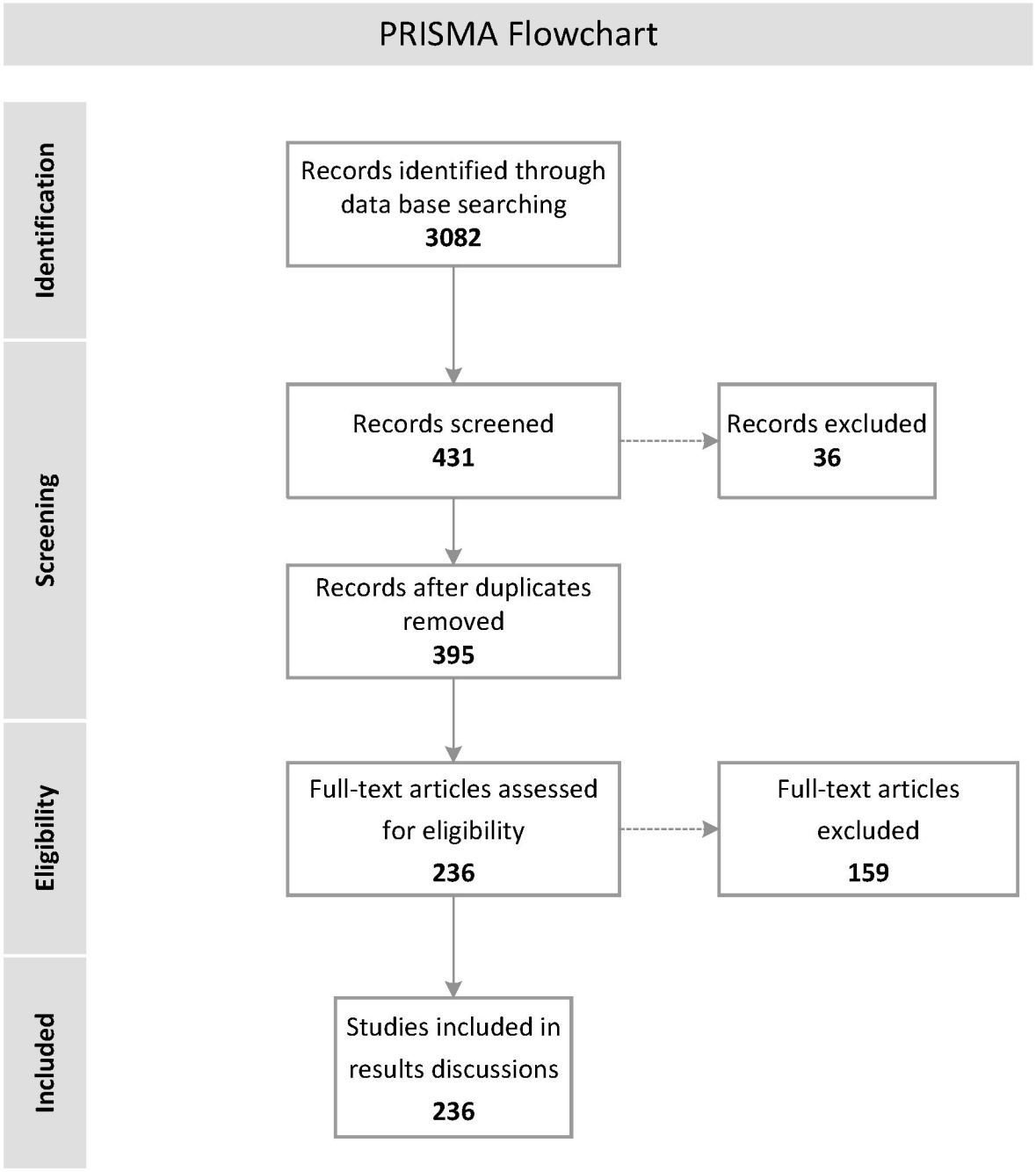

Figure 13 – Flowchart of the application of the PRISMA statement and the results obtained in this work in each of the four steps of the method.
Source: Adapted from Liberati et al. (2020).

With this well-established database, it was possible to categorize these works into general results and compare them, as discussed in the next section.

6 RESULTS AND DISCUSSION

6.1 GENERAL VIEWS

As the first step for general results, the number of publications per year within the determined period was analyzed (Figure 14). As expected, it was observed that the absolute number of publications increased over the years, in line with the growing interest in the processes and products offered by biorefineries. In comparison, 2019 presented, for example, a growth of 13.5% in the number of publications related to the theme in relation to 2018. When this comparison is made between 2019 and the initial year of the review, 2010, this growth is even more expressive, reaching 366.7%. It is also noted that almost half of the total number (48.3%) of publications included in this review were published in the last three years (2017-2020). Notably 2020 is no longer the rule, due to the current pandemic that has strongly affected the conduct of experimental research.

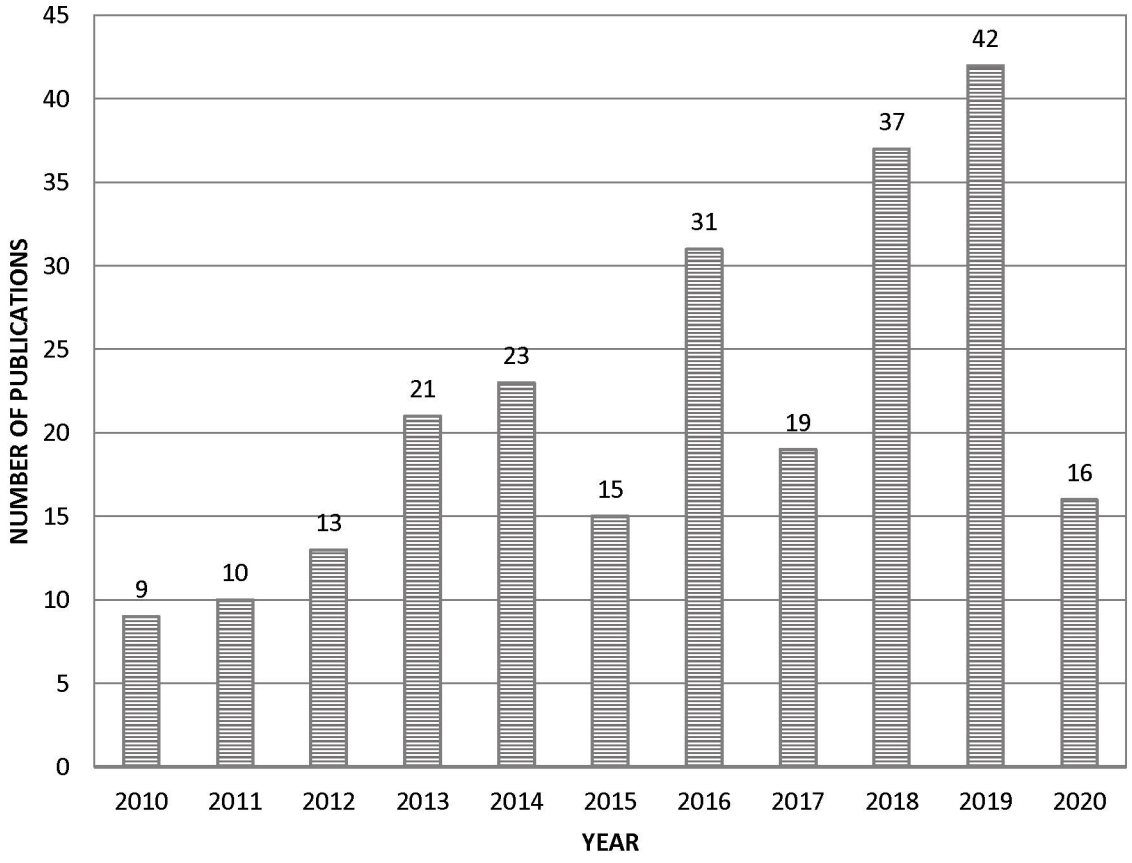

Figure 14 – Absolut number of publication per years of the studies reviewed in this work.
Source: Author's figure (2020).

The relation between the articles under study and their countries of origin was established. It is important to note that it is common in the scientific community that a single article has contributions from more than one country, which is why the number of mentions presented is greater than the absolute number of articles reviewed. In total, 41 countries were included in this work. Figure 15 shows those with at least 5 collaborations published, in descending order.

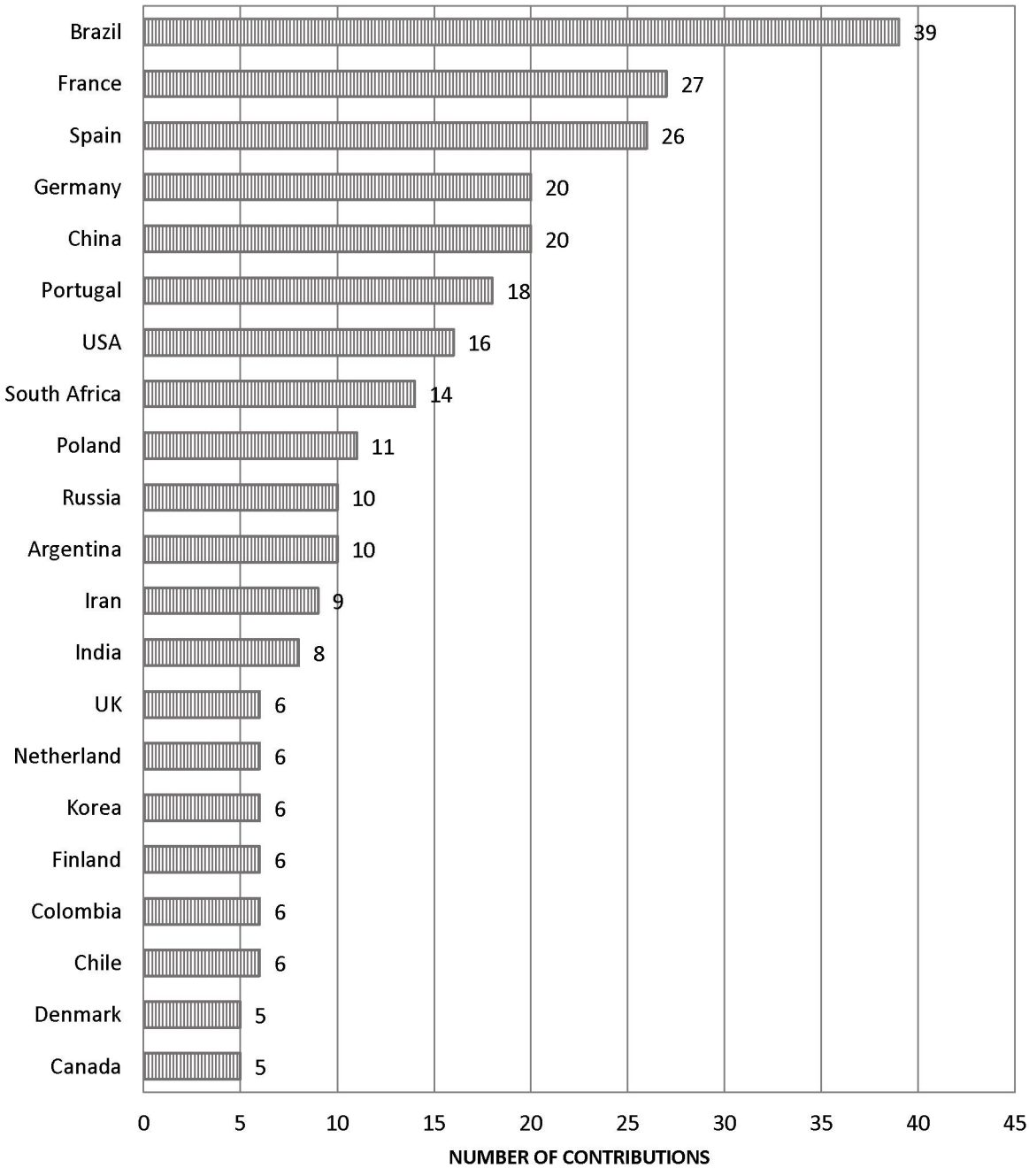

Figure 15 – Number of mentions of each country included in this systematic review.
Source: Author's figure (2020).

The largest contributor country to publications included in this systematic review was Brazil. This data is in agreement with the fact that this country currently has 44.7% of its energy production based on renewable resources, occupying the second position in the world ranking of bioethanol and biodiesel production (BRANCO, 2014). Of the 39 mentions, it can be highlighted the group of Professor Eduardo Augusto Caldas Batista, at the University of Campinas (UNICAMP), as the biggest contributor, since his research associate Antonio José de Almeida Meirelles was mentioned in 10 works. Then, the research group Applied Thermodynamics and Kinetics (LACTA), at the Federal University of Paraná (UFPR), leaded by Prof. Marcos L. Corazza contributed with 7 other works of the review. In addition, the group of Professor Marcos L. Corazza also stands out for being the only Brazilian group that uses a different approach to model the phase equilibria, the PC-SAFT model. In general, Brazilian groups applying classical thermodynamic models for this modeling.

During the catalog by collaborating country, it was observed a trend that countries with a large territorial area, such as Brazil (1st), China (5th), and USA (7th) received these mentions from different research groups, generating a greater variety of models and systems of study. Whereas, smaller countries tend to concentrate their publications in the same group for the same interest, be it the evaluation of a specific model or a certain system. In this way, it was possible to highlight the research groups with the largest number of publications, as can be seen in Table 5:

Table 5 – Research groups with greater number of contributions in a specific topic as model or system of interest in this systematic review.

Country	Group	Contributions	Interest	Model
Spain	TermoCal – Universidad de Valladolid	7	Alkanes mixtures	G^E
France	IFP Energies Nouvelles	7	Hydrocarbons mixtures	GC-PPC-SAFT
Argentina	PLAPIQUI - Universidad Nacional del Sur	9	Diverse	GCA
Portugal	CICECO – Universidade de Aveiro	13	Diverse	Mostly CPA
Germany	Technische Universität Dortmund	9	DES and Ionic Liquids	PC-SAFT
Poland	Politechnika Warszawska	9	Ionic Liquids	NRTL, PC-SAFT

Source: Author's table (2020).

As for the compounds, more than 50 substances were mentioned in this work. This great diversity, although already expected, made any attempt of categorization difficult. The best way found to represent this result was through the list of the main chemical classes considering those that received more than 10 mentions (Figure 16).

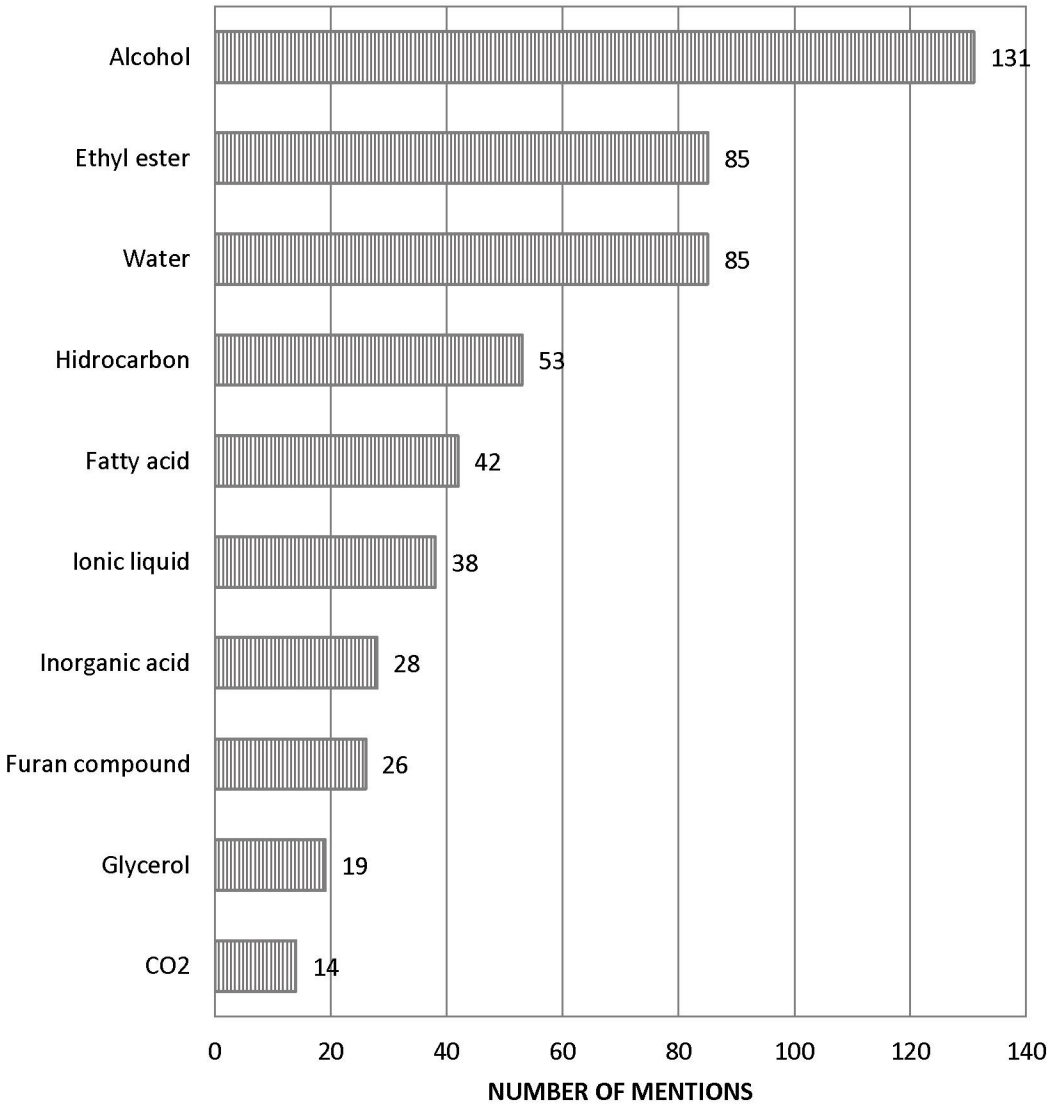

Figure 16 - Chemical classes or compounds with specific interest that received more than 10 mentions in this systematic review.

Source: Author's figure (2020).

In the alcohol class, the substance mentioned more often was ethanol (59). From the graph it can also be seen that 6 out of 10 results are directly related to the production of biodiesel since this biofuel is obtained through esterification/transesterification of a fatty acid with an alcohol, usually, methanol or ethanol, giving rise to a mixture of esters and glycerol (KNOTHE et al., 2006).

Regarding the phase equilibria, in turn, four types of equilibrium were found among the studies: vapor-liquid (VLE), vapor-liquid-liquid (VLLE), liquid-liquid (LLE), and solid-liquid (SLE). Figure 17 shows the number of articles that included in their studies the equilibria mentioned in absolute number and percentage. Once again, it is highlighted that the number of mentions is greater than the number of articles reviewed because a single article can verify more than one type of equilibrium.

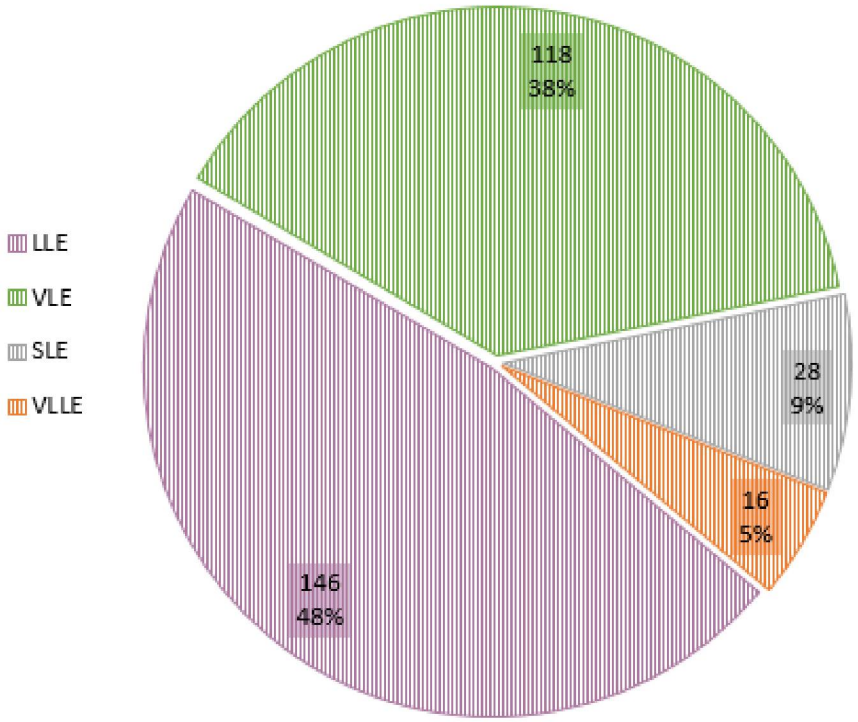

Figure 17 - Number of mentions of each type of phase equilibria founded in this review in absolute number and percentage.

Source: Author's figure (2020).

The analyses of Figure 17 shows that almost half of the works (48%) focused on the study of liquid-liquid equilibrium. This can be related to the fact that the main focus of studies on biorefining continues to be in the development of biofuels, which, in turn, are produced and processes from liquid mixtures. Besides that, LLE measurements are obtained in a relatively simpler way, using few equipment, material and experiments that can be conducted in ambient conditions, while VLE and SLE need greater attention with the pressure and decomposing of the substances under study. Then, the large number of studies related to the vapor-liquid equilibrium (38%) can be associated with the need of binary parameters in classical thermodynamic models, which are usually obtained through VLE experiments. Finally, it is worth

mentioning the small number of studies on SLE (28%) and VLLE (5%), which are quite complex to be carried out in experimental procedures.

The greatest impact assessment for this work, however, is the thermodynamic models applied in the works included in this review. In total, 36 different modeling methods were mentioned, which were categorized in Figure 18 in the three major division groups previously explained. Again, the number of mentions is greater than the absolute number of works evaluated, because hardly an article contemplates only one thermodynamic model.

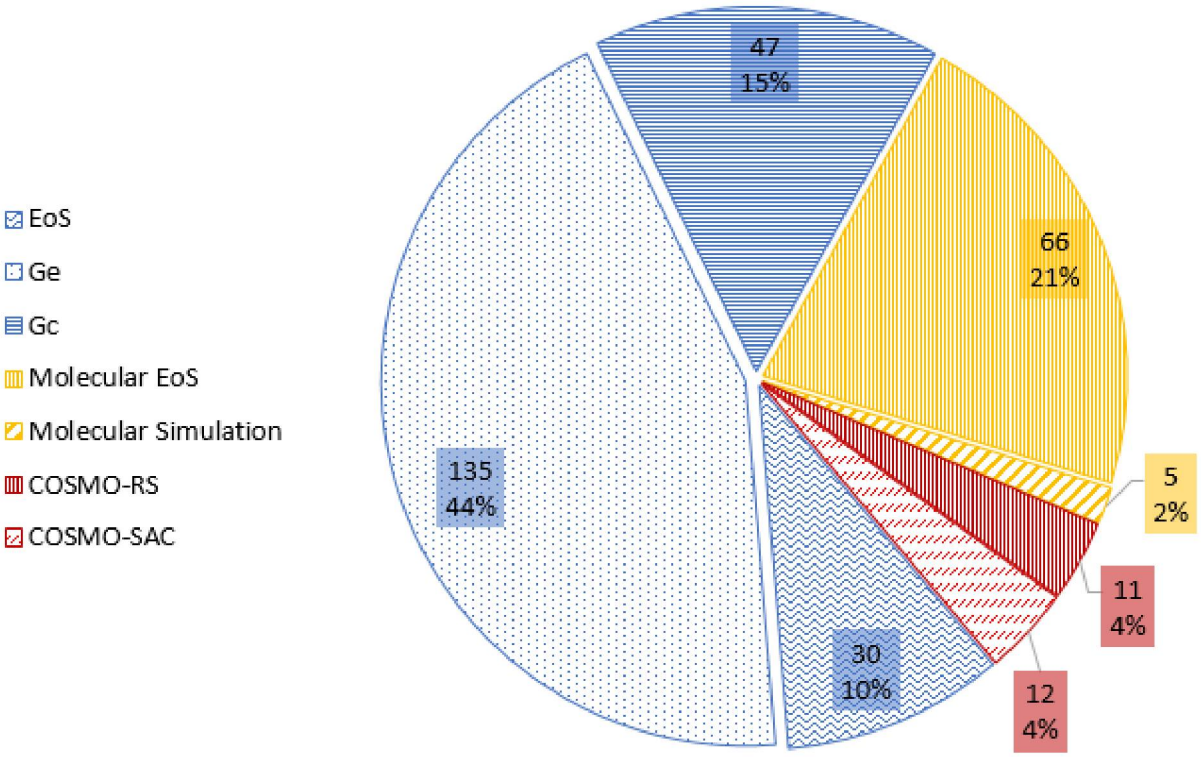

Figure 18 - Number of mentions of each class of thermodynamic modeling included in this review in absolute number and percentage. Classical models are in blue, statistical models in yellow, and quantum chemistry models in red.

Source: Author's figure (2020).

Analyzing the results obtained, the preference for classical methods (almost 70%) is remarkable. It is still evident the more specific predilection for the G^E models (44%). Here, it is valid to state that, within the various possible G^E equations, the method that obtained the greatest number of mentions was the NRTL (110), followed by UNIQUAC (71). Figure 19 and Figure 20, which allows the visualization of the types of equilibria and models over the years, can complement these last results.

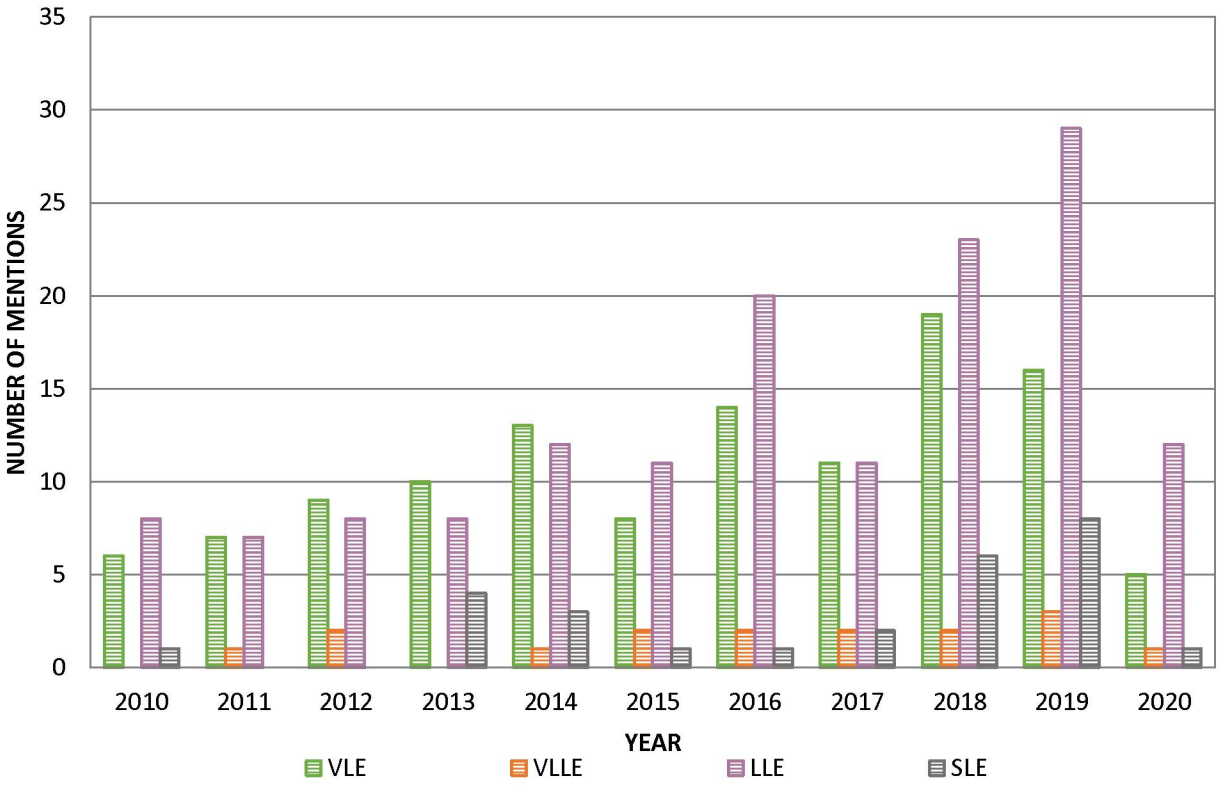

Figure 19 – Absolute number of mentions of each type of phase equilibria over the years.
Source: Author's figure (2020).

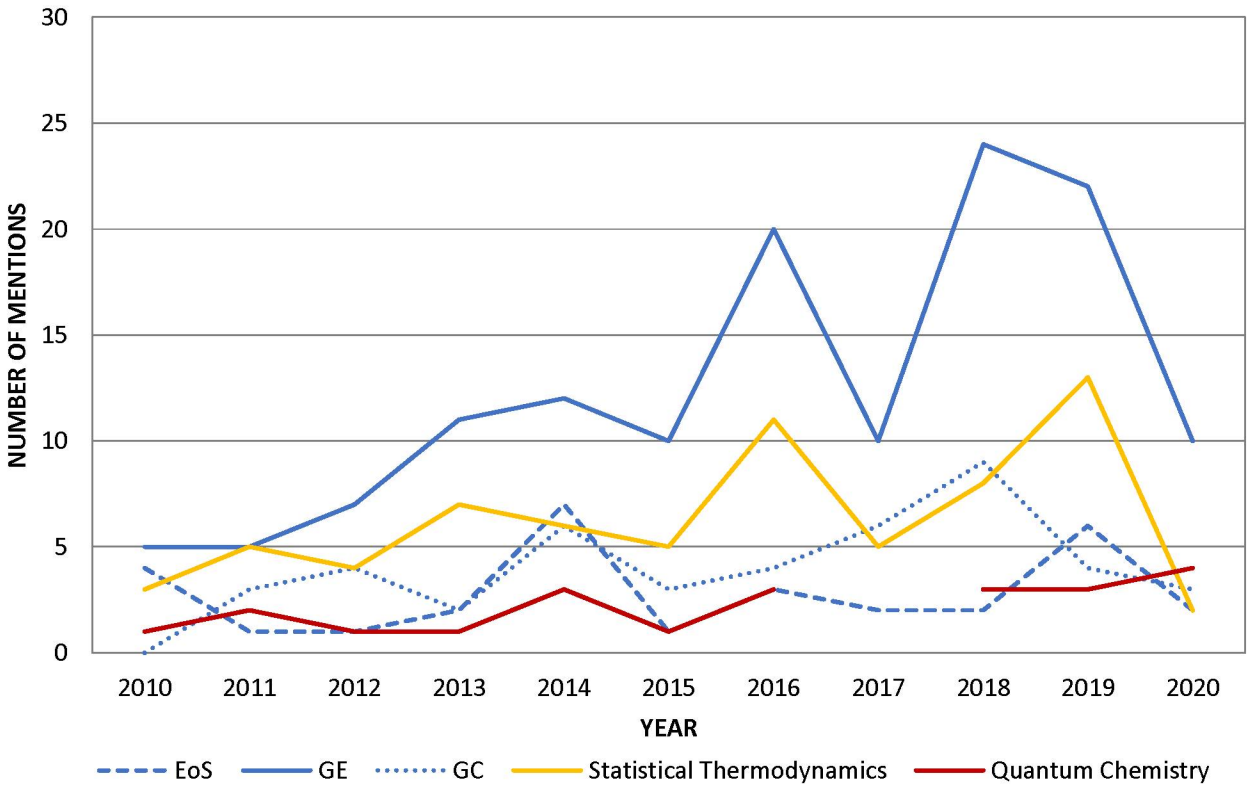

Figure 20 - Absolute number of mentions of each type of thermodynamic modeling over the years.
Source: Author's figure (2020).

In this new form of visualization, it is possible to observe some new information, which was not shown in the pie charts. For instance, despite the relatively low number of studies related to the solid-liquid equilibrium, the interest in this type of phenomenon has been increasing over the years (1 in 2010, and 8 in 2019). This observation is in agreement with the fact that, although biofuels are still the main focus, other areas of the biorefineries sector have received more attention. The reuse of waste and the use of lignocellulose materials, for example, demand greater interest in processes such as solid-liquid extraction, which depends on data from SLE.

Another important conclusion that can be interpreted from Figure 20 is the increase in the use of statistical models over the years (3 in 2010, and 13 in 2019). This data, in turn, can be related to the computational improvement of recent years, which makes more complex mathematical programming less painful, but also to the fact that new matrices and processes are been explored. In this context, the growing interest in phenomena with the solid phase, multiphase processes, oxygen compounds with association, and substances in which hydrogen bonds play a significant role, as the deep eutectic solvents, encourage the use of more robust models.

Lastly, Table 6 was constructed as an overview of the systematic review carried out in this work. At first, it was listed all thermodynamic modeling methods mentioned in the review. These models followed, once again, the division into the three main groups of this work: classical, statistical, and quantum chemistry. Subsequently, it was evaluated in what types of phase equilibria each model was applied. The third category related the model according to the generation of the system under study previously defined in Table 1 and summarized as: harvest from forest or agricultural fields as 1^{st}, residual raw materials with cellulose as 2^{nd}, microalgae as 3^{rd}, and human or industrial waste and use of green solvents as 4^{th} generation . Then, it was measured how many of the reviewed studies applied the model in question and, finally, these studies were listed as references.

Table 6 – Overview of the studies included in this systematic review.

	Model	Phase Equilibria			Generation Biorefinery Systems				Mentions	References
		VLE	*LLE*	*SLE*	*1st*	*2nd*	*3rd*	*4th*		
Classical Thermodynamics	*Equations of State*									
	PR	✓	✓			✓		✓	9	[1]–[9]
	PPR78	✓				✓		✓	3	[10]–[12]
	RK	✓	✓			✓		✓	4	[13]–[16]
	SRK	✓	✓			✓		✓	12	[1], [5], [17]–[26]
	PSRK	✓	✓			✓			5	[18], [20], [24], [27], [28]
	Virial	✓				✓			1	[29]
	WS	✓	✓			✓			1	[21]
	Excess Gibbs free energy									
	Flory-Huggins			✓		✓		✓	5	[30]–[34]
	NRTL	✓	✓	✓	✓	✓	✓	✓	110	[1], [3], [13], [18], [23], [29], [34]–[136] [137], [138]
	eNRTL	✓						✓	3	[14], [18], [60]
	NRTL-HOC	✓	✓		✓	✓			5	[108], [139]–[142]
	Margules	✓				✓			6	[36], [43], [47], [133]–[135]
	UNIQUAC	✓	✓	✓	✓	✓	✓	✓	71	[3], [4], [18], [23], [27]–[29], [34], [36], [37], [39], [40], [42], [44]–[47], [49], [51], [52], [54], [58]–[60], [63], [64], [66]–[72], [76]–[79], [84], [86]–[88], [90], [96], [98], [101], [106], [107], [109]–[111], [116], [117], [122], [125], [129], [130], [132]–[135], [138], [143]–[152]
	UNIQUAC-HOC		✓					✓	2	[141], [153]
	Wilson	✓	✓		✓	✓			19	[3], [36], [37], [39], [42]–[44], [47], [59], [64]–[66], [68], [105], [133]–[135], [154], [155]
	Group Contribution									
	ASOG	✓	✓			✓			1	[156]
	UNIFAC	✓	✓	✓	✓	✓		✓	37	[2] [4], [18], [21], [39], [55], [65], [67], [71], [73], [75], [76], [80], [82], [85], [94], [98], [102], [111], [136], [142]–[144], [157]–[170]

	UNIFAC-Dortmund	✓	✓	✓	✓	✓	✓	10	[30], [31], [57], [68], [112], [155], [167], [171]–[173]
Statistical Thermodynamics	SAFT	✓					✓	1	[174]
	SAFT-VR	✓	✓			✓		1	[175]
	GC-SAFT-VR	✓				✓		1	[176]
	SAFT-MIE	✓				✓		1	[177]
	soft-SAFT	✓	✓			✓	✓	2	[178], [179]
	PC-SAFT	✓	✓	✓		✓	✓	23	[15], [20], [24], [74], [120], [136], [143], [173], [180]–[194]
	ePC-SAFT	✓	✓				✓	4	[195]–[198]
	GC-PC-SAFT	✓	✓				✓	1	[166]
	PPC-SAFT	✓	✓	✓		✓		6	[59], [194], [199]–[202]
	ePPC-SAFT	✓					✓	1	[203]
	PCIP-SAFT		✓				✓	1	[56]
	GC-PPC-SAFT	✓	✓	✓		✓	✓	8	[53], [192], [201], [204]–[208]
	GCA	✓	✓	✓		✓	✓	10	[21], [209]–[217]
	CPA	✓	✓			✓	✓	12	[18], [21], [22], [112], [166], [194], [218]–[223]
	PHSC	✓	✓	✓		✓		1	[224]
	Monte Carlo	✓	✓			✓	✓	5	[225]–[229]
Quantum Chemistry	COSMO-RS	✓	✓	✓			✓	12	[61], [68], [121], [158], [192], [198], [230]–[235]
	COSMO-SAC	✓	✓				✓	11	[18], [21], [48], [52], [61], [72], [97], [158], [169], [192], [236]

Source: Author's table (2020).

6.2 PHASE EQUILIBRIA

The best thermodynamic model was determined by comparing the results presented by the different methods under the same process conditions. For this purpose, the studies were initially filtered by type of equilibrium, as in Figure 17. In this step, however, it was observed that, for the vapor-liquid-liquid and solid-liquid equilibrium, the number of papers was relatively small. Thus, in these cases, the comparison could be made directly.

For the vapor-liquid-liquid category it was found 16 papers. Just two of these reviewed articles used Equations of State for modeling procedure. In the first of them, Pinto et al. (2012) applied the Peng Robinson correlation for binary and ternary mixtures containing CO_2, methanol, and soybean methyl esters. This model choice is in agreement with the theory previously discussed, since these systems were evaluated at high pressures (above 210 bar), region where EoSs demonstrate the best results. Besides that, classical van der Waals (PR-vdW2) and Wong-Sandler (PR–WS) mixing rules were investigated, having the PR–WS the best performance with an average RMSD of 0.42 for binary, and 0.38 for ternary systems. The other study was conducted by Zheng et al. (2019), which selected the Soave−Redlich−Kwong EoS with the modified Huron−Vidal second-order mixing rule (SRK/MHV2) and the predictive SRK (PSRK) EoS, for the comparison with the PC-SAFT performance in VLE, LLE, and VLLE modeling related to Fischer−Tropsch synthesis (FTS). In this paper, PC-SAFT with a single set of parameters was capable of accurately modeling the phase equilibria for complex mixtures over a wide range of temperatures at ambient pressure, whereas the other two methods performed well for some cases, but delivered poor results for some others. These observations are also in agreement with theory, since cubic EoSs are inaccurate in the prediction of vapor pressures, the most decisive factor in VLE calculations, of heavier hydrocarbons, such as olefins found in FTS process. This is because large components deviate strongly from the ideal assumption that considers the spherical shape of molecules. Besides that, the presence of non-condensable gases (CO, H_2, CO_2, and CH_4), nonpolar components (paraffins and olefins), associating (water and alcohols), and highly polar components (ketones and aldehydes), leading to the formation of azeotropes and significant deviations from the ideal gas reference state.

Excess Gibbs free energy and group contributions models, in contrast, appeared in 10 VLLE studies with NRTL, UNIQUAC, and UNIFAC applications at atmospheric pressure. All these works demonstrated poor thermodynamic modeling, exhibiting important discrepancies in predictions of heterogeneous region and azeotrope behavior. These results can be explained by the difficulty to find a unique set of parameters that properly reproduces VLLE, as well as the quality and consistency of experimental data. Zheng et al. (2018) also made the comparison between UNIQUAC and UNIFAC with PC-SAFT performance in VLE, LLE, and VLLE modeling of a large variety of binary and ternary mixtures containing water, alcohols, ketones, aldehydes, ethers, esters, and hydrocarbons to reach unbiased conclusions. Once again, it was presented the superior capacity of PC-SAFT equation, since UNIQUAC and UNIFAC showed unreliable results for LLE and VLLE calculations, predicting artificial liquid−liquid phase splitting for miscible mixtures. These gaps in condensed phase performance were attributed to the fact that LLE calculations are very sensitive to small changes in activity coefficients.

Lastly, a total of 6 reviewed articles used statistical methods to perform VLLE predictions. Besides the excellent results obtained by PC-SAFT model discussed above, in general, the other works focused on improving this equation for specific cases. For example, Ahmed et al. (2016) modified GC-PPC-SAFT to describe accurately pure water properties, while Llovell and Vega (2015) used soft-SAFT to overcome critical region issues of this type of equation for supercritical fluid process.

As for solid-liquid equilibria, 28 articles were reviewed. None of them used Equations of State in their modeling. This result adheres to the discussion made in section 3.2, in which since the reference state of EoS is the ideal gas, it is expected that these methods will not be able to predict solid systems, given the need for data in a very large range of densities. Still in this thought, it could wait that the solid-state also strongly distances itself from the excess Gibbs free energy methods that, despite the closest reference to solids, do not account for the strong molecular interactions present in these systems. Although that, 13 of the cataloged studies tried to use G^E equations in SLE modeling, being Flory Huggins, NRTL, and UNIQUAC models evaluated.

For these cases, Lee et al. (2018) showed that the NRTL and UNIQUAC models have a similar predictive capacity for SLE modeling, the former being slightly better than the latter, with an average RSMD of 0.38 for NRTL and 0.43 for UNIQUAC

for ethanoic acid and carboxylic acids mixtures. Hassan et al. (2012 and 2013) presented this same conclusion, with an average RMSD of 1.93 for NRTL and 2.13 for UNIQUAC for ionic liquids and sugars systems. This small difference can be attributed to the fact that being a 3-parameter model, the NRTL model adapted itself better to the experimental data. Galeotti et al. (2019) also pointed out this importance of adjusting data, showing how NRTL model was sufficient for some regions, but as soon as there was a shortage of data due to the imposition of some difficulty, such as increased temperatures, concentrated systems or the extrapolation for three or more components, it started to depart from the experience. Zarei et al. (2019), in turn, showed that Flory-Huggins method was worse than the two G^E models mentioned above for ionic liquids and sugars, with an average RSMD of 3.13 against 1.64 for NRTL and 1.79 to UNIQUAC. Bessa et al. (2014a, 2014b, 2018 and 2019), however, presented the good performance of Flory-Huggins for ethyl esters systems, reaching until best results than UNIFAC-Dortmund model, in case of insufficient data for the parametrization of this last one, with an average RSMD of 0.99 against 1.41 of GC method. All models described until here were not able to predict complex solid-phase phenomena such as metatectic or inverse peritectic transitions.

It was also noted that UNIFAC was the only GC method used for SLE description, appearing in 8 studies. Yui et al. (2016), Yoshidomi et al. (2017), Perederic et al. (2018), and Damaceno et al. (2018) showed that, even for the best version of this method (UNIFAC-Dortmund) its predictions of SLE for fatty acids had poor performances. In special, it was not able to adequately predict the non-ideality in the liquid phase.

In this category of phase equilibria, 7 of the works presented statistical for the modeling procedure. Once more time, the PC-SAFT model stands out, used in a total of 5 studies, presenting good results even so for strongly non-ideal systems such as heterocyclic compounds (Razavi et al., 2019), and ionic liquids (Paduszynski et al., 2012, 2013, 2015; Körner et al., 2019). In this context, Paduszynski et al. (2012) still presented an alternative approach of solid-liquid phase modeling, which tried to unite the contributions of the association calculations of the PC-SAFT model and the predictive capacity of the UNIFAC method. Although the reliability of the proposed equation for a great number of binary systems, it was shown that in some exceptional cases, satisfactory results can be obtained only when more experimental data were adopted for calculating some corrections.

Thus, two other methods proposed for the study of the SLE were evaluated. The first of them was the COSMO-RS model. In this sense, Wu et al. (2020) presented the SLE predictions of ionic liquids systems, while Martins et al. (2019) focused in deep eutectic mixtures. The quantum method was capable to predict phase behavior with good agreement, being able to describe even so a phase diagram with seven regions. Despite the good results, it must be remembered that, as discussed in section 3.2.3, COSMO-methods are still under development, which ends up having as difficulty the lack of data for parameterization. The other attempt was the GCA equation, Ille et al. (2019) applied this model to monoaromatic oxygenated compounds in mixtures of interest for lignocellulosic biomass conversion processes. The families of compounds evaluated comprised anisole, phenol, linear and cyclic alkanes, alkenes, aromatic hydrocarbons, ketones, alcohols, and water under diverse conditions. The model predictions average deviations reached a remarkable 4.7%.

The works evaluated so far confirm the expected challenge in modeling the solid-liquid phase equilibrium. The difficulty in carrying out experimental procedures due to the instability of the systems and, in some cases, decomposition of compounds, consequently impairs the achievement of parameters of interaction of these systems. This flawed parameterization further reinforces errors in predicting complex phenomena and interactions found in crystalline systems.

Liquid-liquid equilibria, as explained in section 6.1, included most of the articles reviewed in this work (146). For this reason, it was not possible to compare these studies directly and other strategies had to be adopted. In this context, initially, these papers were categorized into the 7 classes of main methods, previously used in Figure 18. The graph obtained (Figure 21) shows that, as expected, G^E were the thermodynamic models most used for LLE evaluation (90). However, at this moment, the indication of greatest interest found in this diagram was the relatively small number of works that applied molecular simulation (3), which can be then evaluated directly.

Harwood et al. (2016), for example, applied Monte Carlo simulations to investigate binary and ternary systems of n-dodecane, ethanol, and water at pressures of 0.1 and 100 MPa. As a result, only qualitatively reproduction of LLE was found, with overestimated miscibility gaps, and UCSTs shifted up by about 50 K compared to experimental values. On the other hand, Rocha et al. (2020) and Yang and Bae (2019)

showed that molecular dynamics represented even isomeric differences for ionic liquids and polymers mixtures, respectively.

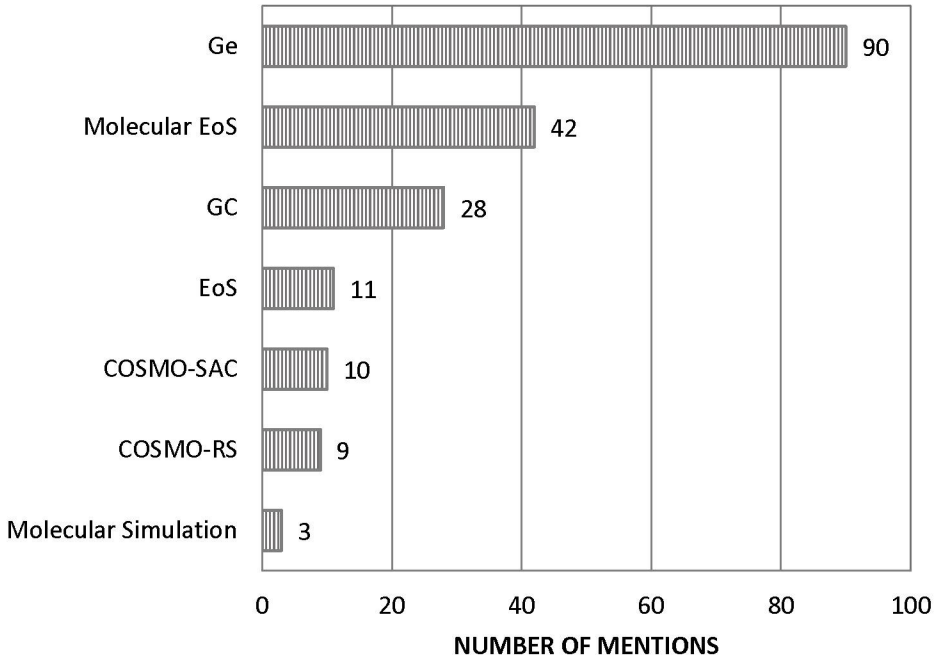

Figure 21 – The seven main thermodynamic methods for phase equilibria modeling and how many times each of them were mentioned in liquid-liquid equilibria studies reviewed in this work.
Source: Author's figure (2020).

Subsequently, another categorization was attempted, this time into low (up to 10 bar) and high pressures (above 20 bar). Only 11 studies were included in this last group, being 4 of them already presented in VLLE section (Zheng et al. (2018), Llovell and Veja (2015), Pinto et al. (2012), and Rodriguez and Beckman (2018)). The other 7 works, in turn, followed similar reasoning to that discussed in vapor-liquid-liquid results that EoS or statistical methods are preferable at high pressures. In an evaluation of solvent and process simultaneous design (PC-SAFT) (Stavrou et al., 2014), near-critical bioethanol extraction processes (GCA) (Paulo et al., 2012), carboxylic acids recovery with sCO_2 (GC-PPC-SAFT and SRK) (Novella et al., 2018, 2019), and biodiesel systems equilibria (PSRK and SRK) (Pokki et al., 2018; Cunico and Guirardello, 2015) good results were obtained without exceptions. In this selection, the work of Coniglio et al. (2014) is still highlighted, because it compared EoS and statistical models for several systems-related to biodiesel. In its results, it was reinforced the best performance of EoS for a realistic representation of phase equilibria at high pressure/critical conditions. Besides that, it also proposed the same discussion

made previously in this work that the complex chemical structure of biomass induces important molecular associations, and how new models that combine different methods, such as GCA and CPA equation, could be better for representing these interactions.

Lastly, in view of the still high number of papers to be analyzed, one more strategy was used, in which the process conditions (temperature and pressure) were defined as inclusion boundaries. Figure 22 shows the application regions of each thermodynamic model and allows the visualization of the common area (in gray). In this way, for this type of equilibrium, it was compared only studies in which the modeling procedure was made inside this region defined by the pressure range of [0.9; 1.5] bar, and temperatures between [293; 386] K. The y-axis is in logarithmic scale for better visualization.

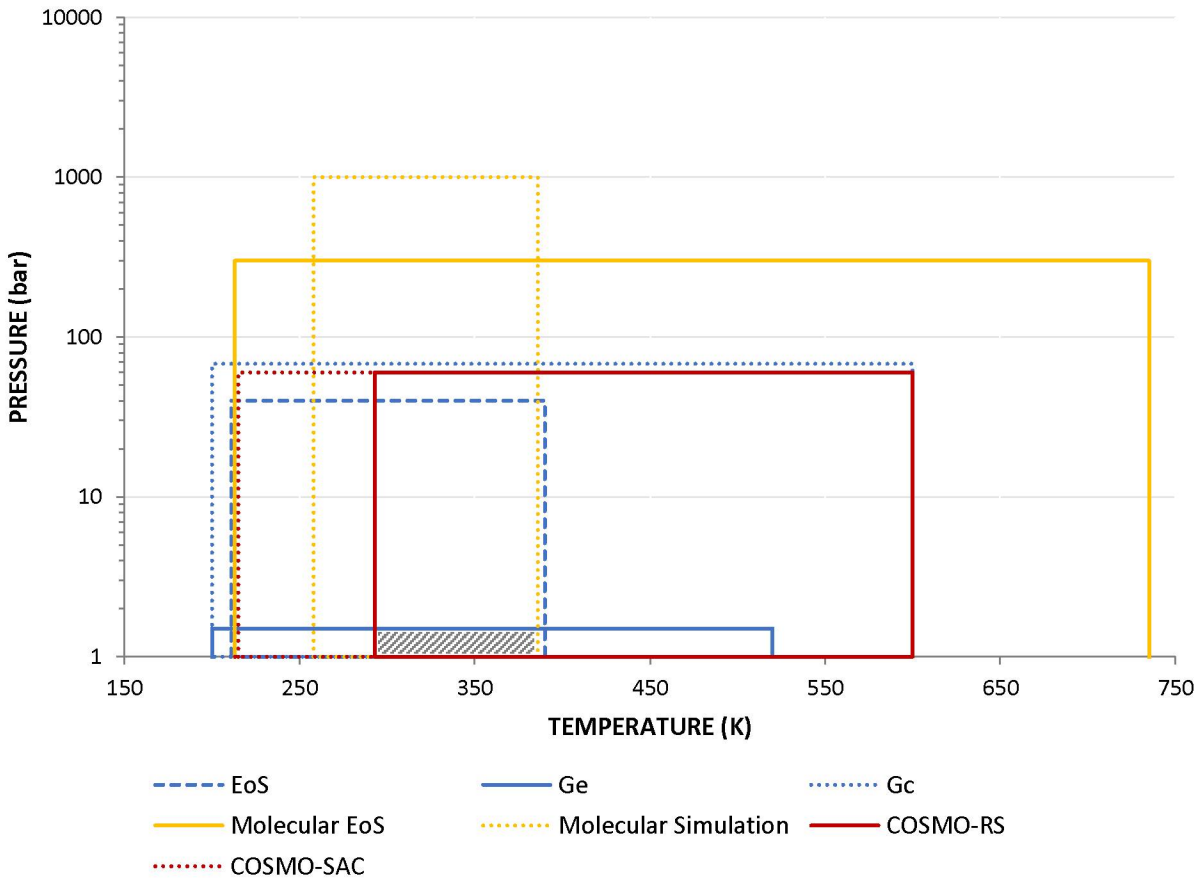

Figure 22 – Region of application of each thermodynamic model in the liquid-liquid equilibria study. In gray the common area, delimited by pressures and temperatures that encompass all class of methods. Source: Author's figure (2020).

These criteria resulted in 104 works. Although it is still a high number, the comparison procedure has been made much easier. This because Gmehling et al. (2006) obtained an interesting result in the study of 3563 best adjustments from the DECHEMA database using G^E models. They showed that the distribution of the best results among the main excess Gibbs free energy models (Wilson, NRTL, and UNIQUAC) was equivalent (around 30% each). So, extending this conclusion to the reviewed studies, it was assumed that for those works that used only excess Gibbs free energy methods for liquid-liquid equilibria evaluation (68 works), there is no preference for one or another model.

Among the 36 articles rest, 5 used EoS for LLE modeling, being four of them previously discussed in VLLE information (Zheng et al. (2018), and high pressure (Novella and Condoret (2019), Pokki et al. (2018), Cunico and Guirardello (2015)). Zerpa et al. (2014) were the only ones that tried to use EoS for low pressures, applying Peng Robinson with Huron–Vidal mixing rules, for the prediction of phase equilibrium of vegetable oils and methanol. As expected, it was found predictions less than satisfactory, being this method unable to represent any of the LLE systems evaluated. Then, excluding 5 papers already mentioned in SLE (Wu et al. (2020), Khoshima et al. (2018)) and VLLE (Ahmed et al. (2016), Zheng et al. (2019), and Sanchez et al. (2011)), only 26 articles remained for comparison.

In this selection, once again, SAFT based models stood out with 15 papers. In comparison with other models, NguyenHuynh and Mai (2019) showed that this equation provided better LLE calculation results over CPA for acetic acid and alkanes mixtures. Samarov et al. (2019) also presented its more robust capacity in relation to NRTL in estimations for alcohol separation from esters using deep eutectic solvents. Auger et al. (2016), in turn, compared these last two models for furan systems. In this case, none of them was able to predict LLE well. The unexpected failure of the association method was justified by the use of VLE parameters in the modeling, which can result in the observed deviations of the condensed phase. However, the factor with the greatest impact on the result obtained was the process conditions used, close to the critical region. Understanding the behavior of LLE close to this region has been widely investigated in the literature, but the solution to this problem has not yet been found. The best results for these cases still being obtained by EoSs.

It was also noted that despite its original form presenting a good performance, there are a wide variety of adaptations that allow the creation of new versions of PC-

SAFT expression for specific systems, or further refinement of its results. For example, the model specific for electrolytes systems, ePC-SAFT, presented excellent results for ionic liquids systems and salting-out effects, reaching an overall absolute average deviation lower than 0.005, against usual values of 0.05 in the literature for other methods (Mohammad et al. (2016)). In addition, its polar versions, PPC-SAFT and GC-PPC-SAFT, improved the phase behavior original predictions of biodiesel-related systems with highly polar components, such as glycerol (Rodriguez and Beckman (2019)), or GVL (Klajmon et al. (2015)).

Finally, 12 works applied quantum models for liquid-liquid equilibria calculations, 9 of them for new solvents (ionic liquids and deep eutectic solvents). Despite the great proposal presented by quantum models, the studies demonstrated that it will still be some years before these methods develop a sufficient database for their complete parameterization. COSMO-models presented the worst performance in all paper reviewed in relation to ePC-SAFT (Mohammad et al. (2016)), NRTL and UNIQUAC (Bharti et al. (2015, 2018), Franzani et al. (2020), Verma and Banerjee (2018)), and even so UNIFAC equation (Silveira and Salau (2019)), with an average RSMD of 7.60% in these studies against 1.33% to the other methods.

Vapor-liquid with 118 studies was the last type of equilibrium analyzed. For this reason, many of the articles included in this category have been already previously discussed in the other sections. Even so, the same analyzes performed for LLE were applied here, in an attempt to obtain relevant information for this specific phenomenon. In this scenario, the division into the 7 categories of methods (Figure 23), for example, showed an interesting observation that the statistical EoSs were the most used approach for the study of VLE (51). In addition, it was noticed that, similarly to LLE, the number of papers that used quantum chemistry models (6) and molecular simulations (2) were small, which could be then evaluated directly.

Ferrando et al. (2011) proposed a Monte Carlo simulation of phase equilibrium and interfacial properties of systems involving ethers and glycol ethers. Accurate predictions were achieved for pure compound saturated and critical properties, surface tensions of the liquid-vapor interface, as well as for binary mixture diagrams, with deviations on bubble pressures around 5%. Yiannourakou et al. (2013), in turn, used Monte Carlo to study a wide range of systems of interest for biomass conversion into high-added value chemicals and biofuels. It was determined the equilibrium properties

for approximately 100 compounds (alcohols, ethers, ketones, aldehydes, esters, glycols) with a good prediction of liquid density, saturation pressures, and vapor-liquid diagrams.

COSMO-based models, however, presented deviations as showed by Zaitseva et al. (2014) for furfural + 2-butanol mixture, in which COSMO-RS underestimated the activity coefficients, being G^E models better for this system. Nala et al. (2013) also showed that, furan + n-hexane phase envelopes were under predicted by COSMO methods, while GC-PPC-SAFT and MC simulation could provide an accurate representation of VLE diagram and excess enthalpy for this mixture.

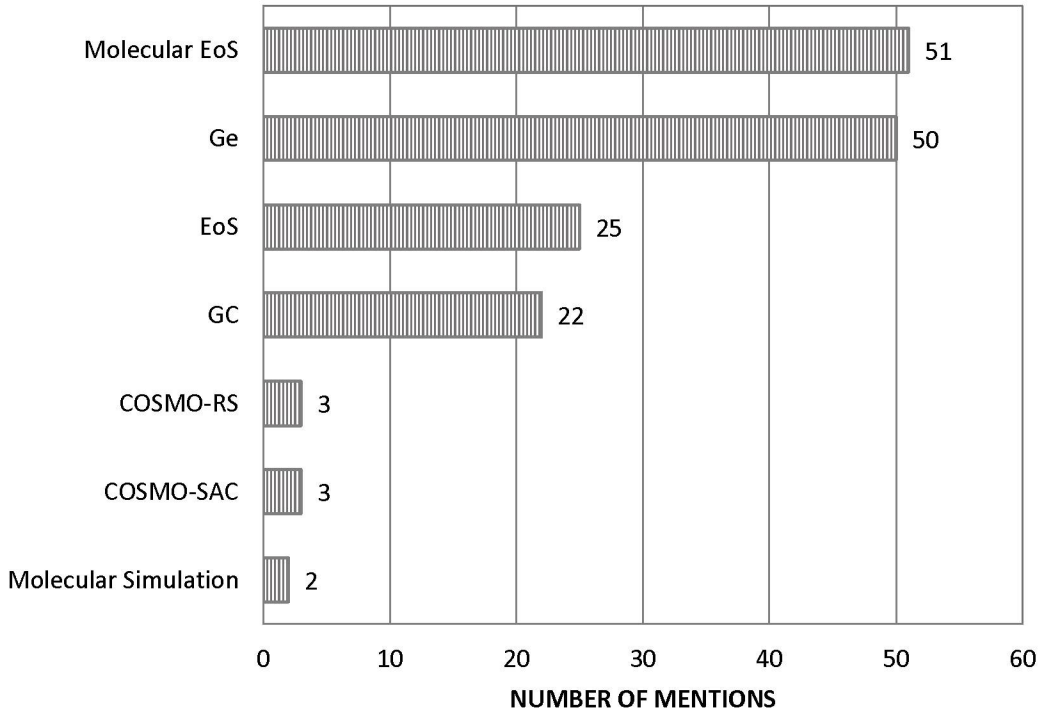

Figure 23 - The seven main thermodynamic methods for phase equilibria modeling and how many times each of them were mentioned in vapor-liquid equilibria studies reviewed in this work.
Source: Author's figure (2020).

Subsequently, the categorization of low (up to 10 bar) and high pressure (above 15 bar) resulted in 32 studies in this last group, the highest absolute number for this type of condition among the 4 types of equilibrium reviewed. These works sustained the reasoning discussed earlier that EoS or statistical methods are preferable under high pressure. This time, however, some new equations were evaluated, such as PPR78 (Privat et al. (2014), Qian et al. (2013)) and PHSC (Khoshsima and Shahriari (2018)). In general, once again, the best EoS performance

for critical conditions was recognized and hybrid models were presented as promises in this area of study.

Finally, the strategy already used for the LLE was applied, in which the conditions of the process were defined as inclusion limits. Figure 24 shows the common area (in gray) obtained with a pressure range between [0.01; 1] bar and temperatures between [298; 363] K. The y-axis was once again in logarithmic scale for better visualization.

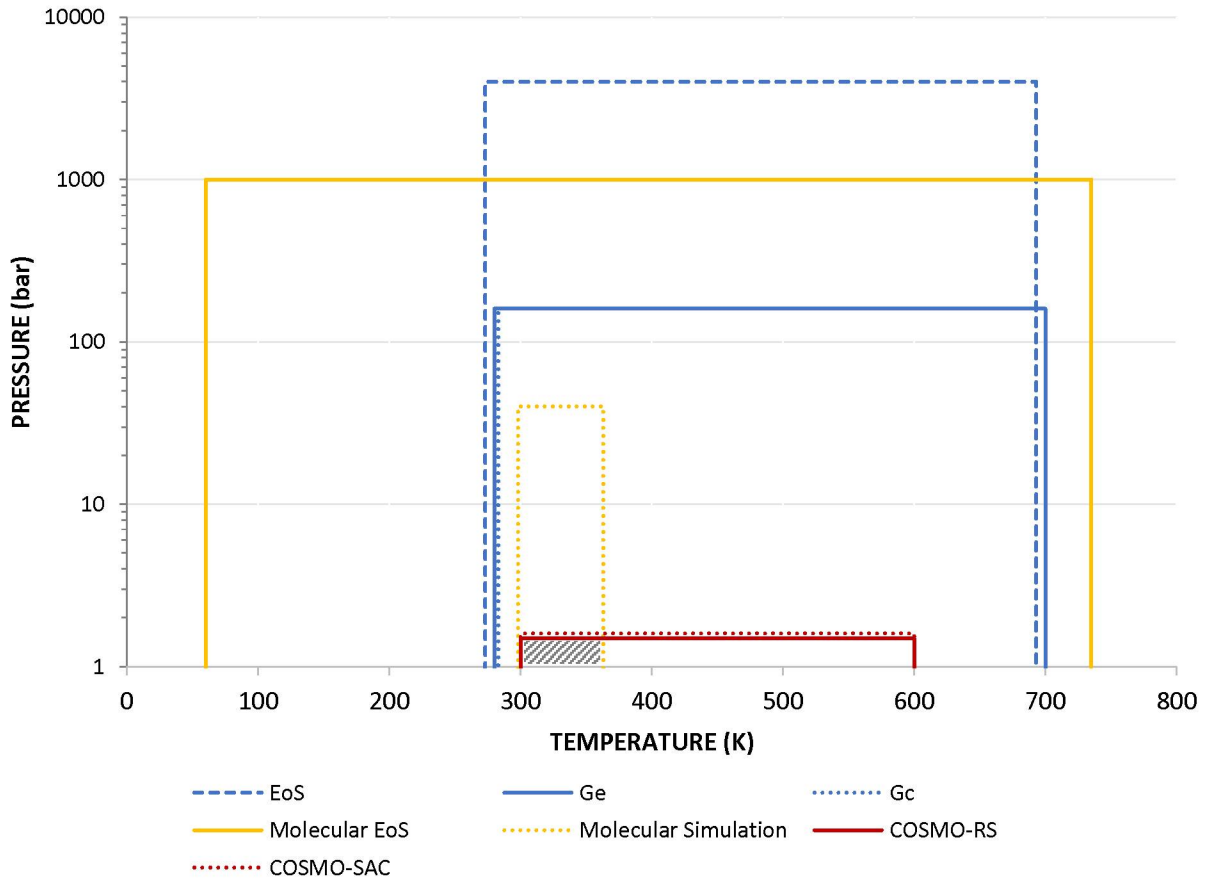

Figure 24 - Region of application of each thermodynamic model in the vapor-liquid equilibria study. In gray the common area, delimited by pressures and temperatures that encompass all class of methods. Source: Author's figure (2020).

These inclusion criteria resulted in 19 papers, 5 of which have already been discussed in the VLLE (Zheng et al. (2018), Ahmed et al. (2016), and Marcilla et al. (2016)) and LLE sections (Warrag et al. (2018), Coniglio et al. (2014)). Among the 14 remaining articles, 11 of them used G^E equations to estimate binary parameters and all showed good results. What stood out most about these works, however, was the appearance of simpler equations, such as Margules and Van Laar. This result is in line

with the theory, since these models are unable to represent efficiently the more complex equilibria previously evaluated. Although, as discussed earlier, there is still no definition of which of G^E methods is the best, conclusion once more time extended for this work. The other three works selected, in turn, applied SAFT on associating compounds (Fouad et al. (2016)), PCP-SAFT on furan mixtures (Liebergesell et al. (2018)), and RK for ionic liquids (Yokozeki and Shiflett (2010)), demonstrating that for compounds that deviate more from ideality, more robust methods are necessary.

Reviewing the information discussed above, it can be highlighted that for the VLLE the Equations of State obtained good results, especially in the high pressure regions studied. Despite this, there was a strong tendency to use statistical models for this type of equilibrium, given the increase in the complexity of the system of interest. For SLE, on the other hand, no Equation of State was used since the theoretical development of these expressions are strongly distant from the solid phase. For this case, once again, the statistical models stood out, being the methods that best represent the complexity of the phenomena present in the solid region. In both cases, the G^E and GC methods showed poor results, in addition to the strong dependence on a large number of data.

For LLE, the G^E methods were definitely the majority. This result was already expected due to the large number of studies in the liquid phase of systems related to biodiesel, in which these methods are quite traditional. Here, the important result of Gmehling et al. (2006) that Gibbs' models are statistically equivalent in the best equilibrium prediction, makes it impossible to establish which of these equations is the best. Still for this type of equilibrium, it is important to highlight that for more complex systems, only the statistical models came close to satisfactory results, with the possibility of the development of specific models for each case under study. In addition, the low number of papers that evaluated systems under high pressures, and the failures of the quantum models, related to their weak database still under development, stands out.

Finally, for VLE it was observed that, surprisingly, the number of statistical methods used to assess this phenomenon already exceeds classical methods. Once again, the best results were attributed to these molecular EoS, except for high pressure and/or critical regions, where the classical EoS still presents better predictions.

These discussions were summarized in a simplified way in Table 7.

Table 7 – Summary of the discussions held in this section for the four types of phase equilibrium, as well as the best resulting thermodynamic model for each.

	VLLE	SLE	LLE	VLE
Equation of State (EoS)	✓		✓	✓
Excess Gibbs free energy (G^E)	✓	✓	✓	✓
Group Contribution (GC)	✓	✓	✓	✓
Molecular EoS	✓	✓	✓	✓
Molecular Simulation			✓	✓
COSMOS-RS		✓	✓	✓
COSMO-SAC			✓	✓
Best model	PC-SAFT	PC-SAFT	PC-SAFT	PC-SAFT*

*For high pressures cases, EoSs presented the best results, or adaptations must be made in the SAFT structure, such as changing the reference fluid (Llovell and Veja, 2014, 2015).
Source: Author's table (2020).

Another very important idea presented in this section that deserves to be highlighted is that despite the smaller absolute number of studies and, therefore, the lower weight in the evaluations carried out, the promises deposited in the hybrid models were very significant. Among these, the most promising model for the specific purpose of this work is the GCA equation. This is because the development of this model by the group PLAPIQUI, Argentina, has focused precisely on systems of interest for biorefineries. In this way, the resolution of the obstacle normally faced by GC models, which is the lack of data, is already quite advanced, having this method currently an extensive database of the main compounds present in the biorefining industries.

The numbers from the analyzes performed on the articles included in this systematic review, however, indicate another answer. Due to the good results in a wider range of systems and conditions, including the four types of equilibrium evaluated, and the possibility of adaptations for specific cases, the figures conclude that, the PC-SAFT model is the best thermodynamic model for modeling phase equilibrium of systems related to biorefineries.

7 CONCLUSIONS

This work initially focused on understanding the development of thermodynamic modeling over time. It was constructed the definitions of phase equilibria and the premises of each thermodynamic model, as well as to highlight the origins of their limitations. Still, an effort was made to point out how the next method tried to overcome previous problems and what differs it from the others.

Then, a systematic review of the state of the art published in the last decade on thermodynamic modeling of phase equilibria in systems related to biorefineries was carried out using the PRISMA systematization of information method, which resulted in an overview of 236 papers. The methodology adopted used as inclusion criteria: being published between 2010 and 2020, English as language, only papers, excluding patents, citations, and thesis, and presentation of phase equilibria modeling in comparison with experimental data in graphic format.

The studies were then cataloged by year, country, type of equilibrium studied, and thermodynamic models used, highlighting relevant points as research groups with greater impact and compounds most studied. At this time, it was observed an increase in publications in this research area in the period under evaluation, and Brazil stood out as the country with the higher number of contributions (39). It was also noted the greater predilection for the LLE and excess Gibbs free energy models, which can be explained by the concentration of articles in biodiesel studies. Still, the growth in the use of statistical models was related to the computational improvement of recent years, and also to the fact that more complex compounds and phenomena have been more explored in the biorefinery sector.

Finally, a comparison of the prediction capacity of phase behavior for different models was performed. In this context, the highlight were hybrid models that synergistically combine different classes of thermodynamic models. In this scenario, the GCA model stood out, given its high capacity to adapt to the diversity found in systems under study. The analyzes, however, presented due to the good results in a wider range of systems and conditions, the PC-SAFT model as the best thermodynamic model for modeling phase equilibrium of systems related to biorefineries.

REFERENCES

ABRAMS, D. S.; PRAUSNITZ, J. M. Statistical thermodynamics of liquid mixtures: A new expression for the excess Gibbs energy of partly or completely miscible systems. **AIChE Journal**, v. 21, n. 1, p. 116–128, 1975.

ABUTAQIYA, M. I. L. Advances in Thermodynamic Modeling of Nonpolar Hydrocarbons and Asphaltene Precipitation in Crude Oils. 235 f. Doctoral Thesis in Chemical Engineering. Rice University. Houston, Texas, USA. April 2019.

BCC RESEARCH. Market Research Reports. Energy – EGY054C. Biorefinery Technologies: Global Markets. Available from: <https://www.bccresearch.com/market-research/energy-and-resources/biorefinery-technologies-global-markets-markets.html>. Access in: 16 jun. 2020.

BENAZZOUZ, A.; MOITY, L.; PIERLOT, C.; MOLINIER, V.; AUBRY, J. M. Hansen approach versus COSMO-RS for predicting the solubility of an organic UV filter in cosmetic solvents. **Colloids and Surfaces A: Physicochemical and Engineering Aspects**, v. 458, n. 1, p. 101–109, 2014. Elsevier B.V. Available in: <http://dx.doi.org/10.1016/j.colsurfa.2014.03.065>.

BRANCO, L. Biocombustíveis: Vantagens E Desafios. **Revista Eletrônica de Energia**, v. 3, n. 1, p. 16–33, 2014.

BUSINESS WIRE – A Berkshire Hathaway company. Global Biorefinery Market 2018-2022 I 12% CAGR Projection over the next four years. Available from: <https://www.businesswire.com/news/home/20180717005605/en/Global-Biorefinery-Market-2018-2022-12-CAGR-Projection>. Access in: 16 jun. 2020.

CHAPMAN, W. G.; GUBBINS, K. E.; JACKSON, G.; RADOSZ, M. SAFT: Equation-of-state solution model for associating fluids. **Fluid Phase Equilibria**, v. 52, n. C, p. 31–38, 1989.

CHAPMAN, W. G. Applications of Molecular Simulation and Statistical Mechanics. Chemical and Biochemical Engineering Department. Rice University. Houton, Texas - USA. 2020.

CHEN, C. C.; MATHIAS, P. M. Applied Thermodynamics for Process Modeling. **AIChE Journal**, v. 48, n. 2, p. 194–200, 2002.

CHERUBINI, F.; WELLISCH, M.; WILLKE, T. Toward a common classification approach for biorefinery systems. **Biofuels, Bioproducts & Biorefining**, v.3 , p. 534–546, 2009.

CRESPO, E. A.; COUTINHO, J. A. P. A Statistical Associating Fluid Theory Perspective of the Modeling of Compounds Containing Ethylene Oxide Groups. **Industrial and Engineering Chemistry Research**, v. 58, n. 9, p. 3562–3582, 2019.

ECKERT, F.; KLAMT, A. Fast Solvent Screening via Quantum Chemistry: COSMO-

RS Approach. **AIChE Journal**, v. 48, n. 2, p. 369–385, 2002.

EMPRESA BRASILEIRA DE PESQUISA AGROPECUÁRIA (EMBRAPA). Ministério da Agricultura, Pecuária e Abastecimento. Biblioteca – Busca de Publicações. Biorrefinarias. Available from: <https://www.embrapa.br/busca-de-publicacoes/-/publicacao/908142/biorrefinarias>. Access in: 13 jun. 2020.

FATIH DEMIRBAS, M. Biorefineries for biofuel upgrading: A critical review. **Applied Energy**, v. 86, n. SUPPL. 1, p. S151–S161, 2009. Elsevier Ltd. Available in: <http://dx.doi.org/10.1016/j.apenergy.2009.04.043>.

FERNANDO, S.; ADHIKARI, S.; CHANDRAPAL, C.; MURALI, N. Biorefineries: Current status, challenges, and future direction. **Energy and Fuels**, v. 20, n. 4, p. 1727–1737, 2006.

FINGERHUT, R.; CHEN, W. L.; SCHEDEMANN, A.; et al. Comprehensive Assessment of COSMO-SAC Models for Predictions of Fluid-Phase Equilibria. **Industrial and Engineering Chemistry Research**, v. 56, n. 35, p. 9868–9884, 2017.

FREDENSLUND, A.; JONES, R. L.; PRAUSNITZ, J. M. Group-Contribution Estimation of Activity Coefficients in Nonideal Liquid Mixtures. **AIChe Journal**, v. 21, n. 6, 1975.

GMEHLING, J.; CONSTANTINESCU, D.; SCHMID, B. Group Contribution Methods for Phase Equilibrium Calculations. **Annual Review of Chemical and Biomolecular Engineering**, v. 6, n. 1, p. 267–292, 2015.

GONZÁLEZ PRIETO, M.; SÁNCHEZ, F. A.; PEREDA, S. Thermodynamic model for biomass processing in pressure intensified technologies. **Journal of Supercritical Fluids**, v. 96, p. 53–67, 2015. Elsevier B.V. Available in: <http://dx.doi.org/10.1016/j.supflu.2014.08.024>. .

GROS, H. P.; BOTTINI, S.; BRIGNOLE, E. A. A group contribution equation of state for associating mixtures. **Fluid Phase Equilibria**, v. 116, n. 1–2, p. 537–544, 1996.

GROSS, J.; SADOWSKI, G. Perturbed-chain SAFT: An equation of state based on a perturbation theory for chain molecules. **Industrial and Engineering Chemistry Research**, v. 40, n. 4, p. 1244–1260, 2001

GUO, N.; CARATZOULAS, S.; DOREN, D. J.; SANDLER, S. I.; VLACHOS, D. G. A perspective on the modeling of biomass processing. **Energy and Environmental Science**, v. 5, n. 5, p. 6703–6716, 2012.

HQS QUANTUM SIMULATIONS. QAD Cloud Beta. Available from: <https://qad.quantumsimulations.de/>. Access in: 23 jun. 2020.

INTERNATIONAL ENERGY AGENCY (IEA). World energy statistics. Available from: <http://www.iea.org/publications/freepublications/publication/key_world_energy_stats-1.pdf>. Access in: 13 jun. 2020.

JONG, E. DE; JUNGMEIER, G. **Biorefinery Concepts in Comparison to Petrochemical Refineries**. In: PANDEY, A.; HÖFER, R.; TAHERZADEH, M.; NAMPOOTHIRI, K. M.; LARROCHE, C. (Ed). Industrial Biorefineries & White Biotechnology. Elsevier B.V., 2015. p. 3-33.

KLAMT, A. Conductor-like screening model for real solvents: A new approach to the quantitative calculation of solvation phenomena. **Journal of Physical Chemistry**, v. 99, n. 7, p. 2224–2235, 1995.

KLAMT, A.; ECKERT, F.; ARLT, W. COSMO-RS: An alternative to simulation for calculating thermodynamic properties of liquid mixtures. **Annual Review of Chemical and Biomolecular Engineering**, v. 1, p. 101–122, 2010.

KONTOGEORGIS, G. M.; VOUTSAS, E. C.; YAKOUMIS, I. V.; TASSIOS, D. P. An equation of state for associating fluids. **Industrial and Engineering Chemistry Research**, v. 35, n. 11, p. 4310–4318, 1996.

KORETSKY, M. D. Engineering and Chemical Thermodynamics. First Edition. John Wiley & Sons, Inc. 2004.

LIBERATI, A.; ALTMAN, D. G.; TETZLAFF, J.; et al. The PRISMA statement for reporting systematic reviews and meta-analyses of studies that evaluate health care interventions: Explanation and elaboration. **PLoS Medicine**, 2009.

LIN, S. T.; SANDLER, S. I. A priori phase equilibrium prediction from a segment contribution solvation model. **Industrial and Engineering Chemistry Research**, v. 41, n. 5, p. 899–913, 2002.

LOVINS, A. B. Winning the Oil Endgame: Innovation for Profits, Jobs, and Security. First Edition. Colorado: Rocky Mountain Institute. 2005.

MAITY, S. K. Opportunities, recent trends and challenges of integrated biorefinery: Part i. **Renewable and Sustainable Energy Reviews**, v. 43, p. 1427–1445, 2015. Elsevier. Available in: <http://dx.doi.org/10.1016/j.rser.2014.11.092>.

NATIONAL RENEWABLE ENERGY LABORATORY (NREL) – Transforming Energy. Bioenergy. Biorefinery Research. Available from: < https://www.nrel.gov/bioenergy/research.html>. Access in: 13 jun. 2020.

PANAGIOTOPOULOS, A. Z. Molecular simulation of phase equilibria: simple, ionic and polymeric fluids. **Fluid Phase Equilibria**, v. 76, n. C, p. 97–112, 1992.

PARIKKA, M. Global biomass fuel resources. **Biomass and Bioenergy**, v. 27, n. 6, p. 613–620, 2004.

PENG, D. Y.; ROBINSON, D. B. A New Two-Constant Equation of State. **Industrial and Engineering Chemistry Fundamentals**, v. 15, n. 1, p. 59–64, 1976.

PRAUSNITZ, J. M. Molecular Thermodynamics of Fluid-Phase Equilibria. Third Edition. New Jersey: Prentice-Hall, Inc. 1999.

PRESCIENT & STRATEGIC INTELLIGENCE – where knowledge inspires strategy. Chemicals and Materials. Biorefinery Market (2011-2020). Available from: <https://www.psmarketresearch.com/market-analysis/biorefinery-market>. Access in: 16 jun. 2020.

REDLICH, O.; KWONG, J. N. S. On the thermodynamics of solutions. V. An equation of state. Fugacities of gaseous solutions. **Chemical Reviews**, v. 44, n. 1, p. 233–244, 1949.

RENON, H.; PRAUSNITZ, J. M.. Local Compositions in Thermodynamic Excess Functions for Liquid Mixtures. **AIChE Journal**, v. 14, n. 1, p. 135- 144, 1968.

ROWLEY, R. VAN DER WAALS EQUATION OF STATE. Available from: <https://www.et.byu.edu/~rowley/ChEn273/Topics/Mass_Balances/Single_Phase_Systems/Van_der_Waals_Equation_of_State.htm>. Access in: 26 jun. 2020.

SADHUKHAN, J.; MARTINEZ-HERNANDEZ, E.; NG, K. S. Biorefinery value chain creation. **Chemical Engineering Research and Design**, v. 107, p. 1–3, 2016. Institution of Chemical Engineers. Available in: <http://dx.doi.org/10.1016/j.cherd.2016.02.026>.

SANDLER, S. I. Chemical, Biochemical, and Engineering Thermodynamics. Fourth Edition. John Wiley & Sons, Inc. 2006.

SISCO, C. Thermodynamic Modeling of Hydrocarbon Mixtures with Application to Polymer Phase Behavior and Asphaltene Precipitation. 177 f. Doctoral Thesis in Chemical Engineering. Rice University - Houston, Texas, USA. August 2018.

SMITH, J. M.; VAN NESS, H. C.; ABBOTT, M. M. Introduction to chemical engineering thermodynamics. Seventh Edition. The McGraw-Hill Companies, Inc. 2005.

SOAVE, G. Equilibrium Constants from a Modified Redkh-Kwong EOS. **Chemical Engineering Science**, v. 27, n. 6, p. 1197–1203, 1972. Available in: <http://dns2.asia.edu.tw/~ysho/YSHO-English/2000 Engineering/PDF/Che Eng Sci27, 1197.pdf>.

VON SOLMS, N.; KOUSKOUMVEKAKI, I. A.; MICHELSEN, M. L.; KONTOGEORGIS, G. M. Capabilities, limitations and challenges of a simplified PC-SAFT equation of state. **Fluid Phase Equilibria**, v. 241, n. 1–2, p. 344–353, 2006.

UNGERER, P.; NIETO-DRAGHI, C.; ROUSSEAU, B.; AHUNBAY, G.; LACHET, V. Molecular simulation of the thermophysical properties of fluids: From understanding toward quantitative predictions. **Journal of Molecular Liquids**, v. 134, n. 1-3 SPEC. ISS., p. 71–89, 2007.

US DEPARTMENT OF ENERGY (DOE). Biomass resources. Available from: <http://www.eere.energy.gov/basics/renewable_energy/biomass_resources.html>. Access in: 13 jun. 2020.

WERTHEIM, M. S. Fluids with highly directional attractive forces. II. Thermodynamic perturbation theory and integral equations. **Journal of Statistical Physics**, v. 35, n. 1–2, p. 35–47, 1984.

WERTHEIM, M. S. Fluids with highly directional attractive forces. I. Statistical thermodynamics. **Journal of Statistical Physics**, v. 35, n. 1–2, p. 19–34, 1983.

WILSON, G. M. Vapor-Liquid Equilibrium. XI. A New Expression for the Excess Free Energy of Mixing. **Journal of the American Chemical Society**, v. 86, n. 2, p. 127–130, 1964.

WILSON, G. M.; DEAL, C. H. Activity coefficients and molecular structure: Activity coefficients in changing environments'solutions of groups. **Industrial and Engineering Chemistry Fundamentals**, v. 1, n. 1, p. 20–23, 1962.

REFERENCES INCLUDED IN PRISMA SYSTEMATIC REVIEW

[1] S. Mandal and A. K. Jana. A comparative performance of thermodynamic models for a quaternary (HI–H2O–I2–H2) HIx system: Experimental verification. **Int. J. Hydrogen Energy**, v. 41, n. 31, p. 13350–13358, 2016. doi: 10.1016/j.ijhydene.2016.05.030.

[2] S. Zerpa, M. Satyro, and M. A. Clarke. A short note on the use of an equation of state (EOS) based approach to modelling the thermodynamics of biodiesel systems. **Fuel Process. Technol.**, v. 121, p. 70–75, 2014. doi: 10.1016/j.fuproc.2014.01.010.

[3] A. Mejía, H. Segura, and M. Cartes. Experimental determination and theoretical prediction of the vapor-liquid equilibrium and interfacial tensions of the system methyl-tert-butyl ether + 2,5-dimethylfuran. **Fuel**, v. 116, p. 183–190, 2014. doi: 10.1016/j.fuel.2013.07.107.

[4] W. Sakdasri, R. Sawangkeaw, Y. Medina-Gonzalez, S. Camy, J. S. Condoret, and S. Ngamprasertsith. Experimental Study and Modeling of Phase Equilibrium of the Methanol-Tripalmitin System: Application to Palm Oil Transesterification with Supercritical Methanol. **Ind. Eng. Chem. Res**., v. 55, n. 18, p. 5190–5199, 2016. doi: 10.1021/acs.iecr.5b04588.

[5] A. C. D. Freitas, L. P. Cunico, M. Aznar, and R. Guirardello. Modeling vapor liquid equilibrium of ionic liquids + gas binary systems at high pressure with cubic equations of state. **Brazilian J. Chem. Eng.**, v. 30, n. 1, p. 63–73, 2013. doi: 10.1590/S0104-66322013000100008.

[6] L. F. Pinto, D. I. S. Da Silva, F. Rosa Da Silva, L. P. Ramos, P. M. Ndiaye, and M. L. Corazza. Phase equilibrium data and thermodynamic modeling of the system (CO 2 + biodiesel + methanol) at high pressures. **J. Chem. Thermodyn.**, v. 44, n. 1, p. 57–65, 2012. doi: 10.1016/j.jct.2011.07.019.

[7] W. R. Giacomin Junior, C. A. Capeletto, F. A. P. Voll, and M. L. Corazza. Phase Equilibrium Measurements and Thermodynamic Modeling of the Systems (CO2 + Ethyl Levulinate) and (CO2 + Levulinic Acid). **J. Chem. Eng. Data**, v. 64, n. 5, p. 2011–2017, 2019. doi: 10.1021/acs.jced.8b01023.

[8] B. A. Veiga, J. T. F. dos Santos, L. F. de Lima Luz Junior, and M. L. Corazza. Phase equilibrium measurements and thermodynamic modelling for the systems involving valeric acid, ethanol, ethyl valerate and water plus CO2. **J. Chem. Thermodyn.**, v. 112, p. 240–248, 2017. doi: 10.1016/j.jct.2017.05.011.

[9] A. R. C. Morais, A. M. Da Costa Lopes, and R. Bogel-Lukasik.The phase equilibrium phenomenon in model hydrogenation of oleic acid. **Monatshefte fur Chemie**, v. 145, n. 10, p. 1555–1560, 2014. doi: 10.1007/s00706-014-1268-8.

[10] N. Juntarachat, R. Privat, L. Coniglio, and J. N. Jaubert. Development of a predictive equation of state for CO2+ ethyl ester mixtures based on critical points measurements. **J. Chem. Eng. Data**, v. 59, n. 10, p. 3205–3219, 2014. doi:

10.1021/je5002494.

[11] J. W. Qian, R. Privat, and J. N. Jaubert. Predicting the phase equilibria, critical phenomena, and mixing enthalpies of binary aqueous systems containing alkanes, cycloalkanes, aromatics, alkenes, and gases (N2, CO2, H2S, H2) with the PPR78 equation of state. **Ind. Eng. Chem. Res.**, v. 52, n. 46, p. 16457–16490, 2013. doi: 10.1021/ie402541h.

[12] Z. Esina, Z. Esina, A. Miroshnikov, A. Miroshnikov, M. Korchuganova, and M. Korchuganova. LIQUID- SOLID AND LIQUID-VAPOR PHASE EQUILIBRIUM IN SECONDARY ALCOHOL - n-ALKANE SYSTEM. **Sci. Evol.**, v. 2, n. 2, p. 33–39, 2017. doi: 10.21603/2500-1418-2017-2-2-33-39.

[13] T. Knorr, E. Aust, and K. H. Jacob. Calculation of vapor-liquid equilibrium data of binary mixtures using vapor pressure data. **Chem. Eng. Technol.**, v. 33, n. 12, p. 2089–2094, 2010. doi: 10.1002/ceat.201000356.

[14] C. Fu, W. Song, C. Yi, and S. Xie. Creating efficient novel aqueous two-phase systems: Salting-out effect and high solubility of salt. **Fluid Phase Equilib.**, v. 490, p. 77–85, 2019. doi: 10.1016/j.fluid.2019.03.002.

[15] C. Silva, L. Soh, A. Barberio, J. Zimmerman, and W. D. Seider. Phase equilibria of triolein to biodiesel reactor systems. **Fluid Phase Equilib.**, v. 409, p. 171–192, 2016. doi: 10.1016/j.fluid.2015.09.049.

[16] A. Yokozeki and M. B. Shiflett. Water solubility in ionic liquids and application to absorption cycles. **Ind. Eng. Chem. Res.**, v. 49, n. 19, p. 9496–9503, 2010. doi: 10.1021/ie1011432.

[17] S. Sima, C. Secuianu, V. Feroiu, and D. Geană. New high-pressures vapor-liquid equilibrium data for the carbon dioxide + 2-methyl-1-propanol (isobutanol) binary system. **Cent. Eur. J. Chem.**, v. 12, n. 9, p. 953–961, 2014. doi: 10.2478/s11532-013-0394-1.

[18] M. R. Shah and G. D. Yadav. Prediction of liquid-liquid equilibria for biofuel applications by quantum chemical calculations using the Cosmo-SAC method. **Ind. Eng. Chem. Res.**, v. 50, n. 23, p. 13066–13075, 2011. doi: 10.1021/ie201454m.

[19] P. Uusi-Kyyny, M. S. Qureshi, J. P. Pokki, V. Alopaeus, and D. Richon. 110th Anniversary: Critical Properties and High Temperature Vapor Pressures for Furan, 2-Methylfuran, 2-Methoxy-2-methylpropane, 2-Ethoxy-2-methylbutane, n-Hexane, and Ethanol and Bubble Points of Mixtures with a New Apparatus. **Ind. Eng. Chem. Res.**, v. 58, n. 49, p. 22350–22362, 2019. doi: 10.1021/acs.iecr.9b02912.

[20] K. Zheng, R. Yang, H. Wu, G. Wang, Y. Yang, and Y. Li. Application of the Perturbed-Chain SAFT to Phase Equilibria in the Fischer-Tropsch Synthesis. **Ind. Eng. Chem. Res.**, v. 58, n. 19, p. 8387–8400, 2019. doi: 10.1021/acs.iecr.9b00174.

[21] L. Coniglio et al. Biodiesel via supercritical ethanolysis within a global analysis 'feedstocks-conversion-engine' for a sustainable fuel alternative. **Prog. Energy**

Combust. Sci., v. 43, p. 1–35, 2014. doi: 10.1016/j.pecs.2014.03.001.

[22] M. F. Monteiro, M. H. Moura-Neto, C. G. Pereira, and O. Chiavone-Filho. Description of phase equilibrium and volumetric properties for CO2+water and CO2+ethanol using the CPA equation of state. **J. Supercrit. Fluids**, v. 161, p. 104841, 2020. doi: 10.1016/j.supflu.2020.104841.

[23] M. A. Guevara, F. A. Guevara, and L. C. Belalcazar. Experimental data and new binary interaction parameters for ethanol-water VLE at low pressures using NRTL and UNIQUAC. **Tecciencia**, v. 13, n. 24, p. 17–26, 2018. doi: 10.18180/tecciencia.2018.24.3.

[24] H. Wu, K. Zheng, G. Wang, Y. Yang, and Y. Li. Modeling of Gas Solubility in Hydrocarbons Using the Perturbed-Chain Statistical Associating Fluid Theory Equation of State. **Ind. Eng. Chem. Res.**, v. 58, n. 27, p. 12347–12360, 2019. doi: 10.1021/acs.iecr.9b01383.

[25] L. P. Cunico and R. Guirardello. Modeling of phase and chemical equilibria for systems involved in biodiesel production. **Chem. Eng. Trans.**, v. 43, n. June, p. 1855–1860, 2015. doi: 10.3303/CET1543310.

[26] S. Sima, C. Secuianu, V. Feroiu, and D. Geană. New high-pressures vapor-liquid equilibrium data for the carbon dioxide + 2-methyl-2-propanol binary system. **Cent. Eur. J. Chem.**, v. 12, n. 9, p. 893–900, 2014. doi: 10.2478/s11532-013-0392-3.

[27] A. Novella, S. Camy, and J. S. Condoret. Fractionation of a dilute acetic acid aqueous mixture in a continuous countercurrent packed column using supercritical CO2: Experiments and simulation of external extract reflux. **J. Supercrit. Fluids**, v. 157, p. 104680, 2020. doi: 10.1016/j.supflu.2019.104680.

[28] J. P. Pokki, H. Q. Lê, P. Uusi-Kyyny, H. Sixta, and V. Alopaeus. Isobaric Vapor-Liquid Equilibrium of Furfural + γ-Valerolactone at 30 kPa and Isothermal Liquid-Liquid Equilibrium of Carbon Dioxide + γ-Valerolactone + Water at 298 K. **J. Chem. Eng. Data**, v. 63, n. 12, p. 4381–4391, 2018. doi: 10.1021/acs.jced.8b00451.

[29] S. Mavalal and K. Moodley. Isothermal vapour-liquid equilibrium measurements for the water + butane-1,4-diol/butane-2,3-diol system within 353.1–373.2 K. **Fluid Phase Equilib.**, v. 512, p. 112518, 2020. doi: 10.1016/j.fluid.2020.112518.

[30] L. C. B. A. Bessa, M. D. Robustillo, A. J. de A. Meirelles, and P. de A. Pessôa Filho. (Solid + liquid) equilibrium of binary mixtures containing ethyl esters and p-xylene by differential scanning calorimetry. **J. Therm. Anal. Calorim.**, v. 137, n. 6, p. 2017–2028, 2019. doi: 10.1007/s10973-019-08085-z.

[31] L. C. B. A. Bessa, M. D. Robustillo, B. C. Marques, C. C. Tadini, and P. de A. Pessôa Filho. Experimental determination and thermodynamic modeling of solid-liquid equilibrium of binary systems containing representative compounds of biodiesel and fossil fuels: Ethyl esters and n-dodecane. **Fuel**, v. 237, n. October 2018, p. 1132–1140, 2019. doi: 10.1016/j.fuel.2018.10.080.

[32] M. D. Robustillo, D. F. Barbosa, A. J. de A. Meirelles, and P. de A. Pessoa Filho. Solid-liquid equilibrium in ternary mixtures of ethyl laurate, ethyl palmitate and ethyl myristate. **Fluid Phase Equilib.**, v. 361, p. 188–199, 2014. doi: 10.1016/j.fluid.2013.10.024.

[33] M. D. Robustillo, D. F. Barbosa, A. J. de A. Meirelles, and P. de A. Pessôa Filho. Solid-liquid equilibrium of binary and ternary mixtures containing ethyl oleate, ethyl myristate and ethyl stearate. **Fluid Phase Equilib.**, v. 370, p. 85–94, 2014. doi: 10.1016/j.fluid.2014.03.001.

[34] S. Zarei, S. Abdolrahimi, and G. Pazuki. Thermophysical characterization of sorbitol and 1–ethyl–3–methylimidazolium acetate mixtures. **Fluid Phase Equilib.**, v. 497, p. 140–150, 2019. doi: 10.1016/j.fluid.2019.06.006.

[35] H. E. Reynel-Ávila, A. Bonilla-Petriciolet, and J. C. Tapia-Picazo. An artificial neural network-based NRTL model for simulating liquid-liquid equilibria of systems present in biofuels production. **Fluid Phase Equilib.**, v. 483, p. 153–164, 2019. doi: 10.1016/j.fluid.2018.11.009.

[36] A. Moreau, J. J. Segovia, M. D. Bermejo, and M. C. Martín. Vapor-liquid equilibria and excess enthalpies of the binary systems 1-pentanol or 2-pentanol and 1-hexene or 1,2,4-trimethylbenzene for the development of biofuels. **Fluid Phase Equilib.**, v. 460, p. 85–94, 2018. doi: 10.1016/j.fluid.2017.12.031.

[37] S. Li et al. Vapor-liquid equilibrium in the binary and ternary systems containing ethyl propionate, ethanol and alkane at 101.3 kPa. **Fluid Phase Equilib.**, v. 476, p. 103–111, 2018. doi: 10.1016/j.fluid.2018.07.013.

[38] N. Galeotti, J. Burger, and H. Hasse. Vapor-liquid equilibrium in the ternary systems acetic acid + water + (xylose or glucose). **Fluid Phase Equilib.**, v. 473, p. 323–329, 2018. doi: 10.1016/j.fluid.2018.06.011.

[39] J. Garcia-Cano, V. Gomis, A. Font, V. Calemma, and E. F. Gambarotta. Vapor-liquid equilibrium of 3-ethoxy-1,2-propanediol + water/ethanol/diethyl ether/glycerol/1,2-propanediol at different pressures. **Fluid Phase Equilib.**, v. 512, p. 112519, 2020. doi: 10.1016/j.fluid.2020.112519.

[40] J. A. Duran, F. P. Córdoba, I. D. Gil, G. Rodríguez, and A. Orjuela. Vapor-liquid equilibrium of the ethanol+3-methyl-1-butanol system at 50.66, 101.33 and 151.99kPa. **Fluid Phase Equilib.**, v. 338, p. 128–134, 2013. doi: 10.1016/j.fluid.2012.11.004.

[41] L. Zhang, B. Yang, and W. Zhang. Vapor-Liquid Equilibrium of Water + Ethanol + Glycerol: Experimental Measurement and Modeling for Ethanol Dehydration by Extractive Distillation. **J. Chem. Eng. Data**, v. 60, n. 6, p. 1892–1899, 2015. doi: 10.1021/acs.jced.5b00116.

[42] A. Mejía, H. Segura, M. Cartes, and J. A. P. Coutinho. Vapor-liquid equilibrium, densities, and interfacial tensions of the system hexane + 2,5-dimethylfuran. **J. Chem. Eng. Data**, v. 57, n. 10, p. 2681–2688, 2012. doi: 10.1021/je300631s.

[43] A. Moreau, M. C. Martín, F. Aguilar, and J. J. Segovia. Vapour-liquid equilibria and excess enthalpies of the binary mixtures 1-pentanol with 2,2,4-trimethylpentane or n-heptane. **Fluid Phase Equilib.**, v. 338, p. 95–99, 2013. doi: 10.1016/j.fluid.2012.11.005.

[44] A. Moreau, J. J. Segovia, M. A. Villamañán, and M. C. Martín. Vapour-liquid equilibria of the ternary mixture (1-pentanol+2,2,4-trimethylpentane+heptane) and the binary mixture (2,2,4-trimethylpentane+heptane) at T=313.15K for the characterization of second generation biofuels. **Fluid Phase Equilib.**, v. 405, p. 101–106, 2015. doi: 10.1016/j.fluid.2015.07.049.

[45] J. Pla-Franco, E. Lladosa, S. Loras, and J. B. Montón. Azeotropic distillation for 1-propanol dehydration with diisopropyl ether as entrainer: Equilibrium data and process simulation. **Sep. Purif. Technol.**, v. 212, n. November 2018, p. 692–698, 2019. doi: 10.1016/j.seppur.2018.11.082.

[46] D. Rabari and T. Banerjee. Biobutanol and n-propanol recovery using a low density phosphonium based ionic liquid at T=298.15K and p=1atm. **Fluid Phase Equilib.**, v. 355, p. 26–33, 2013. doi: 10.1016/j.fluid.2013.06.047.

[47] A. Moreau, J. J. Segovia, M. D. Bermejo, and M. C. Martín. Characterizing second generation biofuels: Excess enthalpies and vapour-liquid equilibria of the binary mixtures containing 1-pentanol or 2-pentanol and n-hexane. **Fluid Phase Equilib.**, v. 425, pp. 177–182, 2016, doi: 10.1016/j.fluid.2016.05.031.

[48] Y. Song et al. Dehydration of 1-Butanol with a Deep Eutectic Solvent by Liquid-Liquid Extraction. **Ind. Eng. Chem. Res.**, v. 59, n. 2, p. 846–855, 2020. doi: 10.1021/acs.iecr.9b04371.

[49] R. R. Ginting, A. Mustain, and G. Wibawa. Determination of ternary liquid-liquid equilibria for dimethyl carbonate + 2-methyl-1-propanol or 2-methyl-2-propanol + water systems at T = 303.15 and 313.15 K. **J. Chem. Eng. Data**, v. 62, n. 1, p. 463–468, 2017. doi: 10.1021/acs.jced.6b00763.

[50] S. Altway, S. C. Pujar, and A. B. de Haan. Effect of 1-ethyl-3-methylimidazolium tetrafluoroborate on the phase equilibria for systems containing 5-hydroxymethylfurfural, water, organic solvent in the absence and presence of sodium chloride. **J. Chem. Thermodyn.**, v. 132, p. 257–267, 2019. doi: 10.1016/j.jct.2019.01.001.

[51] T. Wannachod, M. Hronec, T. Soták, K. Fulajtárová, U. Pancharoen, and A. Arpornwichanop. Effects of salt on the LLE and tie-line data for furfuryl alcohol - N-butanol-water at T = 298.15 K. **J. Mol. Liq.**, v. 218, p. 50–58, 2016. doi: 10.1016/j.molliq.2016.02.027.

[52] A. Bharti and T. Banerjee. Enhancement of bio-oil derived chemicals in aqueous phase using ionic liquids: Experimental and COSMO-SAC predictions using a modified hydrogen bonding expression. **Fluid Phase Equilib.**, v. 400, p. 27–37, 2015, doi: 10.1016/j.fluid.2015.04.029.

[53] E. Auger, C. Coquelet, A. Valtz, M. Nala, P. Naidoo, and D. Ramjugernath. Equilibrium data and GC-PC SAFT predictions for furanic extraction. **Fluid Phase Equilib.**, v. 430, p. 57–66, 2016. doi: 10.1016/j.fluid.2016.09.019.

[54] S. J. Park, J. K. Moon, and B. H. Um. Evaluation of the efficiency of solvent systems to remove acetic acid derived from pre-pulping extraction. **J. Korean Wood Sci. Technol.**, v. 41, n. 5, p. 447–455, 2013. doi: 10.5658/WOOD.2013.41.5.447.

[55] K. Moodley, C. L. Dorsamy, C. Narasigadu, and Y. Vemblanathan. Excess Properties and Phase Equilibria for the Potential Biofuel System of Propan-2-ol and 2-Methyl-propan-1-ol at 333.15, 343.15, and 353.15 K. **J. Chem. Eng. Data**, v. 63, n. 6, p. 2106–2113, 2018. doi: 10.1021/acs.jced.8b00103.

[56] M. Klajmon, K. Řehák, M. Matoušová, and P. Morávek. Experimental and Computational Study on Liquid-Liquid Equilibrium in Ternary Systems of γvalerolactone, Toluene, and Hydrocarbons. **J. Chem. Eng. Data**, v. 61, n. 1, p. 391–397, 2016. doi: 10.1021/acs.jced.5b00611.

[57] R. C. Basso, A. J. D. A. Meirelles, and E. A. C. Batista. Experimental data, thermodynamic modeling and sensitivity analyses for the purification steps of ethyl biodiesel from fodder radish oil production. **Brazilian J. Chem. Eng.**, v. 34, n. 1, pp. 341–353, 2017, doi: 10.1590/0104-6632.20170341s20140197.

[58] A. Cháfer, J. De La Torre, J. B. Montón, and E. Lladosa; Experimental Determination and Correlation of Liquid-Liquid Equilibria Data for a System of Water + Ethanol + 1-Butyl-3-methylimidazolium Hexafluorophosphate at Different Temperatures. **J. Chem. Eng. Data**, v. 62, n. 2, p. 773–779, 2017. doi: 10.1021/acs.jced.6b00829.

[59] H. Quinteros-Lama, M. Cartes, A. Mejía, and H. Segura. Experimental determination and theoretical modeling of the vapor-liquid equilibrium and densities of the binary system butan-2-ol+tetrahydro-2H-pyran. **Fluid Phase Equilib.**, v. 342, n. 2010, p. 52–59, 2013. doi: 10.1016/j.fluid.2012.12.021.

[60] L. D. Simoni, A. Chapeaux, J. F. Brennecke, and M. A. Stadtherr. Extraction of biofuels and biofeedstocks from aqueous solutions using ionic liquids. **Comput. Chem. Eng.**, v. 34, n. 9, p. 1406–1412, 2010. doi: 10.1016/j.compchemeng.2010.02.020.

[61] M. I. Campos-Franzani et al. Extraction of guaiacol from hydrocarbons as an alternative for the upgraded bio-oil purification: Experimental and computational thermodynamic study. **Fuel**, v. 280, n. May, p. 118405, 2020. doi: 10.1016/j.fuel.2020.118405.

[62] E. Suarez Garcia, C. A. Suarez Ruiz, T. Tilaye, M. H. M. Eppink, R. H. Wijffels, and C. van den Berg. Fractionation of proteins and carbohydrates from crude microalgae extracts using an ionic liquid based-aqueous two phase system. **Sep. Purif. Technol.**, v. 204, n. April, p. 56–65, 2018. doi: 10.1016/j.seppur.2018.04.043.

[63] E. S. R. E. Hassan, F. Mutelet, and J. C. Moïse. From the dissolution to the extraction of carbohydrates using ionic liquids. **RSC Adv.**, v. 3, n. 43, p. 20219–20226, 2013. doi: 10.1039/c3ra42640h.

[64] A. Mejía, H. Segura, and M. Cartes. Isobaric vapor-liquid equilibrium and isothermal interfacial tensions for the system ethanol + 2,5-dimethylfuran. **J. Chem. Eng. Data**, v. 58, n. 11, p. 3226–3232, 2013. doi: 10.1021/je400683g.

[65] J. Hou, S. Xu, H. Ding, and T. Sun. Jun Hou, Shimin Xu, Hui Ding, and Tao Sun. **J. Chem. Eng. Data**, v. 57, p. 2632–2639, 2012.

[66] G. Rubio-Pérez, N. Muñoz-Rujas, A. Srhiyer, E. A. Montero, and F. Aguilar. Isobaric vapor-liquid equilibrium, density and speed of sound of binary mixtures 2,2,4-trimethylpentane + 1-butanol or dibutyl ether (DBE) at 101.3 kPa. **Fluid Phase Equilib.**, v. 475, p. 10–17, 2018. doi: 10.1016/j.fluid.2018.07.027.

[67] L. Brits, A. C. Kouakou, A. J. Burger, and C. E. Schwarz. Isobaric Vapor-Liquid-Liquid Phase Equilibria Measurements of Three Ternary Water + 2-Butanone + Aliphatic Alcohol (Ethanol, 1-Propanol, 2-Propanol) Systems at 101.3 kPa. **J. Chem. Eng. Data**, v. 62, n. 6, p. 1767–1775, 2017. doi: 10.1021/acs.jced.6b00725.

[68] A. Zaitseva, H. Laavi, J. P. Pokki, P. Uusi-Kyyny, and V. Alopaeus. Isothermal vapor-liquid equilibrium and excess molar enthalpies of the binary mixtures furfural+methyl isobutyl ketone, +2-butanol and +2-methyl-2-butanol. **Fluid Phase Equilib.**, v. 372, p. 85–99, 2014. doi: 10.1016/j.fluid.2014.03.033.

[69] K. Moodley, P. Naidoo, J. D. Raal, and D. Ramjugernath. Isothermal Vapor-Liquid Equilibrium Measurements for Alcohol + Water/ n-Hexane Azeotropic Systems Using Both Dynamic and Automated Static-Synthetic Methods. **J. Chem. Eng. Data**, v. 64, n. 6, p. 2657–2670, 2019. doi: 10.1021/acs.jced.9b00102.

[70] A. Shariati, A. Azaribeni, P. Hajighahramanzadeh, and Z. Loghmani. Liquid – Liquid Equilibria of Systems Containingsunflower Oil, Ethanol and Water. **APCBEE Procedia**, v. 5, p. 486–490, 2013. doi: 10.1016/j.apcbee.2013.05.082.

[71] M. Maghami, J. Yousefi Seyf, S. M. Sadrameli, and A. Haghtalab. Liquid-liquid phase equilibrium in ternary mixture of waste fish oil biodiesel-methanol-glycerol: Experimental data and thermodynamic modeling. **Fluid Phase Equilib.**, v. 409, p. 124–130, 2016. doi: 10.1016/j.fluid.2015.09.046.

[72] A. Bharti et al. Liquid-liquid equilibria and COSMO-SAC modeling of organic solvent/ionic liquid - hydroxyacetone - water mixtures. **Fluid Phase Equilib.**, v. 462, p. 73–84, 2018. doi: 10.1016/j.fluid.2018.01.026.

[73] A. Kilina, G. Kuranov, I. Pukinsky, and N. Smirnova. Liquid-liquid equilibria for multicomponent mixtures of 2,2-dimethyl-1,3-dioxolane with n-heptane, toluene, ethanol and water. **Fluid Phase Equilib.**, v. 380, p. 93–99, 2014. doi: 10.1016/j.fluid.2014.08.002.

[74] A. Samarov, I. Prikhodko, N. Shner, G. Sadowski, C. Held, and A. Toikka. Liquid-Liquid Equilibria for Separation of Alcohols from Esters Using Deep Eutectic Solvents Based on Choline Chloride: Experimental Study and Thermodynamic Modeling. **J. Chem. Eng. Data**, v. 64, n. 12, p. 6049–6059, 2019. doi:

10.1021/acs.jced.9b00884.

[75] M. Yakovleva, E. Vorobyov, I. Pukinsky, I. Prikhodko, G. Kuranov, and N. Smirnova. Liquid-liquid equilibria for ternary mixtures of 2,2-dimethyl-1,3-dioxolane-4-methanol with n-heptane, toluene, ethanol and water. **Fluid Phase Equilib.**, v. 405, p. 107–113, 2015. doi: 10.1016/j.fluid.2015.07.016.

[76] A. Asoodeh, F. Eslami, and S. M. Sadrameli. Liquid–liquid equilibria of systems containing linseed oil biodiesel + methanol + glycerol: Experimental data and thermodynamic modeling. **Fuel**, v. 253, n. April, p. 460–473, 2019. doi: 10.1016/j.fuel.2019.04.170.

[77] S. Altway, S. C. Pujar, and A. B. de Haan. Liquid-liquid equilibria of ternary and quaternary systems involving 5-hydroxymethylfurfural, water, organic solvents, and salts at 313.15 K and atmospheric pressure. **Fluid Phase Equilib.**, v. 475, p. 100–110, 2018. doi: 10.1016/j.fluid.2018.07.034.

[78] A. Cháfer, J. De La Torre, A. Font, and E. Lladosa. Liquid-Liquid Equilibria of Water + Ethanol + 1-Butyl-3-methylimidazolium Bis(trifluoromethanesulfonyl)imide Ternary System: Measurements and Correlation at Different Temperatures. **J. Chem. Eng. Data**, v. 60, n. 8, p. 2426–2433, 2015. doi: 10.1021/acs.jced.5b00301.

[79] C. Stephan, M. Dicko, P. Stringari, and C. Coquelet. Liquid-liquid equilibria of water + solutes (acetic acid/ acetol/furfural/guaiacol/methanol/phenol/propanal) + solvents (isopropyl acetate/toluene) ternary systems for pyrolysis oil fractionation. **Fluid Phase Equilib.**, v. 468, p. 49–57, 2018. doi: 10.1016/j.fluid.2018.04.016.

[80] M. Toikka, D. Trofimova, and A. Samarov. Liquid-liquid equilibrium and critical states for the quaternary system propionic acid–n-butanol–n-butyl propionate–water at 303.15 K. **Fluid Phase Equilib.**, v. 460, p. 17–22, 2018. doi: 10.1016/j.fluid.2017.12.023.

[81] J. L. A. Dagostin, D. Carpiné, P. R. S. Dos Santos, and M. L. Corazza. Liquid-liquid equilibrium and kinetics of ethanolic extraction of soybean oil using ethyl acetate as co-solvent. **Brazilian J. Chem. Eng.**, v. 35, n. 2, p. 415–427, 2018. doi: 10.1590/0104-6632.20180352s20160175.

[82] S. Shiozawa, D. Gonçalves, M. C. Ferreira, A. J. A. Meirelles, and E. A. C. Batista. Liquid-liquid equilibrium data and thermodynamic modeling of systems involved in the biodiesel production in terms of acylglycerols, free fatty acids, ethyl esters, and ethanol at 303.2 and 318.2 K and local pressure. **Fluid Phase Equilib.**, v. 507, p. 112431, 2020. doi: 10.1016/j.fluid.2019.112431.

[83] L. Hadlich de Oliveira, G. P. Morgado, R. Boni, L. R. Roque, R. R. Pinto, and S. C. Rabelo. Liquid-liquid equilibrium data and thermophysical properties for ternary systems composed of water, acetic acid and different solvents. **Fluid Phase Equilib.**, v. 482, p. 48–63, 2019. doi: 10.1016/j.fluid.2018.10.021.

[84] K. V. M. Cavalcanti, L. M. Follegatti-Romero, I. Dalmolin, and L. A. Follegatti-Romero. Liquid-liquid equilibrium for (water + 5-hydroxymethylfurfural + 1-pentanol/1-

hexanol/1-heptanol) systems at 298.15 K. **J. Chem. Thermodyn.**, v. 138, p. 59–66, 2019. doi: 10.1016/j.jct.2019.06.010.

[85] J. Liu, Y. Yuan, Y. Pan, Z. Huang, and B. Yang. Liquid-liquid equilibrium for systems of glycerol and glycerol tert-butyl ethers. **Fluid Phase Equilib.**, v. 365, p. 50–57, 2014. doi: 10.1016/j.fluid.2013.12.012.

[86] T. Santos, J. F. Gomes, and J. Puna. Liquid-liquid equilibrium for ternary system containing biodiesel, methanol and water. **J. Environ. Chem. Eng.**, v. 6, n. 1, p. 984–990, 2018. doi: 10.1016/j.jece.2017.12.068.

[87] F. M. R. Mesquita, N. S. Evangelista, H. B. De Sant'Ana, and R. S. De Santiago-Aguiar. Liquid-liquid equilibrium for the glycerol + alcohol + coconut biodiesel system at different temperatures and atmospheric pressure. **J. Chem. Eng. Data**, v. 57, n. 12, p. 3557–3562, 2012. doi: 10.1021/je300749n.

[88] L. Zhang et al. Liquid-Liquid Equilibrium for the Ternary Systems Water + 1-Butanol + 1-Hexanol or 1-Octanol at 303.15, 313.15, and 323.15 K. **J. Chem. Eng. Data**, v. 65, n. 2, p. 477–486, 2020. doi: 10.1021/acs.jced.9b00479.

[89] A. L. Esipovich, A. E. Rogozhin, A. S. Belousov, E. A. Kanakov, K. V. Otopkova, and S. M. Danov. Liquid–liquid equilibrium in the systems FAMEs + vegetable oil + methyl alcohol and FAMEs + glycerol + methyl alcohol. **Fuel**, v. 217, n. December 2017, p. 31–37, 2018. doi: 10.1016/j.fuel.2017.12.083.

[90] J. H. Yim, K. W. Park, J. S. Lim, and K. Y. Choi. Liquid-Liquid Equilibrium Measurements for the Ternary System of Water/2,3-Butanediol/4-Methyl-2-pentanol at Various Temperatures. **J. Chem. Eng. Data**, v. 64, n. 9, p. 3882–3888, 2019. doi: 10.1021/acs.jced.9b00290.

[91] M. Glass, M. Aigner, J. Viell, A. Jupke, and A. Mitsos. Liquid-liquid equilibrium of 2-methyltetrahydrofuran/water over wide temperature range: Measurements and rigorous regression. **Fluid Phase Equilib.**, v. 433, p. 212–225, 2017. doi: 10.1016/j.fluid.2016.11.004.

[92] M. Trofimova et al. Liquid-liquid equilibrium of acetic acid – ethanol – ethyl acetate – water quaternary system: Data review and new results at 323.15 K and 333.15 K. **Fluid Phase Equilib.**, v. 503, 2020. doi: 10.1016/j.fluid.2019.112321.

[93] A. Samarov, N. Shner, E. Mozheeva, and A. Toikka. Liquid-liquid equilibrium of alcohol–ester systems with deep eutectic solvent on the base of choline chloride. **J. Chem. Thermodyn.**, v. 131, p. 369–374, 2019. doi: 10.1016/j.jct.2018.11.019.

[94] M. C. Ferreira, L. C. B. A. Bessa, S. Shiozawa, A. J. A. Meirelles, and E. A. C. Batista. Liquid-liquid equilibrium of systems containing triacylglycerols (canola and corn oils), diacylglycerols, monoacylglycerols, fatty acids, ester and ethanol at T/K=303.15 and 318.15. **Fluid Phase Equilib.**, v. 404, p. 32–41, 2015. doi: 10.1016/j.fluid.2015.06.027.

[95] N. Montesantos, M. Chirullo, and M. Maschietti. Liquid-Liquid Equilibrium of

Water + 2-Methoxyphenol + Methyl Isobutyl Ketone and Water + 1,2-Benzenediol + Methyl Isobutyl Ketone at 303.15 K and 328.15 K. **J. Chem. Eng. Data**, v. 63, n. 3, pp. 712–722, 2018. doi: 10.1021/acs.jced.7b00887.

[96] S. Shekarsaraee. Liquid-liquid equilibrium study for the system (water + phosphoric acid + propylene carbonate) at different temperatures. **J. Chem. Thermodyn.**, v. 104, p. 16–23, 2017. doi: 10.1016/j.jct.2016.09.008.

[97] R. Verma and T. Banerjee. Liquid-Liquid Extraction of Lower Alcohols Using Menthol-Based Hydrophobic Deep Eutectic Solvent: Experiments and COSMO-SAC Predictions. **Ind. Eng. Chem. Res.**, v. 57, n. 9, p. 3371–3381, 2018. doi: 10.1021/acs.iecr.7b05270.

[98] V. Gomis, A. Font, M. D. Saquete, and J. García-Cano. LLE, VLE and VLLE data for the water-n-butanol-n-hexane system at atmospheric pressure. **Fluid Phase Equilib.**, v. 316, p. 135–140, 2012. doi: 10.1016/j.fluid.2011.11.025.

[99] N. Galeotti, J. Burger, and H. Hasse. Measurement and Modeling of Phase Equilibria in Systems Containing Water, Xylose, Furfural, and Acetic Acid. **J. Chem. Eng. Data**, v. 64, n. 6, p. 2634–2640, 2019. doi: 10.1021/acs.jced.9b00095.

[100] S. Mardani, H. Laavi, E. Bouget, J. P. Pokki, P. Uusi-Kyyny, and V. Alopaeus. Measurements and modeling of LLE and HE for (methanol + 2,4,4-trimethyl-1-pentene), and LLE for (water + methanol + 2,4,4-trimethyl-1-pentene). **J. Chem. Thermodyn.**, v. 85, p. 120–128, 2015. doi: 10.1016/j.jct.2015.01.013.

[101] A. Merzougui, A. Bonilla-Petriciolet, A. Hasseine, D. Laiadi, and N. Labed. Modeling of liquid-liquid equilibrium of systems relevant for biodiesel production using Backtracking Search Optimization. **Fluid Phase Equilib.**, v. 388, p. 84–92, 2015. doi: 10.1016/j.fluid.2014.12.041.

[102] L. Fernández, E. Pérez, J. Ortega, J. Canosa, and J. Wisniak. Multiproperty modeling for a set of binary systems. Evaluation of a model to correlate simultaneously several mixing properties of methyl ethanoate+alkanes and new experimental data. **Fluid Phase Equilib.**, v. 341, p. 105–123, 2013. doi: 10.1016/j.fluid.2012.12.027.

[103] X. Wang, S. Li, H. Bai, and C. Liu. New Predictive Nonrandom Two Liquid Equation for Solid-Liquid Phase Equilibrium in n-Alkanes Mixture with Multiple Solid Solutions. **Ind. Eng. Chem. Res.**, v. 58, n. 39, p. 18411–18421, 2019. doi: 10.1021/acs.iecr.9b03678.

[104] J. F. O. Granjo, D. S. Nunes, B. P. M. Duarte, and N. M. C. Oliveira. A comparison of process alternatives for energy-efficient bioethanol downstream processing. **Sep. Purif. Technol.**, v. 238, p. 116414, 2020. doi: 10.1016/j.seppur.2019.116414.

[105] M. Hakim, H. Abedini Najafabadi, G. Pazuki, and M. Vossoughi. Novel approach for liquid-liquid phase equilibrium of biodiesel (canola and sunflower) + glycerol + methanol. **Ind. Eng. Chem. Res.**, v. 53, n. 2, p. 855–864, 2014. doi: 10.1021/ie4031902.

[106] C. C. R. S. Rossi, L. Cardozo-Filho, and R. Guirardello. Parameter estimation and thermodynamic model fitting for components in mixtures for bio-diesel production. **Clean Technol. Environ. Policy**, v. 14, n. 3, p. 435–442, 2012. doi: 10.1007/s10098-012-0463-8.

[107] P. Dehury, U. Mahanta, and T. Banerjee. Partitioning of butanol between a hydrophobic ionic liquid and aqueous phase: Insights from Liquid Liquid Equilibria measurements and Molecular Dynamics simulations. **Fluid Phase Equilib.**, v. 425, p. 421–431, 2016. doi: 10.1016/j.fluid.2016.06.007.

[108] A. J. Resk, L. Peereboom, A. K. Kolah, D. J. Miller, and C. T. Lira. Phase equilibria in systems with levulinic acid and ethyl levulinate. **J. Chem. Eng. Data**, v. 59, n. 4, p. 1062–1068, 2014. doi: 10.1021/je400814n.

[109] K. Bayazit, A. Gök, H. Uslu, and Ş. I. Kirbaşla. Phase equilibria of (water+butyric acid+butyl acetate) ternary systems at different temperatures. **Fluid Phase Equilib.**, v. 379, p. 185–190, 2014. doi: 10.1016/j.fluid.2014.07.023.

[110] V. Gomis, M. D. Saquete, A. Font, J. García-Cano, and I. Martínez-Castellanos. Phase equilibria of the water + 1-butanol + 2-pentanol ternary system at 101.3 kPa. **J. Chem. Thermodyn.**, v. 123, p. 38–45, 2018. doi: 10.1016/j.jct.2018.03.024.

[111] V. Gomis, A. Font, M. D. Saquete, and J. García-Cano. Phase equilibria of the water+1-butanol+toluene ternary system at 101.3 kPa. **Fluid Phase Equilib.**, v. 385, p. 29–36, 2015. doi: 10.1016/j.fluid.2014.10.038.

[112] F. Muhammad, M. B. Oliveira, P. Pignat, J. N. Jaubert, S. P. Pinho, and L. Coniglio. Phase equilibrium data and modeling of ethylic biodiesel, with application to a non-edible vegetable oil. **Fuel**, v. 203, p. 633–641, 2017. doi: 10.1016/j.fuel.2017.05.007.

[113] U. Domańska, M. Królikowski, M. Wlazlo, and M. Wieckowski. Phase Equilibrium Investigation on 2-Phenylethanol in Binary and Ternary Systems: Influence of High Pressure on Density and Solid-Liquid Phase Equilibrium. **J. Phys. Chem. B**, v. 122, n. 23, p. 6188–6197, 2018. doi: 10.1021/acs.jpcb.8b02500.

[114] A. A. Albuquerque, F. T. T. Ng, L. Danielski, and L. Stragevitch. Phase equilibrium modeling in biodiesel production by reactive distillation. **Fuel**, v. 271, n. December 2019, p. 117688, 2020. doi: 10.1016/j.fuel.2020.117688.

[115] T. H. E. D. Zation, O. F. Ternary, and P. Diagrams - The determination and characterization of ternary phase diagrams, 2019.

[116] J. Pla-Franco, E. Lladosa, S. Loras, and J. B. Montón. Proposal of Isobutyl Alcohol as Entrainer To Separate Mixtures Formed by Ethanol and Water and 1-Propanol and Water. **J. Chem. Eng. Data**, v. 62, n. 9, p. 2697–2707, 2017. doi: 10.1021/acs.jced.7b00098.

[117] G. R. Harvianto et al. Purification of 2,3-butanediol from fermentation broth:

Process development and techno-economic analysis. **Biotechnol. Biofuels**, v. 11, n. 1, p. 1–16, 2018. doi: 10.1186/s13068-018-1013-3.

[118] A. Smirnov, A. Sadaeva, K. Podryadova, and M. Toikka. Quaternary liquid-liquid equilibrium, solubility and critical states: Acetic acid – n-butanol – n-butyl acetate – water at 318.15 K and atmospheric pressure. **Fluid Phase Equilib.**, v. 493, p. 102–108, 2019. doi: 10.1016/j.fluid.2019.04.020.

[119] Y. Xie, F. Yu, Y. Wang, X. He, S. Zhou, and H. Cui. Salt effect on liquid–liquid equilibria of tetrahydrofuran/water/5-hydroxymethylfurfural systems. **Fluid Phase Equilib.**, v. 493, p. 137–143, 2019. doi: 10.1016/j.fluid.2019.04.018.

[120] U. Domańska, K. Paduszyński, M. Królikowski, and A. Wróblewska. Separation of 2-Phenylethanol from Water by Liquid-Liquid Extraction with Ionic Liquids: New Experimental Data and Modeling with Modern Thermodynamic Tools. **Ind. Eng. Chem. Res.**, v. 55, n. 19, p. 5736–5747, 2016. doi: 10.1021/acs.iecr.6b00375.

[121] C. M. S. S. Neves, J. F. O. Granjo, M. G. Freire, A. Robertson, N. M. C. Oliveira, and J. A. P. Coutinho. Separation of ethanol–water mixtures by liquid–liquid extraction using phosphonium-based ionic liquids. **Green Chem.**, v. 13, n. 6, p. 1517–1526, 2011. doi: 10.1039/c1gc15079k.

[122] L. Zhang et al. Separation of the mixture pyridine + methylbenzene via several acidic ionic liquids: Phase equilibrium measurement and correlation. **Fluid Phase Equilib.**, v. 440, p. 103–110, 2017. doi: 10.1016/j.fluid.2017.03.009.

[123] U. Domańska, M. Wlazło, and M. Karpińska. Separation of water/butan-1-ol with ionic liquids in ternary liquid-liquid phase equilibrium. **J. Chem. Thermodyn.**, v. 134, p. 76–83, 2019. doi: 10.1016/j.jct.2019.03.001.

[124] A. Marcilla, M. M. Olaya, and J. A. Reyes-Labarta. Simultaneous VLLE data correlation for ternary systems: Modification of the NRTL equation for improved calculations. **Fluid Phase Equilib.**, v. 426, p. 47–55, 2016. doi: 10.1016/j.fluid.2015.12.047.

[125] K. H. Lee, J. E. Gu, H. Y. Oh, and S. J. Park. Solid-liquid phase equilibria, excess molar volume, and molar refraction deviation for the mixtures of ethanoic acid with propanoic, butanoic, and pentanoic acid. **Korean J. Chem. Eng.**, v. 35, n. 8, p. 1710–1715, 2018, doi: 10.1007/s11814-018-0072-2.

[126] U. Domańska, M. Wlazło, Z. Dąbrowski, and A. Wiśniewska. Ammonium ionic liquids in separation of water/butan-1-ol using liquid-liquid equilibrium diagrams in ternary systems. **Fluid Phase Equilib.**, v. 485, p. 23–31, 2019. doi: 10.1016/j.fluid.2018.12.009.

[127] M. Okuniewski, D. Ramjugernath, P. Naidoo, and U. Domańska. Solubility data and modeling for sugar alcohols in ionic liquids. **J. Chem. Thermodyn.**, v. 77, p. 23–30, 2014. doi: 10.1016/j.jct.2014.04.021.

[128] E. S. R. E. Hassan, F. Mutelet, S. Pontvianne, and J. C. Moïse. Studies on the

dissolution of glucose in ionic liquids and extraction using the antisolvent method. **Environ. Sci. Technol.**, v. 47, n. 6, p. 2809–2816, 2013. doi: 10.1021/es303884n.

[129] A. Cháfer, J. de la Torre, E. Lladosa, and S. Loras. Study of liquid–liquid equilibria at different temperatures of water + ethanol + 1-butyl-1-methylpyrrolidinium bis(trifluoromethylsulfonyl)imide ternary system. **Fluid Phase Equilib.**, v. 426, p. 3–9, 2016. doi: 10.1016/j.fluid.2016.02.003.

[130] M. D. Saquete, A. Font, J. García-Cano, and I. Blasco. Study of the LLE, VLE, and VLLE of the Ternary System Water + 1-Butanol + Isoamyl Alcohol at 101.3 kPa. **J. Chem. Eng. Data**, v. 63, n. 10, p. 3733–3743, 2018. doi: 10.1021/acs.jced.8b00308.

[131] A. Marciniak, M. Wlazło, and J. Gawkowska. Ternary (liquid + liquid) equilibria of {bis(trifluoromethylsulfonyl)-amide based ionic liquids + butan-1-ol + water. **J. Chem. Thermodyn.**, v. 94, p. 96–100, 2016. doi: 10.1016/j.jct.2015.11.002.

[132] X. Xu, W. Liu, M. Li, Y. Ri, and Y. Wang. Ternary liquid-liquid equilibrium of azeotropes (Ester + Alcohol) with Different Ionic Liquids at T = 298.15 K. **J. Chem. Eng. Data**, v. 62, n. 1, p. 532–538, 2017. doi: 10.1021/acs.jced.6b00811.

[133] A. Moreau, J. J. Segovia, R. M. Villamañán, and M. C. Martín. Thermodynamic behaviour of second generation biofuels: Vapour-liquid equilibria and excess enthalpies of the binary mixtures 2-pentanol and n-heptane or 2,2,4-trimethylpentane. **Fluid Phase Equilib.**, v. 384, p. 89–94, 2014. doi: 10.1016/j.fluid.2014.10.016.

[134] A. Moreau, M. C. Martín, C. R. Chamorro, and J. J. Segovia. Thermodynamic characterization of second generation biofuels: Vapour-liquid equilibria and excess enthalpies of the binary mixtures 1-pentanol and cyclohexane or toluene. **Fluid Phase Equilib.**, v. 317, p. 127–131, 2012. doi: 10.1016/j.fluid.2012.01.007.

[135] A. Moreau, J. J. Segovia, J. Rubio, and M. C. Martín. Thermodynamics properties, VLE and HE, of the systems 2-pentanol and cyclohexane or methylbenzene for contributing to the knowledge of new biofuels. **Fluid Phase Equilib.**, v. 409, p. 92–97, 2016. doi: 10.1016/j.fluid.2015.09.035.

[136] L. R. S. Kanda, K. C. dos Santos, J. T. F. Santos, F. C. Paes, F. A. P. Voll, and M. L. Corazza. Vapor-liquid and liquid-liquid equilibrium modeling of systems involving ethanol, water, and ethyl valerate (valeric acid) using the PC-SAFT equation of state. **Fluid Phase Equilib.**, v. 474, 2018. doi: 10.1016/j.fluid.2018.07.014.

[137] C. B. S. Araújo, Leonete Cristina de. Brazilian Journal of Development. **J. Dev.**, v. 6, n. 1, p. 4303–4308, 2020. doi: 10.34117/bjdv5n10-057.

[138] P. Parthasarathy and S. K. Narayanan. Effect of Hydrothermal Carbonization Reaction Parameters. **Environ. Prog. Sustain. Energy**, v. 33, n. 3, p. 676–680, 2014. doi: 10.1002/ep.

[139] L. Salemme, G. Olivieri, F. Raganati, P. Salatino, and A. Marzocchella. Analysis of the energy efficiency of some butanol recovery processes. **Chem. Eng. Trans.**, v. 49, n. November 2017, p. 109–114, 2016. doi: 10.3303/CET1649019.

[140] A. F. Martínez, C. A. Sánchez, A. Orjuela, and G. Rodríguez. Isobutyl acetate by reactive distillation. Non-reactive phase equilibrium and topological analysis. **Fluid Phase Equilib.**, v. 516, 2020. doi: 10.1016/j.fluid.2020.112612.

[141] A. Orjuela, A. J. Yanez, D. T. Vu, D. Bernard-Brunel, D. J. Miller, and C. T. Lira. Phase equilibria for reactive distillation of diethyl succinate. Part I. System diethyl succinate + ethanol + water. **Fluid Phase Equilib.**, v. 290, n. 1–2, p. 63–67, 2010. doi: 10.1016/j.fluid.2009.11.014.

[142] A. Orjuela, A. J. Yanez, J. Evans, A. M. Hassan, D. J. Miller, and C. T. Lira. Phase equilibria in binary mixtures with monoethyl succinate. **Fluid Phase Equilib.**, v. 309, n. 2, p. 121–127, 2011. doi: 10.1016/j.fluid.2011.06.020.

[143] K. Zheng, H. Wu, C. Geng, G. Wang, Y. Yang, and Y. Li. A Comparative Study of the Perturbed-Chain Statistical Associating Fluid Theory Equation of State and Activity Coefficient Models in Phase Equilibria Calculations for Mixtures Containing Associating and Polar Components. **Ind. Eng. Chem. Res.**, v. 57, n. 8, p. 3014–3030, 2018, doi: 10.1021/acs.iecr.7b04758.

[144] N. S. Graça, L. S. Pais, V. M. T. M. Silva, and A. E. Rodrigues. Dynamic study of the synthesis of 1,1-dibutoxyethane in a fixed-bed adsorptive reactor. **Sep. Sci. Technol.**, v. 46, n. 4, p. 631–640, 2011. doi: 10.1080/01496395.2010.534121.

[145] S. Doungsri, T. Sookkumnerd, A. Wongkoblap, and A. Nuchitprasittichai. Equilibrium study for ternary mixtures of biodiesel. **IOP Conf. Ser. Mater. Sci. Eng.**, v. 273, p. 012008, 2017. doi: 10.1088/1757-899x/273/1/012008.

[146] Y. Y. Wu, D. T. Pan, J. W. Zhu, K. Chen, B. Wu, and Y. L. Shen. Isobaric Vapor-Liquid-Liquid Equilibria for 1-Butanol + Water + 2,3-Butanediol at 101.3 kPa. **Chem. Eng. Commun.**, v. 202, n. 2, p. 175–180, 2015. doi: 10.1080/00986445.2013.836632.

[147] Q. Zhang, W. Peng, and Y. Chen. Liquid–Liquid Equilibria for Ethanol or 2-Propanol Aqueous Solutions with sec-Butyl Acetate at Four Temperatures. **J. Solution Chem.**, v. 48, n. 6, p. 807–817, 2019. doi: 10.1007/s10953-019-00894-y.

[148] A. A. Evangelista Neto, J. C. C. Sobrinho, H. N. M. Oliveira, H. F. S. Freitas, F. F. M. Silva, and E. L. Barros Neto. Liquid-Liquid Equilibrium Data for the Pseudo-Ternary Biodiesel of Chicken Fat + Methanol + Glycerol. **Brazilian J. Pet. Gas**, v. 12, n. 2, p. 123–133, 2018. doi: 10.5419/bjpg2018-0012.

[149] J. A. P. Coutinho et al. Measurement and modeling of biodiesel cold-flow properties. **Energy and Fuels**, v. 24, n. 4, p. 2667–2674, 2010. doi: 10.1021/ef901427g.

[150] M. Detcheberry et al. Thermodynamic modeling of the condensable fraction of a gaseous effluent from lignocellulosic biomass torrefaction. **Fluid Phase Equilib.**, v. 409, p. 242–255, 2016. doi: 10.1016/j.fluid.2015.09.025.

[151] M. A. Mazutti et al. Thermophysical properties of biodiesel and related systems:

(Liquid + liquid) equilibrium data for castor oil biodiesel. **J. Chem. Thermodyn.**, v. 62, p. 17–26, 2013. doi: 10.1016/j.jct.2013.02.016.

[152] O. Ershova, J. P. Pokki, A. Zaitseva, V. Alopaeus, and H. Sixta. Vapor pressure, vapor-liquid equilibria, liquid-liquid equilibria and excess enthalpy of the system consisting of isophorone, furfural, acetic acid and water. **Chem. Eng. Sci.**, v. 176, p. 19–34, 2018. doi: 10.1016/j.ces.2017.10.017.

[153] M. Männistö, J. P. Pokki, H. Haapaniemi, and V. Alopaeus. Quaternary, ternary, and binary lle measurements for 2-methoxy-2-methylpropane + furfural + acetic acid + water at temperatures between 298 and 307 K. **J. Chem. Eng. Data**, v. 61, n. 7, p. 2458–2466, 2016. doi: 10.1021/acs.jced.6b00149.

[154] M. R. Urdaneta, S. I. Garc, A. M. Faneite, D. Soto, and A. A. Cesar. Isothermal Vapor À Liquid Equilibrium Data of Propan-1-ol + 2,2. p. 3346–3350, 2011.

[155] M. Benziane, K. Khimeche, I. Mokbel, D. Trache, N. Yagoubi, and J. Jose. Phase equilibrium properties of binary mixtures containing a diesel compound (n-dodecane) + biodiesel compounds (ethyl hexanoate, ethyl decanoate and ethyl tetradecanoate). **J. Therm. Anal. Calorim.**, v. 126, n. 2, p. 845–854, 2016. doi: 10.1007/s10973-016-5561-0.

[156] C. E. S. Dantas and R. Ceriani. Prediction of liquid-liquid equilibria of multicomponent fatty systems using the ASOG method. **Fluid Phase Equilib.**, v. 506, p. 112400, 2020. doi: 10.1016/j.fluid.2019.112400.

[157] M. Hajiw, A. Valtz, E. El Ahmar, and C. Coquelet. Apparent Henry's law constants of furan in different n-alkanes and alcohols at temperatures from 293 to 323K. **J. Environ. Chem. Eng.**, v. 5, n. 1, p. 1205–1209, 2017. doi: 10.1016/j.jece.2017.02.001.

[158] J. Li and P. Paricaud. Application of the conduct-like screening models for real solvent and segment activity coefficient for the predictions of partition coefficients and vapor-liquid and liquid-liquid equilibria of Bio-oil-related mixtures. **Energy and Fuels**, v. 26, n. 6, p. 3756–3768, 2012. doi: 10.1021/ef300181j.

[159] G. D. Machado, M. Castier, A. P. Voll, V. F. Cabral, L. Cardozo-Filho, and D. A. G. Aranda. Ethanol and methanol Unifac subgroup parameter estimation in the prediction of the liquid-liquid equilibrium of biodiesel systems. **Fluid Phase Equilib.**, v. 488, p. 79–86, 2019. doi: 10.1016/j.fluid.2019.01.012.

[160] D. S. Damaceno, O. A. Perederic, R. Ceriani, G. M. Kontogeorgis, and R. Gani. Improvement of predictive tools for vapor-liquid equilibrium based on group contribution methods applied to lipid technology. **Fluid Phase Equilib.**, v. 470, p. 249–258, 2018. doi: 10.1016/j.fluid.2017.12.009.

[161] M. A. Noriega, P. C. Narváez, A. D. Imbachi, J. G. Cadavid, and A. C. Habert. Liquid-liquid equilibrium for biodiesel-glycerol-methanol or ethanol systems using UNIFAC correlated parameters. **Energy**, v. 111, p. 841–849, 2016. doi: 10.1016/j.energy.2016.06.031.

[162] A. C. de S. Maia, I. S. e Silva, and L. Stragevitch. Liquid-Liquid Equilibrium of Methyl Esters of Fatty Acid/Methanol/Glycerol and Fatty Acid Ethyl Esters/Ethanol/Glycerol: A Case Study for Biodiesel Application. **Int. J. Chem. Eng. Appl.**, v. 4, n. 5, p. 285–289, 2013. doi: 10.7763/ijcea.2013.v4.311.

[163] L. C. B. A. Bessa, E. A. C. Batista, and A. J. A. Meirelles. Liquid-liquid equilibrium of systems composed of soybean oil + monoacylglycerols + diacylglycerols + ethyl oleate + oleic acid + ethanol at 303.15 and 318.15 K. **Brazilian J. Chem. Eng.**, v. 35, n. 2, p. 373–382, 2018. doi: 10.1590/0104-6632.20180352s20160271.

[164] M. C. Ferreira, L. C. B. A. Bessa, C. R. A. Abreu, A. J. A. Meirelles, and E. A. Caldas Batista. Liquid-liquid equilibrium of systems containing triolein + (fatty acid/ partial acylglycerols/ester) + ethanol: Experimental data and UNIFAC modeling. **Fluid Phase Equilib.**, v. 476, p. 186–192, 2018. doi: 10.1016/j.fluid.2018.07.030.

[165] O. A. Perederic et al. Process Analysis of Shea Butter Solvent Fractionation Using a Generic Systematic Approach. **Ind. Eng. Chem. Res.**, v. 59, n. 19, p. 9152–9164, 2020. doi: 10.1021/acs.iecr.9b06719.

[166] N. H. Dong, de H. Jean-Charles, L. Rafael, P. Jean-Philippe, and T. Pascal. Simultaneous liquid-liquid and vapour-liquid equilibria predictions of selected oxygenated aromatic molecules in mixtures with alkanes, alcohols, water, using the polar GC-PC-SAFT. **Chem. Eng. Res. Des.**, v. 92, n. 12, p. 2912–2935, 2014. doi: 10.1016/j.cherd.2014.05.018.

[167] K. Yui et al. Solid-liquid equilibria in the binary systems of saturated fatty acids or triglycerides (C12 to C18) + hexadecane. **J. Chem. Eng. Data**, v. 62, n. 1, p. 35–43, 2017. doi: 10.1021/acs.jced.6b00355.

[168] O. A. Perederic et al. Systematic identification method for data analysis and phase equilibria modelling for lipids systems. **J. Chem. Thermodyn.**, v. 121, p. 153–169, 2018. doi: 10.1016/j.jct.2018.02.007.

[169] C. L. da Silveira and N. P. G. Salau. The UNIFAC-LLE and COSMO-SAC ternary aqueous LLE calculations. **Fluid Phase Equilib.**, v. 501, p. 112278, 2019. doi: 10.1016/j.fluid.2019.112278.

[170] D. S. Damaceno and R. Ceriani. Vapor-liquid equilibria of monoacylglicerol + monoacylglicerol or alcohol or fatty acid at subatmospheric pressures. **Fluid Phase Equilib.**, v. 452, p. 135–142, 2017. doi: 10.1016/j.fluid.2017.08.013.

[171] M. D. Robustillo, L. C. B. A. Bessa, A. J. de A. Meirelles, and P. de A. Pessôa Filho. Experimental data and thermodynamic modeling of solid-liquid equilibrium of binary systems containing representative compounds of biodiesel and fossil fuels: Ethyl esters and n-hexadecane. **Fuel**, v. 220, n. November 2017, p. 303–317, 2018. doi: 10.1016/j.fuel.2018.01.117.

[172] S. Yoshidomi, Y. Sugami, E. Minami, N. Shisa, H. Hayashi, and S. Saka. Predicting Solid–Liquid Equilibrium of Fatty Acid Methyl Ester and Monoglyceride Mixtures as Biodiesel Model Fuels. **JAOCS, J. Am. Oil Chem. Soc.**, v. 94, n. 8, p.

1087–1094, 2017. doi: 10.1007/s11746-017-3015-x.

[173] K. Paduszyński and U. Domańska. Thermodynamic modeling of ionic liquid systems: Development and detailed overview of novel methodology based on the PC-SAFT. **J. Phys. Chem. B**, v. 116, n. 16, p. 5002–5018, 2012. doi: 10.1021/jp3009207.

[174] W. A. Fouad et al. Extensions of the SAFT model for complex association in the bulk and interface. **Fluid Phase Equilib.**, v. 416, p. 62–71, 2016. doi: 10.1016/j.fluid.2015.11.011.

[175] F. A. Perdomo and A. Gil-Villegas. Predicting thermophysical properties of biodiesel fuel blends using the SAFT-VR approach. **Fluid Phase Equilib.**, v. 306, n. 1, p. 124–128, 2011. doi: 10.1016/j.fluid.2011.02.021.

[176] J. D. Haley and C. McCabe. Predicting the phase behavior of fatty acid methyl esters and their mixtures using the GC-SAFT-VR approach. **Fluid Phase Equilib.**, v. 411, p. 43–52, 2016. doi: 10.1016/j.fluid.2015.11.012.

[177] J. T. Cripwell, F. J. Kruger, and A. J. Burger. Accounting for cross association in non-self-associating species using a physically consistent SAFT-VR Mie approach. **Fluid Phase Equilib.**, v. 483, p. 1–13, 2019. doi: 10.1016/j.fluid.2018.11.003.

[178] F. Llovell and L. F. Vega. Accurate modeling of supercritical CO2 for sustainable processes: Water + CO2 and CO2 + fatty acid esters mixtures. **J. Supercrit. Fluids**, v. 96, p. 86–95, 2015. doi: 10.1016/j.supflu.2014.09.040.

[179] N. Mac Dowell et al. New experimental density data and soft-SAFT models of alkylimidazolium ([CnC1im]+) chloride (Cl-), methylsulfate ([MeSO4]-), and dimethylphosphate ([Me 2PO4]-) based ionic liquids. **J. Phys. Chem. B**, v. 118, n. 23, p. 6206–6221, 2014. doi: 10.1021/jp501619y.

[180] M. Stavrou, M. Lampe, A. Bardow, and J. Gross. Continuous molecular targeting-computer-aided molecular design (CoMT-CAMD) for simultaneous process and solvent design for CO2 capture. **Ind. Eng. Chem. Res.**, v. 53, n. 46, p. 18029–18041, 2014. doi: 10.1021/ie502924h.

[181] J. Janeček and P. Paricaud. Influence of cyclic dimer formation on the phase behavior of carboxylic acids. II. cross-associating systems. **J. Phys. Chem. B**, v. 117, n. 32, p. 9430–9438, 2013. doi: 10.1021/jp4012125.

[182] J. Janecek and P. Paricaud. Influence of cyclic dimer formation on the phase behavior of carboxylic acids. **J. Phys. Chem. B**, v. 116, n. 27, p. 7874–7882, 2012. doi: 10.1021/jp303051j.

[183] A. Nann, C. Held, and G. Sadowski. Liquid − Liquid Equilibria of 1 - Butanol/Water/IL Systems. 2013.

[184] S. E. E. Warrag et al. Oil desulfurization using deep eutectic solvents as sustainable and economical extractants via liquid-liquid extraction: Experimental and PC-SAFT predictions. **Fluid Phase Equilib.**, v. 467, p. 33–44, 2018. doi:

10.1016/j.fluid.2018.03.018.

[185] M. L. Corazza, W. A. Fouad, and W. G. Chapman. PC-SAFT predictions of VLE and LLE of systems related to biodiesel production. **Fluid Phase Equilib.**, v. 416, p. 130–137, 2016. doi: 10.1016/j.fluid.2015.09.044.

[186] E. Razavi, A. Khoshsima, and R. Shahriari. Phase Behavior Modeling of Mixtures Containing N-, S-, and O-Heterocyclic Compounds Using PC-SAFT Equation of State. **Ind. Eng. Chem. Res.**, v. 58, p. 11038–11059, 2019. doi: 10.1021/acs.iecr.9b01429.

[187] E. Altuntepe, A. Reinhardt, J. Brinkmann, T. Briesemann, G. Sadowski, and C. Held. Phase Behavior of Binary Mixtures Containing Succinic Acid or Its Esters. **J. Chem. Eng. Data**, v. 62, n. 7, p. 1983–1993, 2017. doi: 10.1021/acs.jced.7b00005.

[188] K. Paduszyński, M. Okuniewski, and U. Domańska. Renewable feedstocks in green solvents: Thermodynamic study on phase diagrams of d-sorbitol and xylitol with dicyanamide based ionic liquids. **J. Phys. Chem. B**, v. 117, n. 23, p. 7034–7046, 2013. doi: 10.1021/jp401937p.

[189] K. Paduszyński, M. Okuniewski, and U. Domańska. Solid-liquid phase equilibria in binary mixtures of functionalized ionic liquids with sugar alcohols: New experimental data and modelling. **Fluid Phase Equilib.**, v. 403, p. 167–175, 2015. doi: 10.1016/j.fluid.2015.06.002.

[190] K. Paduszyński, E. V. Lukoshko, M. Królikowski, U. Domańska, and J. Szydłowski. Thermodynamic study of binary mixtures of 1-butyl-1-methylpyrrolidinium dicyanamide ionic liquid with molecular solvents: New experimental data and modeling with PC-saft equation of state. **J. Phys. Chem. B**, v. 119, n. 2, p. 543–551, 2015. doi: 10.1021/jp511621j.

[191] E. Altuntepe, V. N. Emel'yanenko, M. Forster-Rotgers, G. Sadowski, S. P. Verevkin, and C. Held. Thermodynamics of enzyme-catalyzed esterifications: II. Levulinic acid esterification with short-chain alcohols. **Appl. Microbiol. Biotechnol.**, v. 101, n. 20, p. 7509–7521, 2017. doi: 10.1007/s00253-017-8481-4.

[192] M. Nala et al. Vapour-liquid equilibrium (VLE) for the systems furan+n-hexane and furan+toluene. Measurements, data treatment and modeling using molecular models, **Fluid Phase Equilib.**, v. 337, p. 234–245, 2013. doi: 10.1016/j.fluid.2012.08.005.

[193] K. Paduszyński, M. Okuniewski, and U. Domańska. 'Sweet-in-Green' systems based on sugars and ionic liquids: New solubility data and thermodynamic analysis. **Ind. Eng. Chem. Res.**, v. 52, n. 51, p. 18482–18491, 2013. doi: 10.1021/ie4033186.

[194] D. NguyenHuynh and C. T. Q. Mai. Application of the Modified Group Contribution PC-SAFT to Carboxylic Acids and Their Mixtures. **Ind. Eng. Chem. Res.**, v. 58, p. 8923–8934, 2019. doi: 10.1021/acs.iecr.9b02052.

[195] S. Mohammad, G. Grundl, R. Müller, W. Kunz, G. Sadowski, and C. Held.

Influence of electrolytes on liquid-liquid equilibria of water/1-butanol and on the partitioning of 5-hydroxymethylfurfural in water/1-butanol. **Fluid Phase Equilib.**, v. 428, p. 102–111, 2016. doi: 10.1016/j.fluid.2016.05.001.

[196] S. Mohammad, C. Held, E. Altuntepe, T. Köse, and G. Sadowski. Influence of Salts on the Partitioning of 5-Hydroxymethylfurfural in Water/MIBK. **J. Phys. Chem. B**, v. 120, n. 16, p. 3797–3808, 2016. doi: 10.1021/acs.jpcb.5b11588.

[197] Y. Sun, A. Schemann, C. Held, X. Lu, G. Shen, and X. Ji. Modeling Thermodynamic Derivative Properties and Gas Solubility of Ionic Liquids with ePC-SAFT. **Ind. Eng. Chem. Res.**, v. 58, n. 19, p. 8401–8417, 2019. doi: 10.1021/acs.iecr.9b00254.

[198] S. Mohammad et al. Salt influence on MIBK/water liquid-liquid equilibrium: Measuring and modeling with ePC-SAFT and COSMO-RS. **Fluid Phase Equilib.**, v. 416, p. 83–93, 2016. doi: 10.1016/j.fluid.2015.11.018.

[199] B. Liebergesell et al. High-pressure vapor-liquid equilibria of the second generation biofuel blends: Experiments and PCP-SAFT modeling. **Fluid Phase Equilib.**, v. 400, p. 95–102, 2015. doi: 10.1016/j.fluid.2015.05.002.

[200] G. Rodriguez and E. J. Beckman. Modelling phase behavior of biodiesel related systems with CO2 using a polar version of PC-SAFT. **Fluid Phase Equilib.**, v. 485, p. 32–43, 2019. doi: 10.1016/j.fluid.2018.12.003.

[201] G. Rodriguez and E. J. Beckman. Predicting Initial Reactant Miscibility for CO2-Enhanced Transesterification of Triglycerides with Methanol Using a Polar Version of PC-SAFT. **Ind. Eng. Chem. Res.**, v. 58, n. 50, p. 22598–22608, 2019. doi: 10.1021/acs.iecr.9b03235.

[202] B. Liebergesell, T. Brands, H. J. Koß, and A. Bardow. Quaternary isothermal vapor-liquid equilibrium of the model biofuel 2-butanone + n-heptane + tetrahydrofuran + cyclohexane using Raman spectroscopic characterization. **Fluid Phase Equilib.**, v. 472, p. 107–116, 2018. doi: 10.1016/j.fluid.2018.04.009.

[203] S. Ahmed, N. Ferrando, J. C. de Hemptinne, J. P. Simonin, O. Bernard, and O. Baudouin. Modeling of mixed-solvent electrolyte systems. **Fluid Phase Equilib.**, v. 459, p. 138–157, 2018. doi: 10.1016/j.fluid.2017.12.002.

[204] S. Ahmed, N. Ferrando, J. C. De Hemptinne, J. P. Simonin, O. Bernard, and O. Baudouin. A New PC-SAFT Model for Pure Water, Water-Hydrocarbons, and Water-Oxygenates Systems and Subsequent Modeling of VLE, VLLE, and LLE. **J. Chem. Eng. Data**, v. 61, n. 12, p. 4178–4190, 2016. doi: 10.1021/acs.jced.6b00565.

[205] L. Grandjean, J. C. De Hemptinne, and R. Lugo. Application of GC-PPC-SAFT EoS to ammonia and its mixtures. **Fluid Phase Equilib.**, v. 367, p. 159–172, 2014. doi: 10.1016/j.fluid.2014.01.025.

[206] C. G. Pereira et al. Guaiacol and its mixtures: New data and predictive models part 1: Phase equilibrium. **Fluid Phase Equilib.**, v. 470, p. 75–90, 2018. doi:

10.1016/j.fluid.2018.01.035.

[207] D. Nguyen-Huynh, J. C. De Hemptinne, R. Lugo, J. P. Passarello, and P. Tobaly. Modeling liquid-liquid and liquid-vapor equilibria of binary systems containing water with an alkane, an aromatic hydrocarbon, an alcohol or a gas (methane, ethane, CO2 or H2S), using group contribution polar perturbed-chain statistical associating fluid. **Ind. Eng. Chem. Res.**, v. 50, n. 12, p. 7467–7483, 2011. doi: 10.1021/ie102045g.

[208] A. Novella, S. Camy, and E. Monso. Recovery of carboxylic acids from dilute aqueous solutions using a supercritical CO 2 packed column.

[209] M. G. Prieto, F. A. Sánchez, and S. Pereda. A Group Contribution Equation of State for Biorefineries. GCA-EOS Extension to Bioether Fuels and Their Mixtures with n-Alkanes. **J. Chem. Eng. Data**, v. 64, n. 5, p. 2170–2185, 2019. doi: 10.1021/acs.jced.8b01153.

[210] F. A. Sánchez, Y. Ille, N. Dahmen, and S. Pereda. GCA-EOS extension to mixtures of phenol ethers and derivatives with hydrocarbons and water. **Fluid Phase Equilib.**, v. 490, p. 13–21, 2019. doi: 10.1016/j.fluid.2019.02.017.

[211] F. A. Sánchez, S. Pereda, and E. A. Brignole. GCA-EoS: A SAFT group contribution model-Extension to mixtures containing aromatic hydrocarbons and associating compounds. **Fluid Phase Equilib.**, v. 306, n. 1, p. 112–123, 2011. doi: 10.1016/j.fluid.2011.03.024.

[212] C. I. Paulo, M. Soledad Diaz, and E. A. Brignole. Minimizing costs in near-critical bioethanol extraction and dehydration processes. **Energy and Fuels**, v. 26, n. 6, p. 3785–3795, 2012. doi: 10.1021/ef3002907.

[213] T. M. Soria, F. A. Sánchez, S. Pereda, and S. B. Bottini. Modeling alcohol+water+hydrocarbon mixtures with the group contribution with association equation of state GCA-EoS. **Fluid Phase Equilib.**, v. 296, n. 2, p. 116–124, 2010. doi: 10.1016/j.fluid.2010.02.040.

[214] M. G. Prieto, F. A. Sánchez, and S. Pereda. Modeling Phase Equilibria of Ethers and Alcohols with GCA-EOS for Assessing the Coblending of Advanced Biofuels. **J. Chem. Eng. Data**, v. 64, n. 6, p. 2504–2518, 2019. doi: 10.1021/acs.jced.9b00030.

[215] Y. Ille, F. A. Sánchez, N. Dahmen, and S. Pereda. Multiphase Equilibria Modeling of Fast Pyrolysis Bio-Oils. Group Contribution Associating Equation of State Extension to Lignin Monomers and Derivatives. **Ind. Eng. Chem. Res.**, v. 58, n. 17, p. 7318–7331, 2019. doi: 10.1021/acs.iecr.9b00227.

[216] M. González Prieto, F. A. Sánchez, and S. Pereda. Thermodynamic model for biomass processing in pressure intensified technologies. **J. Supercrit. Fluids**, v. 96, p. 53–67, 2015. doi: 10.1016/j.supflu.2014.08.024.

[217] T. M. Soria, A. E. Andreatta, S. Pereda, and S. B. Bottini. Thermodynamic modeling of phase equilibria in biorefineries. **Fluid Phase Equilib.**, v. 302, n. 1–2, p. 1–9, 2011. doi: 10.1016/j.fluid.2010.10.029.

[218] M. B. Oliveira, A. J. Queimada, and J. A. P. Coutinho. Prediction of near and supercritical fatty acid ester + alcohol systems with the CPA EoS. **J. Supercrit. Fluids**, v. 52, n. 3, p. 241–248, 2010. doi: 10.1016/j.supflu.2010.01.014.

[219] A. M. Palma, M. B. Oliveira, A. J. Queimada, and J. A. P. Coutinho. Re-evaluating the CPA EoS for improving critical points and derivative properties description. **Fluid Phase Equilib.**, v. 436, p. 85–97, 2017. doi: 10.1016/j.fluid.2017.01.002.

[220] A. Mejía, M. B. Oliveira, H. Segura, M. Cartes, and J. A. P. Coutinho. Isobaric vapor-liquid equilibrium and isothermal surface tensions of 2,2'-oxybis[propane]+2,5-Dimethylfuran. **Fluid Phase Equilib.**, v. 345, p. 60–67, 2013. doi: 10.1016/j.fluid.2013.02.005.

[221] L. A. Follegatti-Romero, M. B. Oliveira, E. A. C. Batista, J. A. P. Coutinho, and A. J. A. Meirelles. Liquid-liquid equilibria for ethyl esters + ethanol + water systems: Experimental measurements and CPA EoS modeling. **Fuel**, v. 96, p. 327–334, 2012. doi: 10.1016/j.fuel.2011.12.056.

[222] A. M. Palma, A. J. Queimada, and J. A. P. Coutinho. Modeling of the Mixture Critical Locus with a Modified Cubic Plus Association Equation of State: Water, Alkanols, Amines, and Alkanes. **Ind. Eng. Chem. Res.**, v. 57, n. 31, p. 10649–10662, 2018. doi: 10.1021/acs.iecr.8b01960.

[223] M. B. Oliveira, S. I. Miguel, A. J. Queimada, and J. A. P. Coutinho. Phase equilibria of ester + alcohol systems and their description with the cubic-plus-association equation of state. **Ind. Eng. Chem. Res.**, v. 49, n. 7, p. 3452–3458, 2010. doi: 10.1021/ie901470s.

[224] A. Khoshsima and R. Shahriari. Molecular modeling of systems related to the biodiesel production using the PHSC equation of state. **Fluid Phase Equilib.**, v. 458, p. 58–83, 2018. doi: 10.1016/j.fluid.2017.10.029.

[225] D. B. Harwood, C. J. Peters, and J. I. Siepmann. A Monte Carlo simulation study of the liquid-liquid equilibria for binary dodecane/ethanol and ternary dodecane/ethanol/water mixtures. **Fluid Phase Equilib.**, v. 407, p. 269–279, 2015. doi: 10.1016/j.fluid.2015.07.011.

[226] N. Ferrando, V. Lachet, J. Pérez-Pellitero, A. D. MacKie, P. Malfreyt, and A. Boutin. A transferable force field to predict phase equilibria and surface tension of ethers and glycol ethers. **J. Phys. Chem. B**, v. 115, n. 36, p. 10654–10664, 2011. doi: 10.1021/jp203278t.

[227] M. A. A. Rocha, D. Kerlé, J. Kiefer, W. Schroër, and B. Rathke. Liquid-Liquid Phase Behavior of Solutions of 1,3-Diethylimidazoliumamide in n-Alkyl Alcohols. **J. Chem. Eng. Data**, v. 65, n. 3, p. 1345–1357, 2020. doi: 10.1021/acs.jced.9b00800.

[228] M. Yiannourakou, P. Ungerer, B. Leblanc, N. Ferrando, and J. M. Teuler, "Overview of GIBBS capabilities for thermodynamic property calculation and VLE

behaviour description of pure compounds and mixtures: Application to polar compounds generated from ligno-cellulosic biomass. **Molecular Simulation**, v. 39, n. 14–15, p. 1165–1211, 2013. doi: 10.1080/08927022.2013.830182.

[229] H. E. Yang and Y. C. Bae. Thermodynamic analysis of phase equilibrium and surface tension of ternary polymer solutions. **AIChE J.**, v. 65, n. 9, p. 1–10, 2019. doi: 10.1002/aic.16679.

[230] L. Villar, B. González, I. Díaz, Á. Domínguez, and E. J. González. Role of the cation on the liquid extraction of levulinic acid from water using NTf2-based ionic liquids: Experimental data and computational analysis. **J. Mol. Liq.**, v. 302, p. 112561, 2020. doi: 10.1016/j.molliq.2020.112561.

[231] Z. Wu, C. Liu, H. Cheng, L. Chen, and Z. Qi. Tuned extraction and regeneration process for separation of hydrophobic compounds by aqueous ionic liquid. **J. Mol. Liq.**, v. 308, p. 113032, 2020. doi: 10.1016/j.molliq.2020.113032.

[232] B. Ozturk and M. Gonzalez-Miquel. Alkanediol-based deep eutectic solvents for isolation of terpenoids from citrus essential oil: Experimental evaluation and COSMO-RS studies. **Sep. Purif. Technol.**, v. 227, n. February, p. 115707, 2019. doi: 10.1016/j.seppur.2019.115707.

[233] J. Scheffczyk et al. COSMO-CAMPD: A framework for integrated design of molecules and processes based on COSMO-RS. **Mol. Syst. Des. Eng.**, v. 3, n. 4, p. 645–657, 2018. doi: 10.1039/c7me00125h.

[234] R. Anantharaj and T. Banerjee, "COSMO-RS-based screening of ionic liquids as green solvents in denitrification studies," Ind. Eng. Chem. Res., vol. 49, no. 18, pp. 8705–8725, 2010, doi: 10.1021/ie901341k.

[235] M. A. R. Martins et al. Greener Terpene-Terpene Eutectic Mixtures as Hydrophobic Solvents. **ACS Sustain. Chem. Eng.**, v. 7, n. 20, p. 17414–17423, 2019. doi: 10.1021/acssuschemeng.9b04614.

[236] M. A. R. Martins et al. Impact of the cation symmetry on the mutual solubilities between water and imidazolium-based ionic liquids. **Fluid Phase Equilib.**, v. 375, p. 161–167, 2014. doi: 10.1016/j.fluid.2014.05.013.

APPENDIX 1 – EXCESS GIBBS FREE ENERGY MODELS

Excess Gibbs free energy models presented in section 3.2.1.2 and its related expressions, including parameters and activity coefficient final equations.

$$RTln\gamma_i = \left(\frac{\partial G^E}{\partial n_i}\right)_{T,P,n_{j\neq i}}$$

- **Two-Suffix Margules Equation**

$$G^E = Ax_1x_2$$

$$ln\gamma_1 = \frac{A}{RT}x_2^2 \qquad ln\gamma_2 = \frac{A}{RT}x_1^2$$

Where x_i is the molar fraction of component "i" and A is an empirical constant.

- **Van Laar Equation**

$$G^E = x_1x_2\left(\frac{AB}{Ax_1 + Bx_2}\right)$$

$$ln\gamma_1 = \frac{A}{\left(1 + \frac{A}{B}\frac{x_1}{x_2}\right)^2} \qquad ln\gamma_2 = \frac{B}{\left(1 + \frac{B}{A}\frac{x_2}{x_1}\right)^2}$$

Where A and B are empirical constants.

- **Flory-Huggins Equation**

$$G^E = RT\left[\left(x_1ln\frac{\phi_1}{x_1} + x_2ln\frac{\phi_2}{x_2}\right) + \chi\left(x_1 + \frac{\nu_2}{\nu_1}x_2\right)\phi_1\phi_2\right]$$

$$ln\gamma_1 = ln\frac{\phi_1}{x_1} + \left(1 - \frac{1}{\frac{\nu_2}{\nu_1}}\right)\phi_2 + \chi\phi_2^2 \qquad ln\gamma_2 = ln\frac{\phi_2}{x_2} - \left(\frac{\nu_2}{\nu_1} - 1\right)\phi_1 + \frac{\nu_2}{\nu_1}\chi\phi_1^2$$

Where $\nu_i$and ϕ_i are the molar volume and the volume fraction of component "i", respectively, and χ is the Flory-Huggins interaction parameter determined experimentally.

- **Wilson Equation**

$$G^E = -RT\sum_{i=1}^{m} x_i ln\left(\sum_{j=1}^{m} x_j\Lambda_{ij}\right)$$

$$\Lambda_{ij} = \frac{v_j}{v_i} exp\left(-\frac{\lambda_{ij} - \lambda_{ii}}{RT}\right) \qquad \Lambda_{ji} = \frac{v_i}{v_j} exp\left(-\frac{\lambda_{ji} - \lambda_{jj}}{RT}\right)$$

$$ln\gamma_k = 1 - ln\left(\sum_{j=1}^{m} x_j \Lambda_{kj}\right) - \sum_{i=1}^{m} \frac{x_i \Lambda_{ik}}{\sum_{j=1}^{m} x_j \Lambda_{ij}}$$

Where R is the universal gas constant, T is the temperature, m is the total number of components in the mixture, and λ_{ij}'s are interaction parameters adjusted experimentally.

- **Non Random Two Liquids (NRTL)**

$$G^E = -RT \sum_{i=1}^{m} x_i \frac{\sum_{j=1}^{m} \tau_{ji} G_{ji} x_j}{\sum_{l=1}^{m} G_{li} x_l}$$

$$\tau_{ji} = \frac{g_{ji} - g_{ii}}{RT} \qquad G_{ji} = exp(-\alpha_{ji} \tau_{ji})$$

$$ln\gamma_i = \frac{\sum_{j=1}^{m} \tau_{ji} G_{ji} x_j}{\sum_{l=1}^{m} G_{li} x_l} + \sum_{j=1}^{m} \frac{x_j G_{ij}}{\sum_{l=1}^{m} G_{lj} x_l} \left(\tau_{ij} - \frac{\sum_{r=1}^{m} x_r \tau_{rj} G_{rj}}{\sum_{l=1}^{m} G_{lj} x_l}\right)$$

Where g_{ji}'s are interaction parameters adjusted experimentally, and α_{ji} is the non-randomness parameter of the mixture, normally fixed as 0.3.

- **Universal Quasi Chemical (UNIQUAC)**

$$G^E = RT \left[\sum_{i=1}^{m} x_i ln \frac{\phi_i}{x_i} + \frac{z}{2} \sum_{i=1}^{m} q_i x_i ln \frac{\theta_i}{\phi_i} - \sum_{i=1}^{m} x_i q_i ln \left(\sum_{j=1}^{m} \theta_j \tau_{ji}\right)\right]$$

$$\phi_i = \frac{r_i x_i}{\sum_{j=1}^{m} r_j x_j} \qquad \theta_i = \frac{q_i x_i}{\sum_{j=1}^{m} q_j x_j} \qquad \tau_{ij} = exp\left(-\frac{a_{ij}}{T}\right) \qquad \tau_{ji} = exp\left(-\frac{a_{ji}}{T}\right)$$

Where z is the coordinator number defined as 10, r_i and q_i, the volume and the area parameter of component "i", respectively, and a_{ij} are the interaction energy parameters adjusted experimentally.

$$ln\gamma_i = ln\frac{\phi_i}{x_i} + \frac{z}{2} q_i ln \frac{\theta_i}{\phi_i} + l_i - \frac{\phi_i}{x_i} \sum_{j=1}^{m} x_j l_j + q_i \left[1 - ln\left(\sum_{j=1}^{m} \theta_j \tau_{ji}\right) - \sum_{j=1}^{m} \frac{\theta_j \tau_{ij}}{\sum_{k=1}^{m} \theta_k \tau_{kj}}\right]$$

$$l_i = \frac{z}{2}(r_i - q_i) - (r_i - 1)$$

APPENDIX 2 – PRISMA CHECKLIST

PRISMA 27 items-checklist applied to this work.

Section/topic	#	Checklist item	Reported on page #
TITLE			
Title	1	Identify the report as a systematic review, meta-analysis, or both.	1
ABSTRACT			
Structured summary	2	Provide a structured summary including, as applicable: background; objectives; data sources; study eligibility criteria, participants, and interventions; study appraisal and synthesis methods; results; limitations; conclusions and implications of key findings; systematic review registration number.	17
INTRODUCTION			
Rationale	3	Describe the rationale for the review in the context of what is already known.	18
Objectives	4	Provide an explicit statement of questions being addressed with reference to participants, interventions, comparisons, outcomes, and study design (PICOS).	19
METHODS			
Protocol and registration	5	Indicate if a review protocol exists, if and where it can be accessed (e.g., Web address), and, if available, provide registration information including registration number.	61
Eligibility criteria	6	Specify study characteristics (e.g., PICOS, length of follow-up) and report characteristics (e.g., years considered, language, publication status) used as criteria for eligibility, giving rationale.	62
Information sources	7	Describe all information sources (e.g., databases with dates of coverage, contact with study authors to identify additional studies) in the search and date last searched.	62
Search	8	Present full electronic search strategy for at least one database, including any limits used, such that it could be repeated.	62
Study selection	9	State the process for selecting studies (i.e., screening, eligibility, included in systematic review, and, if applicable, included in the meta-analysis).	62
Data collection process	10	Describe method of data extraction from reports (e.g., piloted forms, independently, in duplicate) and any processes for obtaining and confirming data from investigators.	62
Data items	11	List and define all variables for which data were sought (e.g., PICOS, funding sources) and any assumptions and simplifications made.	62
Risk of bias in individual studies	12	Describe methods used for assessing risk of bias of individual studies (including specification of whether this was done at the study or outcome level), and how this information is to be used in any data synthesis.	62
Summary measures	13	State the principal summary measures (e.g., risk ratio, difference in means).	-

Synthesis of results	14	Describe the methods of handling data and combining results of studies, if done, including measures of consistency (e.g., I^2) for each meta-analysis.	-
Risk of bias across studies	15	Specify any assessment of risk of bias that may affect the cumulative evidence (e.g., publication bias, selective reporting within studies).	-
Additional analyses	16	Describe methods of additional analyses (e.g., sensitivity or subgroup analyses, meta-regression), if done, indicating which were pre-specified.	-
RESULTS			
Study selection	17	Give numbers of studies screened, assessed for eligibility, and included in the review, with reasons for exclusions at each stage, ideally with a flow diagram.	62
Study characteristics	18	For each study, present characteristics for which data were extracted (e.g., study size, PICOS, follow-up period) and provide the citations.	72,73
Risk of bias within studies	19	Present data on risk of bias of each study and, if available, any outcome level assessment (see item 12).	-
Results of individual studies	20	For all outcomes considered (benefits or harms), present, for each study: (a) simple summary data for each intervention group (b) effect estimates and confidence intervals, ideally with a forest plot.	72,73
Synthesis of results	21	Present results of each meta-analysis done, including confidence intervals and measures of consistency.	-
Risk of bias across studies	22	Present results of any assessment of risk of bias across studies (see Item 15).	-
Additional analysis	23	Give results of additional analyses, if done (e.g., sensitivity or subgroup analyses, meta-regression [see Item 16]).	64-85
DISCUSSION			
Summary of evidence	24	Summarize the main findings including the strength of evidence for each main outcome; consider their relevance to key groups (e.g., healthcare providers, users, and policy makers).	72,73,85
Limitations	25	Discuss limitations at study and outcome level (e.g., risk of bias), and at review-level (e.g., incomplete retrieval of identified research, reporting bias).	64-85
Conclusions	26	Provide a general interpretation of the results in the context of other evidence, and implications for future research.	86
FUNDING			
Funding	27	Describe sources of funding for the systematic review and other support (e.g., supply of data); role of funders for the systematic review.	6

Source: Liberati et al., 2009.